Hayah, Nurul (2012) *A study of the anatomical variations of the carotid arterial tree in Equidae.* PhD thesis.

A STUDY OF THE ANATOMICAL VARIATIONS OF THE CAROTID ARTERIAL TREE IN EQUIDAE

by

Nurul Hayah (D.V.M)

A thesis submitted for the degree of

Doctor of Philosophy

School of Veterinary Medicine
University of Glasgow

November 2011

SUMMARY

The internal carotid artery in the horse is of significant veterinary importance due to its intimate relationship with the guttural pouch, and mycotic disease thereof. The relevance of recognising and identifying variations involving the internal carotid artery lies in the fact that surgical occlusion of the artery is the treatment of choice for guttural pouch mycosis. However, occlusion could be hampered when there is doubt about the anatomy of this vessel and its variation.

Conventional angiography and automatic rotational angiographic techniques were used to study the anatomy of the carotid trifurcation and the internal carotid artery on cadavers of three species included in the genus *Equus*; 50 horses, 26 donkeys and one zebra. Following angiography, arterial latex casting was performed on the horse and donkey specimens with subsequent dissection to harvest the hardened arterial casts.

Rotational angiography with 3-dimensional image reconstruction represent a major advantage in the angiographic diagnosis of carotid and cerebral vascular variation compared to conventional angiography. This technique generated superior angiographic images of the carotid and cerebral vascular system of horses, donkey and zebra.

In the horse, five variations of the internal carotid artery were identified as follows: [1] the internal carotid artery and occipital artery arising as a common trunk, [2] an aberrant branch of the internal carotid artery that unites with the basilar artery, [3] an aberrant branch of the internal carotid artery that does not unite with the basilar artery, [4] aberrant branch of the internal carotid artery that gives rise to several satellite branches, [5] aberrant branch of the internal carotid artery that has a satellite branch connected to the caudal branch of the ipsilateral occipital artery. Variations of the carotid arterial tree in donkeys were identified as follow: [1] the internal carotid and occipital arteries shared a common trunk, [2] the linguofacial trunk originated from the common carotid artery causing the common carotid artery to terminate as four branches, [3] a short external carotid artery before giving rise to the linguofacial trunk, mimicking the appearance of the

common carotid artery terminating into four branches, [4] the internal carotid artery originating far more caudal from the common carotid artery termination. The carotid arterial anatomy of the one zebra studied here showed no discrepancy to the accepted common anatomical pattern of this structure. Aneurysm formation was not identified in any of the specimens.

TABLE OF CONTENT

LIST OF TABLES

LIST OF FIGURES

LIST OF ACCOMPANYING MATERIAL

One DVD unit entitled: Videos of Cine-Loop function entitled 'An angiographic study of the carotid arterial tree of Equidae'.

List of content:

Video 2-1: An angiographic video of a common/standard anatomy of the carotid trifurcation, the internal carotid artery and the cerebral arterial circle in a horse.

Video 2-2a: An angiographic video of a horse showing the presence of an aberrant branch of the left internal carotid artery (carotid level).

Video 2-2b: An angiographic video of a horse showing the presence of an aberrant branch of the left internal carotid artery (cerebral level).

Video 2-3: An angiographic video of a horse with presence of an aberrant branch of the left internal carotid artery that gives rise to several satellite branches. One of the satellite branches was observed to be connected to the ipsilateral occipital artery. The right internal carotid artery shares a common trunk with the occipital artery.

Video 3-1: An angiographic video of a common/standard anatomy of the carotid trifurcation, the internal carotid artery and the cerebral arterial circle in a donkey.

Video 3-2: An angiographic video of a donkey showing the left internal carotid artery sharing a common trunk with the occipital artery.

Video 3-3: An angiographic video of a donkey showing the linguofacial trunk arising from the common carotid artery.

Video 3-4: An angiographic video of a donkey showing the linguofacial trunk sharing a common origin with the external carotid artery.

Video 3-5: An angiographic video of a donkey showing the left internal carotid artery arising far more caudal than the carotid termination with the left linguofacial trunk arising from the common carotid artery.

Video 3-6: An angiographic video of a donkey with a small and tortuous caudal intercarotid artery.

Video 4-1: An angiographic video of a common/standard anatomy of the carotid trifurcation, the internal carotid artery and the cerebral arterial circle in a zebra.

ACKNOWLEDGEMENT

I am grateful for the opportunity given to me by my supervisor, Patrick Pollock, for accepting me to conduct a PhD research study in this department and at the same time gained knowledge and practical experiences on the equine clinical work done here. He supported me in a number of ways that will shape my future career as an equine veterinary practitioner in Malaysia.

Not to forget my former co-supervisor, Christoph Lischer, whose initial guidance has enabled me to develop an understanding of the C-arm machine and its 3D component; as well as his motivational encouragement and emotional support during transitional period of adjusting to a new country and its environment.

A special thanks right from the heart to Martin Sullivan, my current co-supervisor, the one who stopped me from falling apart, helped re-build my confidence and his ‘thoroughness’ has helped me to finally make this thesis a reality.

We are indebted to the Donkey Sanctuary for their support in this research project. A million thanks to Richard Irvine and Michael McGuigan from the post mortem room, School of Veterinary Medicine, University of Glasgow, for their help in collecting the specimens for this research. I would also like to thank Gordon Reford, from the lab of human anatomy, University of Glasgow, for his help and advice in the technique of arterial latex casting.

A credit of appreciation for Phillipa Broadway for her artistic contribution in drawing two medical figures used in this thesis (Figure 1-1 and Figure 1-2).

It is an honor for me to thank Prof. Olivier Lepage for allowing me to visit the Lyon Veterinary School, France, and share some of his ideas regarding this field of study.

A pleasure to thank the staff of Weipers Centre and BIOPTA, for all the hospitality offered to me that made me feels less homesick and lonely.

Huge thanks Raja Khairul Adli for his willingness to proof read every chapter in this thesis without fail. To my friends; Sarah Othman, Ida Suzaini Pratt, Intan Fatiha, Doyin Thompson, Saa'din, Nani and family. Thanks for being there for me and helping me maintain my sanity while undertaking this challenge.

To my family, Mama and Babah, thank you for the support and prayers from far. Especially to my sister, Khairul Farhah, thanks for your sacrifice to come all the way from Malaysia and take charge of the baby, Airil Hakim, while I write this thesis day and night. Without your help, there is no way I could finish on time.

For my dearest husband, Azrul Azman Abd. Lah, no words could described my deepest gratitude for all the physical and emotional sacrifice you gave for me, for all the love and patience you had for us to keep us holding on and strong. Not to mention your direct involvement in this research, where you helped in lifting and shifting specimens onto the table in preparation for angiograms, latex casting and dissections when the specimens were too heavy for me. Thank you for accompanying me during experimental work on late nights and at weekends and sharing my joy and pain during this whole process.

Lastly, special acknowledgement goes to the Government of Malaysia for funding this PhD and my three and a half year stay here in the UK, including allowances for family by University Putra of Malaysia (Grant number 820626-05-5112-2008/UPM).

With that, I dedicate this piece of old Malay poem called 'pantun' in honour of all the people I have mentioned and for all other people that I have not mentioned directly;

Pulau Pandan jauh ke tengah,

Gunung Daik bercabang tiga,

Hancur badan dikandung tanah,

Budi yang baik dikenang juga

AUTHOR'S DECLARATION

I hereby declare that I am the sole author of this thesis and performed all the works presented here.

Nurul Hayah

Date: 11th November 2011

1 THE CAROTID ARTERIAL TREE

1.1 Important Vessels

1.1.1 Common Carotid Artery

The two common carotid arteries arise from the brachiocephalic trunk (Nanda, 1975) and together with the vagosympathetic trunk, ascend the neck and extend dorsolaterally to the trachea. The length of the common carotid artery may vary, but is usually about 5-7cm, but it may vary between 2.5 (in rare cases) and 20cm (Nanda, 1975).

From the ventral surface of the trachea, the right common carotid artery passes obliquely to the right side and later inclines towards the dorsal surface of the trachea near its termination. Here, it divides into the external carotid, internal carotid and occipital arteries. The right common carotid artery is in contact superficially with the jugular vein at the caudal part of the neck. Towards the end of the common carotid artery, it becomes more deeply located and is related laterally to the mandibular and parotid glands, and medially to the oesophagus.

The pathway of the left common carotid artery differs from the right because it normally separates from the trachea as part of its course. It is usually in contact with the trachea for about 6-8cm at the base of the neck. However, contact of the left common carotid artery with the trachea may be even less when the oesophagus is more ventral than usual and if the horse possesses a long bicarotid trunk (Nanda, 1975).

The common carotid artery gives off several branches, which include the following:

1. Muscular branches of variable size supplying the ventral muscles of the neck, subcutis and skin
2. Oesophageal and tracheal branches that supply the deep cervical lymph nodes
3. The parotid artery (a collateral branch of the common carotid artery). However, its presence is not consistent between horses. Commonly, the parotid artery arises near the termination of common carotid artery and enters the ventral part of the parotid gland
4. The cranial thyroid artery is the largest collateral branch of the common carotid artery and sends several branches to the thyroid gland. It arises from the common carotid artery about 5-7.5cm distal to the carotid trifurcation. It also gives off the caudal laryngeal branch that supplies the extrinsic muscles of the larynx and the constrictors of the pharynx
5. The ascending pharyngeal artery is a collateral branch that generally originates directly from the common carotid artery. Sometimes it arises by way of a common trunk with the cranial thyroid artery
6. The caudal thyroid artery arises from the common carotid artery at a variable distance caudal to the cranial thyroid or parotid artery. Its presence is not always constant where it supplies the caudal part of the thyroid gland

1.1.2 The Equine Carotid Trifurcation

In human beings, the common carotid artery usually bifurcates to form the internal carotid artery and external carotid artery (Gray, 1918). However, the common carotid artery of the horse terminates and branches into three important arteries; the external carotid artery, occipital artery and the internal carotid artery. The termination of the common carotid artery and the beginning of these three branches constitutes the term carotid trifurcation of the horse (Furuhata, 1964).

The external carotid artery is the largest artery of these three branches and makes up the continuation of the common carotid artery (Furuhata, 1964, Nanda, 1975). Normally, the external carotid artery continues straight from the common carotid artery. The occipital artery is usually the second largest branch of the carotid trifurcation. Most commonly, it arises cranial to the internal carotid artery, but sometimes the occipital artery and the internal carotid artery may arise together as a common trunk. Later, at a variable distance, these get separate as individual arteries. In this situation, the common carotid artery is bifurcated instead of the normal trifurcated form (Winogradow, 1928, Meijling, 1938, Furuhata, 1964, Nanda, 1975, Orr et al., 1983, Caron et al., 1987, Greet, 1987).

At the initial portion of the internal carotid artery, there is a prominent swelling termed the 'sinus caroticus' or 'bulbus caroticus' (Tandler, 1901), also known as a carotid body (Nanda, 1975). However, Furuhata (1964) also claimed that there was a sinus-like dilatation at the initial part of the occipital artery that he thought to be similar to the carotid sinus. The carotid body is tightly attached to the wall of the occipital artery, internal carotid artery and external carotid artery by thick connective tissue. Embedded in this connective tissue, between the roots of the external carotid and the occipital arteries, there is the intercarotid bone. The presence of the intercarotid bone at the trifurcate portion of the common carotid artery is to provide support for the carotid body (Furuhata, 1964).

Histological sections of the carotid trifurcation revealed that the carotid body is attached to the afore mentioned thick fibrous tissue and embedded as small mass, a cartilage or bony tissue, with some small blood vessels (Furuhata, 1964). In another histological study of the carotid trifurcation in Thoroughbred horses, various degrees of oedema in the tunica media of the carotid trifurcation were observed (Nakamura et al., 1992). The oedematous lesions were characterized as a loose arrangement of smooth muscle fibres, oedematous swelling with vacuolation, oedematous lesion consisting focal and multi-focal muscle fibre loss and irregular arrangement of the elastic laminae. Tunica media calcification was also observed, but a definitive association of these pathologic changes to the performance in the horse could not be reached and suspected to be a congenital lesion (Nakamura et al., 1992). A similar finding (based on radiography) has also been reported in the dog of where the described feature of unknown significance is recognised as an incidental finding (Schwarz et al., 2002).

1.1.3 Internal Carotid Artery

In horses commonly, the internal carotid artery originates from the trifurcation of the common carotid artery, caudal and ventral to the occipital artery. In size, the internal carotid artery is smaller than the occipital artery. Sometimes, the internal carotid and occipital artery may arise together as a common trunk and after a variable distance, the arteries separate (Winogradow, 1928, Meijling, 1938, Furuhata, 1964, Nanda, 1975, Orr et al., 1983, Caron et al., 1987, Greet, 1987).

The brain of a horse receives arterial blood supply directly from the internal carotid artery (Gillilan, 1974, Baptiste, 1998). It arises at the level of the first cervical vertebrae, caudal to the occipital artery and runs on the dorsal and rostral surface of the medial compartment of the guttural pouch, and then directly pierces the foramen lacerum (Du Boulay et al., 1975, Nanda, 1975).

The intracranial pathway of the internal carotid artery was observed to have an extra-intracavernous course (Nanda, 1975, Nanda and Getty, 1975). After the internal carotid artery pierces the foramen lacerum, it enters the cranial cavity where it passes through the ventral petrosal sinus and enters the venous cavernous sinus, here it forms S-shaped curve. After this tortuous curve in the venous cavernous sinus, the internal carotid artery communicates with the contralateral vessel via the caudal intercarotid artery (Colles and Cook, 1983, Macdonald et al., 1999), where this artery lies in the intercavernous sinus caudal to the hypophysis, beneath the base of the brain (Nanda, 1975, Orr et al., 1983). The caudal intercarotid artery also provides a branch to the posterior (caudal) hypophyseal artery and the anterior (cranial) hypophyseal artery. These arteries perforate the hypophysis and then extend rostromedially to reach the tuber cinereum and then to the optic chiasma (Nanda, 1975).

During the intracavernous course of the internal carotid artery, immediately after the second bend of the internal carotid artery, it may branch into the caroticobasilar artery (Nanda and Getty, 1975, Freeman et al., 1993). This artery courses in a caudomedial direction and leaves the cavernous sinus to join the basilar artery at the pontine region, which is located at the ventral surface of the pons (Nanda, 1975, Orr et al., 1983). After giving off these branches, the internal carotid artery perforates the dura mater and gives off the caudal communicating artery. This artery turns caudad and courses on the ventral surface of the crus and joins the basilar artery and forms the lateral and caudolateral quadrants of the cerebral arterial circle, also known as the Circle of Willis (Martin, 2003).

After the internal carotid artery gives off the caudal communicating artery, it continues rostrally for a short distance and terminates as the rostral and middle cerebral arteries. The rostral cerebral artery courses rostral and unites with the corresponding branch of the opposite side to form the rostrolateral quadrants of the cerebral arterial circle, dorsal to the optic chiasma (Nanda, 1975). The median artery of the corpus collosum is formed by the union of the rostral cerebral arteries of either side (Nanda, 1975).

Arising from the rostrolateral quadrants of the cerebral arterial circle are two vessels that supply extracerebral tissue, which are the internal ophthalmic and the internal ethmoidal arteries (Orr et al., 1983). The internal ophthalmic artery leaves the cranial cavity through the optic foramen along with the optic nerve and terminates by anastomosing with the external ophthalmic artery to supply the eye and other periorbital tissue (Nanda, 1975, Orr et al., 1983). As for the internal ethmoidal artery, it passes through the cribriform plate to supply the ethmoidal turbinates and other tissues in the nasal sinus (Orr et al., 1983).

As a broad generalisation, the internal carotid artery branches from the common carotid artery just caudal and ventral to the occipital artery and continues its course rostro-dorsally to pierce the foramen lacerum into the brain cavity and contributes to the cerebral arterial circle. The blood flow of the internal carotid artery predominantly supply the brain, with insignificant blood flow to associated extracerebral tissue (periorbital and ethmoidal turbinate tissues)(Orr et al., 1983).

1.1.4 Occipital Artery

The occipital artery originates from the terminal branch of the common carotid artery, which is where the common carotid artery forms the carotid trifurcation. It typically arises cranial to the internal carotid artery and is usually larger than the internal carotid artery (Nanda, 1975). From its origin, the artery passes dorsally and slightly lateral to the fossa atlantis, and then divides into a cranial and caudal branch. The cranial branch is the cerebrospinal artery that unites with the contralateral side to form the basilar artery. The caudal branch of the occipital artery contributes to the formation of the vertebral artery (Colles and Cook, 1983).

In certain individuals, the occipital and internal carotid arteries arise as a common trunk of variable length from the common carotid before they separate. The occipital artery is related superficially to the mandibular gland and the brachiocephalicus muscle. Sometimes, the occipital artery may run deep to the guttural pouch and the longus carpitis muscle, but its relation to these structures is not consistent (Nanda and Getty, 1975).

1.1.5 External Carotid Artery

The external carotid artery is the continuation of the common carotid artery. The most important collateral branches of the external carotid artery are the masseteric, linguofacial trunk, caudal auricular and superficial temporal arteries. It also gives off variable branches to the mandibular and parotid glands, the guttural pouch, the retropharyngeal lymph nodes and also several ‘twigs’ to the adjacent muscles (Nanda, 1975).

After the external carotid artery gives off the linguofacial trunk, it travels dorsally and beneath the lateral compartment of the guttural pouch. Here, it continues as the maxillary artery after branching into the caudal auricular and superficial temporal arteries. Generally, the maxillary artery travels along the roof of the lateral compartment of the guttural pouch and passes above the tensor palatine muscle and enters the caudal alar foramen into the alar canal. In the caudal alar foramen, the maxillary artery is covered by the parotid gland and medially is in contact with the guttural pouch. Before and after the caudal alar foramen, the maxillary artery gives rise to the following major arteries; the inferior alveolar, the external ophthalmic and major palatine (Constantinescu and Constantinescu, 2004).

1.2 Association of the Carotid Arterial Tree with the Guttural Pouch in Equidae

Guttural pouches are paired evaginations of the auditory tubes that connect the nasopharynx to the middle ear (Freeman and Hardy, 2006), which have also been termed auditory tube diverticulae (Cook, 1966, Manglai et al., 2000). A number of other mammals also possess guttural pouches including the tapir (Turner, 1850), rhinoceros (Ellenberger and Baum, 1943), bats, hyrax and the South American forest mouse (Hinchcliffe and Pye, 1969).

The presence of guttural pouch or otherwise in the rhinoceros is currently contentious. Ellenberger and Baum (1943) considered it present in this mammal, however, more recent work denied that the rhinoceros, at least the white rhinoceros, has an auditory tube diverticulum (Endo et al., 1998). Intriguingly, there is debate as to whether the hyrax truly has guttural pouches in the way that is accepted in the horse. This is because in the hyrax, the two pouches are not separated by a medial septum but by the strap muscles of the neck as described by Fischer (1989). This author went on to propose that the hyracoids should be returned to the order of Perissodactyla owing to the occurrence of the guttural pouch and the apomorphic characteristics of the locomotor system and the maxilla (Fischer, 1989). A clade uniting Perissodactyla and Hyracoidea has been proposed (McKenna, 1975, Van Valen, 1978, Prothero and Schoch, 1989). However, Wible (1986) cautioned that the position of Hyracoidea within the Grandorder Ungulata was controversial.

In the horse, these air filled pouches are lined by pseudostratified ciliated epithelium, with a membrane thickness of 45-261µm, containing goblet cells

(Sisson, 1975). The guttural pouch is divided into two compartments, lateral and medial, which are separated by the stylohyoid bone (Freeman and Hardy, 2006).

The guttural pouches are located at the caudal aspect of the equine head, ventral to the basisphenoid bone, dorsal to the nasopharynx and larynx, and cranial to the atlanto-occipital joint. The medial compartment has a capacity of 472ml ±12.4ml of air, and the lateral compartment is approximately one third the capacity of the medial compartment (Manglai et al., 2000). Both pouches communicate with the nasopharynx via the pharyngeal orifice; a funnel-shaped opening in the dorsolateral aspect of the pharynx. The guttural pouch ostia (oblique slit-like openings) are about 3cm long and can be found on the lateral wall of the nasopharynx, just ventral to the level of choanae. The ostia are bounded medially by the thin free edge of the auditory tube, where a fold of mucus membrane (*plica salpingopharyngea*) extends in the same direction on the lateral wall of the pharynx for a distance of about 3cm. The outer boundary of each ostium is the lateral wall of the pharynx (Sisson, 1975). The guttural pouches are covered laterally by the pterygoid and digastric muscles, ramus of the mandible, parotid and mandibular salivary glands. Dorsally, the pouches are roofed by the petrous part of the temporal bone, tympanic bulla and auditory meatus (Freeman and Hardy, 2006).

These unique structures caught veterinary attention because they are closely related to several important structures. The medial compartment has close associations with the internal carotid artery, external carotid artery, glossopharyngeal, hypoglossal and vagus nerves, the cranial cervical ganglion, cranial laryngeal nerve and the pharyngeal branch of the vagus nerve (Figure 1-1 and Figure 1-2). The lateral compartment is intimately related to the external carotid, maxillary and superficial temporal arteries, and the facial and mandibular nerves (Figure 1-1 and Figure 1-2). Generally, the vagus, accessory and sympathetic nerves, the cranial cervical ganglion, internal carotid artery and ventral cerebral vein are situated in a fold of the dorsal part of the pouch (Sisson, 1975).

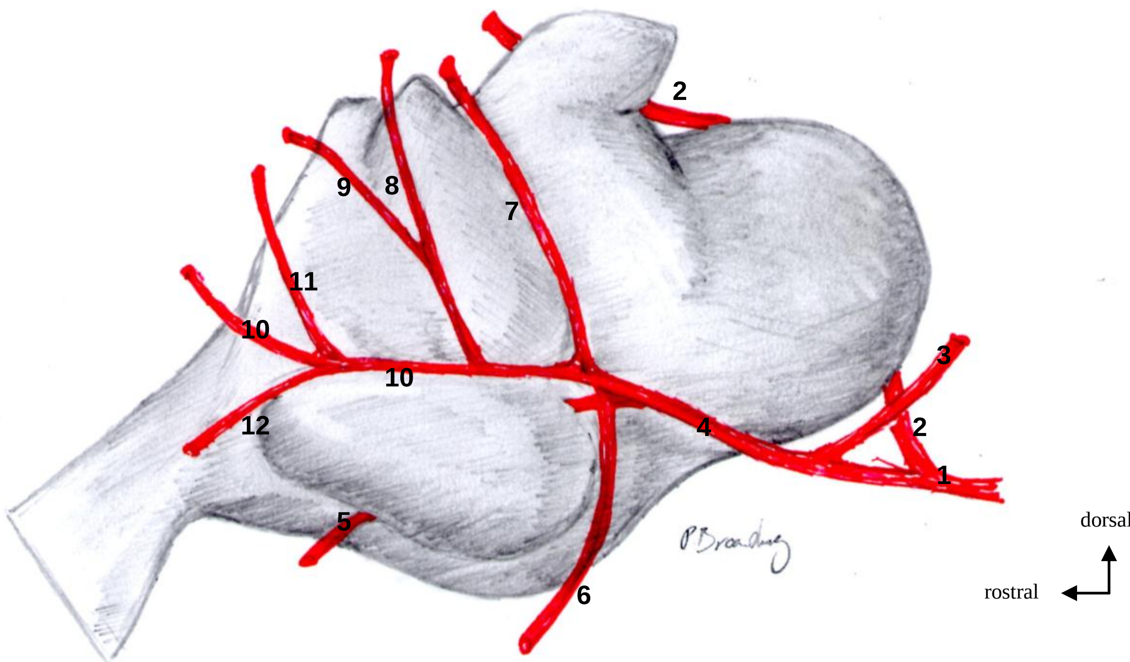

Figure 1-1: Arteries associated with the guttural pouch.
1 common carotid artery; 2 internal carotid artery; 3 occipital artery; 4 external carotid artery; 5 linguofacial trunk; 6 masseteric branch; 7 caudal auricular artery; 8 superficial temporal; 9 transverse facial; 10 maxillary artery; 11 middle meningeal; 12 inferior alveolar.

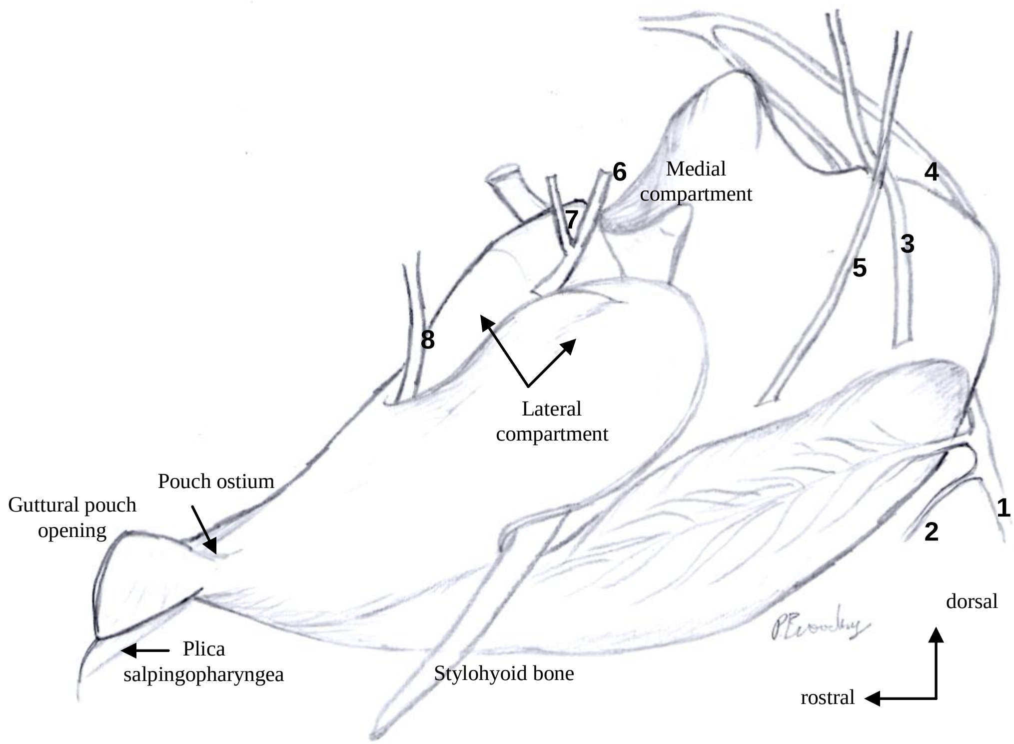

Figure 1-2: Nerves associated with the guttural pouch.
1 vagosympathetic trunk; 2 cranial laryngeal nerve; 3 glossopharyngeal; 4 accessory nerve; 5 hypoglossal nerve; 6 facial nerve; 7 auriculo-temporal nerve; 8 mandibular nerve.

1.2.1 Function of the Guttural Pouch

The function of the guttural pouches in horses remains unclear, however several authors have postulated the role of the guttural pouches as a brain cooling device (McConaghy et al., 1995, Baptiste, 1998, Baptiste et al., 2000). They speculated that the guttural pouches might function during selective brain-cooling to maintain the temperature of blood carried by the internal carotid artery below the core temperature during hyperthermia. Conversely, other work defined selective brain cooling as a mechanism of lowering the temperature of the brain below arterial blood temperature (Mitchell et al., 2006) and thus contradicted the idea of the role of the guttural pouches in selective brain cooling in horses. Despite evidence of cranial cooling, brain temperature still increased by about 2.5ºC during exercise, and consistently exceeded carotid temperature by 0.2-0.5ºC. These authors believed that selective brain cooling does not occur in horses and concluded that guttural pouches are not surrogate carotid retes. However, Baptiste (2000) never proposed that the guttural pouch to be a surrogate carotid rete as claimed by Mitchell et.al (2006). Another proposal mooted was that the guttural pouches are closely involved in the physiology of swallowing (Rooney, 1997). Alternative suggested functions of the pouches include pressure equilibration across the tympanic membrane, air warming device, and vocalization resonance chamber as well as a flotation device for the horse (Hardy and Léveilé, 2003, Freeman and Hardy, 2006).

Diseases directly associated with the guttural pouch include mycosis, empyema and tympany. Indirect afflictions of the pouch are otitis media/externa extending to the pouch, temporohyoid osteoarthropathy and rupture of the capitus muscles. Cysts and neoplasia are encountered rarely (Hardy and Léveilé, 2003).

Examination of the guttural pouch is facilitated by external palpation, endoscopy and radiography. Endoscopic examination of the guttural pouches often provides the most useful information regarding guttural pouch disease.

Several surgical approaches can be used to expose the pouch. However, risk of surgical iatrogenic nerve damage and haemorrhage are high due to adjacent important structures surrounding the pouch. The pouch can be drained and exposed with the horse anaesthetised using a number of approaches including; Viborg's triangle, hyovertebrotomy, Whitehouse and modified Whitehouse techniques (Figure 1-3) (Freeman and Hardy, 2006). A standing surgical approach to the guttural pouch is feasible and was described in ten horses with inspissated guttural pouch exudates (Perkins et al., 2006).

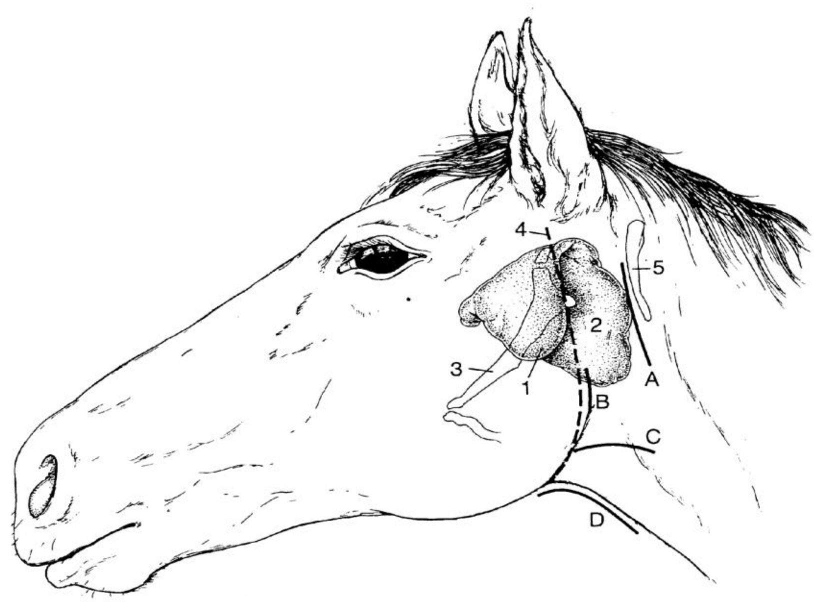

Figure 1-3: Surgical approaches to the guttural pouch.
A, Hyovertebrotomy. B, Viborg's triangle. C, Modified Whitehouse. D, Whitehouse. 1, Lateral compartment. 2, Medial compartment. 3, Stylohyoid bone. 4, Vertical ramus of mandible. 5, Wing of atlas (Reproduced with permission from 'Auer and Stick Equine Surgery', Elsevier).

1.2.2 Neurological Structures Closely Associated with the Guttural Pouch

The guttural pouches of the horse are associated with several important neurological structures; the glossopharyngeal, vagus, hypoglossal and accessory nerves. These nerves are related to the dorsal wall of the pouch of the medial compartment. Conditions affecting the guttural pouch may contribute to neurological dysfunction if these nerves are damaged.

1.2.2.1 Glossopharyngeal nerve

The glossopharyngeal is a mixed nerve, providing sensory and motor fibres to the pharyngeal and laryngeal muscles that control swallowing. The glossopharyngeal nerve is also sensory to the caudal part of the tongue, the palate and the pharynx. This nerve arises from the ventrolateral aspect of the medulla oblongata, where the most rostral rootlets also give origin to the vagus nerve and the medullary part of the accessory nerve (Dyce et al., 1996). The glossopharyngeal nerve runs together with these nerves to the jugular foramen and then bears two small ganglia. The tympanic nerve is the first branch from the ganglia that enters the tympanic cavity and joins the facial and internal carotid nerves to supply the parotid gland. The main branch from the ganglia proceeds to the carotid sinus. The glossopharyngeal nerve then turns rostroventrally and divides into pharyngeal and lingual branches. The lingual branch of the glossopharyngeal nerve is the branch closely associated with conditions affecting the guttural pouch. It is sensory to the mucosa of the caudal part of the tongue, which include the taste buds of this region as well as motor to the levator palatine muscles and the glands of the soft palate. Inflammation of the guttural pouch may lead to damage to this nerve resulting in dysphagia.

1.2.2.2 Vagus Nerve

The vagus nerve is a part of the nerve bundle that passes through the jugular foramen where it bears two small ganglia that lie external to the foramen. Thereafter the vagus runs closely with the glossopharyngeal and the accessory nerve. The vagus then travels caudal and ventral with the accessory nerve in a fold of the guttural pouch. When the vagus and the accessory nerves separate from each other, the hypoglossal nerve passes between them, the vagus nerve then descends along with the internal carotid artery and crosses to the origin of the occipital artery, at its medial face. The vagus nerve is joined by the cervical sympathetic trunk to continue along the common carotid artery in the common sheath, forming the vagosympathetic trunk (Sisson and Grossman, 1975). The most important collateral branch of the vagus associated with the guttural pouch is the pharyngeal branch because it lies closely beneath the mucosa on the floor of the medial compartment of the guttural pouch.

The pharyngeal branch of the vagus nerve is given off at the level of the cranial cervical ganglion, it then runs around the internal carotid artery and travels ventrally and cranially in the medial compartment of the guttural pouch to the dorsal wall of the pharynx. Here the pharyngeal branch of the vagus nerve is concurrent with the pharyngeal branch of the glossopharyngeal nerve, forming the pharyngeal plexus together with filaments of the accessory nerve and the sympathetic nerve. The plexus supplies the muscles of the pharynx and the soft palate. An injury to the vagus nerves result in nasopharyngeal dysfunction and dysphagia, which is sometimes seen in cases of guttural pouch mycosis.

1.2.2.3 Hypoglossal Nerve

The hypoglossal nerve supplies motor innervation to the tongue. It arises from the ventral aspect of the medulla oblongata and passes through the hypoglossal canal and runs ventral and caudal between the guttural pouch and the articulation of the atlanto-occipital capsule (Sisson and Grossman, 1975). The hypoglossal nerve crosses the nerves of the vagus group and continues towards the tongue. Guttural pouch disease may contribute to hypoglossal nerve dysfunction due to its close proximity with the pouch, leading to irreparable lingual paralysis (Kipar and Frese, 1993).

1.2.2.4 Accessory Nerve

The accessory nerve is included in the important nerves associated with the guttural pouch because the spinal branch of the accessory nerve is contained in a fold of mucous membrane along the caudal wall of the medial compartment. This nerve provides motor innervation to the muscles of the neck and the scapula of the horse. Lesions involving this nerve are rare and can be difficult to detect.

1.3 Association of Guttural Pouch Mycosis with Carotid Arterial Tree

The clinical manifestations of guttural pouch mycosis are due to the association of the neurovascular structures with the mycotic infection and the degree of mucosal erosion within the pouches, however, the size of the mycotic lesion is not necessarily associated with the severity of the disease (Cook, 1968a). The condition is characterised by the formation of mycotic plaques on the mucous membrane of the pouch, often on the dorsal portion of the roof of the medial compartment of one pouch (Greet, 1987), but in some cases both pouches can be affected (Cook, 1968a, Freeman and Hardy, 2006). Typically, the lesion is a diphtheritic membrane of variable size and shape composed of necrotic tissue, cell debris, bacteria and fungal mycelia (Cook, 1966) The typical clinical signs related to this disease are epistaxis, dysphagia and nasal discharge. Other reported clinical signs that may accompany the disease are laryngeal hemiplegia, Horner's syndrome, abnormal head extension, head shyness, swelling, pain in the parotid region, and facial paralysis (Cook, 1968a, Church et al., 1986). The most common clinical sign is (mild to severe) epistaxis (Cook, 1968a), which is caused by fungal erosion of the internal carotid artery in most cases (Cook, 1968b).

Mycotic plaques most frequently damage the internal carotid artery which crosses transversely on the dorsocaudal aspect of the medial compartment. Less commonly, the mycotic plaques form on the external carotid or maxillary arteries (Smith and Barber, 1984, Freeman et al., 1989). Untreated epistaxis can result in the death of approximately 50% of horses affected (Cook, 1968a, Lévéille et al., 2000). Epistaxis is usually unilateral from the nostril on the ipsilateral side (Cook, 1968a). Several episodes of epistaxis usually lead to a dramatic fatal epistaxis (Freeman, 2003), but there is no predictable pattern (Hardy and Léveilé, 2003). Most of the time, this epistatic episode occurs spontaneously while the horse is at rest in the stable (Cook, 1966). The haemorrhage from the blood vessels runs into the guttural pouch, from where it flows to the pharynx and out through one or both nostrils.

Sometimes, the guttural pouch may be filled with blood such that it becomes distended and produces a transient dyspnoea and pain around the parotid region.

The second most common clinical sign seen in a horse with guttural pouch mycosis is dysphagia, which may be acute in onset, caused by damage to the pharyngeal branches of the vagus and the glossopharyngeal nerve that may lead to pharyngeal paralysis. Attempts to eat and drink may be difficult as food material, water and discharges are coughed out through the nostrils (Cook, 1966). Abnormal respiratory noise may be accompanied by pharyngeal paresis or laryngeal hemiplegia, where the latter is as a result of recurrent laryngeal nerve damage (Cook, 1968a).

If the cranial cervical ganglion and postganglionic sympathetic fibres are damaged, Horner's syndrome may develop. The horse is susceptible to Horner's syndrome as the cranial cervical ganglion and postganglionic sympathetic fibres are superficial as they pass over the caudodorsal aspect of the guttural pouch, resulting in denervation of these fibres when the pouch is affected by disease (Higgins and Wright, 1995).

Guttural pouch mycosis is considered a relatively rare disease of the horse (Cook, 1966). Yet in 1968, based on his experiences, Cook ranked this disease as the third most common disease of the respiratory tract and the most frequent disease of the guttural pouch (Cook, 1968a). No predilection factors such as age, sex, breed and type of work have been identified for this disease (Cook, 1966, Cook, 1968a, Greet, 1987).

1.3.1 Pathogenesis

At present, the pathogenesis and aetiology of guttural pouch mycosis are not well understood (Cook, 1968b, Lane, 1989, Lepage et al., 2004, Pollock, 2007). *Aspergillus* spp. have been reported as the major organism responsible for this disease formation (Baptiste, 2004, Ludwig et al., 2004), but it is not clear why this ubiquitous respiratory tract commensal organism becomes aggressive. These opportunistic fungi, commonly present in the airways of healthy horses and are also found in soil, decaying vegetation or animal waste. It has been suggested that cases of guttural pouch mycosis tend to arise during the warmer months of the year (Cook, 1968a). On the other hand, it has been postulated that the mycotic infection may occur secondary to aneurysm formation of the affected artery; particularly the internal carotid artery (Colles and Cook, 1983, Greet, 1987, Lévéille et al., 2000).

In terms of definition, an aneurysm is a sac formed by the localised dilatation of the wall of an artery. An aneurysm may form at a degenerated or inflammatory site or at a region where the vessel wall has ruptured partially (Aiello and Mays, 1998, Blood and Studdert, 1999).

Invasion of the mycotic lesion at a very specific anatomical region of the pouch and as already indicated, predisposing factors for mycotic development are still unclear and need further investigation (Lepage et al., 2004). Another study by Lepage (2005), failed to support the hypothesis that an arterial wall defect might be a predisposing factor for guttural pouch mycosis (Colles and Cook, 1983, Greet, 1987, Lévéille et al., 2000) due to the low incidence of aneurysm found in his study. Perhaps the infection weakens the vessel wall leading to aneurysm formation (Lepage, 2005).

1.3.2 Diagnosis

Diagnosis of guttural pouch mycosis is based on history, clinical signs and endoscopy of the pharynx and the guttural pouches. Endoscopically, mucus and blood can be seen draining from the guttural pouch opening, though not in all cases. Usually, the fungal lesion resembles a plaque-like diphtheritic membrane or mass localised on the internal carotid artery in the caudomedial aspect of the pouch. Otherwise, the lesion may be localised at the external carotid artery or maxillary artery in the pouch (Hardy and Léveilé, 2003). Although definitive diagnosis can be reached with the use of modern flexible endoscopes, fatal epistaxis may occur due to the stress of handling of the horse for this procedure (Hardy and Léveilé, 2003). Furthermore, visibility in an affected pouch may be reduced due to the presence of blood. Consequently, after an episode of epistaxis, endoscopic examination may not be rewarding. Extreme care must be taken when introducing the endoscope into the guttural pouch of horses with suspected guttural pouch mycosis so that a blood clot or the fungal plaque does not dislodge and initiate haemorrhage.

In horses with the presenting signs of dysphagia, endoscopic examination of the pharynx reveals persistent dorsal displacement of the palatal arch, presence of saliva and ingesta in the nasopharynx, weak pharyngeal contraction and failure of one or both of the pharyngeal ostia of the guttural pouches to dilate during deglutition (Lane, 1989).

1.3.3 Differential Diagnosis

The most important differential diagnosis for epistaxis originating from the guttural pouch is avulsion of the longus capitis muscle. This condition can also produce acute and profuse epistaxis due to haemorrhage into the guttural pouch (Hardy and Léveilé, 2003). Differentiation of these two conditions can be made on the basis of a history of trauma, endoscopic and radiographic findings, and painful swelling in the region of the throat latch and the parotid.

1.3.4 Treatment

Guttural pouch mycosis is most appropriately treated by surgical intervention if there is haemorrhage as soon as possible. Medical treatment of guttural pouch mycosis, either topically or using systemic antifungal drugs may deliver inconsistent results (Lane, 1989, Speirs et al., 1995).

1.3.5 Surgical Treatment

There are several procedures to occlude the artery or arteries that are involved with guttural pouch mycosis. The goal of occlusion of the internal carotid artery and maxillary artery is to prevent all normograde and retrograde flow of blood from the affected vessel. Earlier attempts at treatment involved surgical removal of the mycotic plaque which sometimes resulted in the rupture of the internal carotid artery followed by death (Johnson et al., 1973, Owen, 1974).

1.3.5.1 Ligation of the arteries

Simple ligation of the internal carotid artery at its origin was described by Owen (1974). Unfortunately, single ligation does not always prevent haemorrhage from the vessel as it is not an end artery. In order to prevent backflow, a double ligation technique of the internal carotid artery was then reported (Owen and McKelvey, 1979). The site for double ligation of the internal carotid artery is immediately distal to its origin (cardiac side), which is outwith the guttural pouch, using an approach that is similar to the hyovertebrotomy approach but more ventral (Figure 1-3). The cardiac side of the internal carotid artery is identified at the occipital artery and deep to that artery. As for the cranial side, the ligation is placed distal to the lesion at the guttural pouch. However, this is technically difficult as the artery must be ligated deep within the guttural pouch, and often the artery is obscured by the mycotic lesion making the risk of fatal haemorrhage high. Due to the high complication rate and degree of difficulty performing this technique, this approach to treatment has largely been abandoned (Hardy and Léveilé, 2003).

1.3.5.2 Balloon catheter occlusion of the internal carotid artery

As the majority of cases of guttural pouch mycosis involved the internal carotid artery, the balloon catheter occlusion technique was developed to overcome the problems of double ligation of this artery (Freeman and Donawick, 1980a). The goal of balloon catheter occlusion was for immediate intravascular occlusion and prevention of retrograde blood flow from the cerebral arterial circle. The internal carotid artery is ligated close to its origin and an arteriotomy is done distal to the ligature. A balloon-tipped catheter is introduced into the lumen of the artery through the arteriotomy site, adjacent to the first ligature. The balloon catheter is inserted for a distance of approximately 13cm (Freeman and Donawick, 1980a). At this distance, the balloon tip of the catheter will be resting at the sigmoid flexure of the internal carotid artery, within the venous sinuses and anticardiac to the mycotic lesion (Freeman and Donawick, 1980a, Freeman and Hardy, 2006). The balloon is inflated with sterile saline and fixed in position by a ligation distal to the arteriotomy site. After a period of 10-14 days, during which time the artery leading to the cerebral arterial circle has been thrombosed, the catheter is withdrawn during a second procedure.

Reported complications associated with the balloon catheter occlusion technique in the internal carotid artery include: Horner's syndrome; excess incisional swelling; catheter displacement into the lumen of guttural pouch and post operative epistaxis (Freeman and Donawick, 1980a, Freeman and Donawick, 1980b, Greet, 1987, Freeman et al., 1993). Differentiation between internal carotid artery and occipital artery may be difficult in some horses, especially those with thick throatlatch or where the internal and occipital arteries share a common origin from the common carotid artery.

1.3.5.3 Balloon catheter occlusion of the external carotid artery and its branches

As cases of guttural pouch mycosis also involved the external carotid artery and its branches, attempts to occlude this artery using a single balloon catheter occlusion technique have been described. However, the tip of the catheter easily enters the superficial temporal artery, instead of the maxillary artery (Caron et al., 1987, Freeman et al., 1989). Severe haemorrhage was then identified originating from the maxillary artery, cranial to the site of catheterisation and ligation. In order to overcome this retrograde flow from the collateral channels, the external carotid and maxillary arteries must be occluded on both sides of the mycotic lesion (Freeman et al., 1989). Another improved technique was developed, where the external carotid artery is ligated after the linguofacial trunk. To facilitate this, a catheter is inserted in retrograde fashion into the major palatine artery for approximately 40-42 cm in a 450-kg horse or up to the level of the articular tubercle of the temporal bone. The balloon is inflated partly and retracted gently until some resistance is encountered. At the point of resistance, the balloon should be resting at the caudal alar foramen (Freeman et al., 1989).

Another alternative to ligation of the external carotid artery is the occlusion of the external carotid artery by a balloon catheter. The balloon-tipped catheter can be inserted through the transverse facial artery and inflated distal to the linguofacial trunk. This procedure has been effective and does not cause blindness, even in combination with internal carotid artery occlusion (Freeman et al., 1989). However, the risk of blindness still exists.

1.3.5.4 Detachable balloon catheter system

A detachable balloon catheter system has been described to occlude the internal carotid artery using a detachable, self-sealing, latex balloon (Cheramie et al., 1999). A balloon delivery system is introduced into the internal carotid artery near its origin and advanced until resistance is met or approximately for a distance of 13cm. At this point, the balloon should be located at the proximal bend or between the proximal and distal bends of the sigmoid flexure of the internal carotid artery (Freeman and Donawick, 1980a). With the aid of angiography, occlusion of aberrant vessels of the internal carotid artery can also be made possible with this technique.

Once the delivery system is positioned appropriately, the balloon is inflated and then released. The carrier and the guiding catheter of the system are then withdrawn from the internal carotid artery. As the balloon is inflated, it will immediately occlude the vessel and subsequently a thrombus will form (Cheramie et al., 1999).

1.3.5.5 Transarterial coil embolisation

The transarterial coil embolisation (TCE) technique is the most effective and rapid procedure for the prevention of haemorrhage as a result of guttural pouch mycosis. This technique can selectively and precisely occlude the arterial segment affected by the mycotic plaque under fluoroscopic guidance (Matsuda et al., 1999, Lévéille et al., 2000, Lepage, 2005). This technique is facilitated by angiographic imaging of the affected vessels, identification of any aberrant branches and or specific sites of bleeding (Lévéille et al., 2000). Although the technique is similar to the balloon catheter occlusion technique, it is less invasive and requires shorter anaesthetic time.

The tornado-like shape of the coil allows it to be inserted smoothly even in the presence of active bleeding (Lévéille et al., 2000). Upon insertion of the coil, the vessel is occluded within minutes (Matsuda et al., 1999, Lévéille et al., 2000). Multiple embolisations of the internal carotid, external carotid and maxillary arteries have been shown to be effective using this technique (Lévéille et al., 2000). The disadvantage with this technique is that a fluoroscopic machine and other specialised equipment and personnel trained in their use are required.

1.3.6 Medical Treatment

In cases where the owners refuse surgical intervention, medical management may be attempted, provided that the mycotic lesion is not located on major blood vessels or nerves (Carmalt and Baptiste, 2004), and there is less risk of bleeding. Medical treatment of guttural pouch mycosis is generally slow, inconsistent and may take months to resolve depending on the size of the mycotic plaque (Hardy and Léveilé, 2003).

Direct lavage of the fungal lesion and topical medication can be achieved by placing a Foley catheter through the guttural pouch opening with the aid of an endoscope (Carmalt and Baptiste, 2004). However, topical treatment may be difficult as the lesion can be located more dorsally and is always covered by a diphtheritic membrane and necrotic debris causing poor penetration of antifungal solution. Antifungal solutions such as natamycin solution (Greet, 1987, Caron et al., 1987), nystatin powder (Church et al., 1986), thiabendazole (Smith and Barber, 1984, Caron et al., 1987), aqueous iodine solution, gentian violet, neomycin (Freeman and Donawick, 1980a) and enilconazole (Carmalt and Baptiste, 2004) have been used to macerate the mycotic membrane. However, topical application of concentrated iodine based solution has been reported to cause severe inflammation and necrosis of the mucosa lining of the guttural pouch (Wilson, 1985, Sherlock et al., 2007).

Parenteral administration of antifungal agents such as amphotericin B, natamycin or combination of natamycin-nystatin has been used before (Caron et al., 1987). However, the penetration of these drugs into the pathologic tissue is uncertain (Caron et al., 1987). In addition, the use of amphotericin B in horses is always limited by its nephrotoxicity, phlebotic reaction and high cost of treatment. Furthermore, if the fungal plaque is located over an artery, the risk of bleeding is not reduced during medical treatment (Hardy and Léveilé, 2003).

1.3.7 Prognosis

Approximately 50% of horses with clinical signs of epistaxis die from guttural pouch mycosis if left untreated (Cook, 1968a). Occlusion of the affected arteries must be performed as soon as possible after the first episode of epistaxis to prevent subsequent episodes of bleeding. Whilst the goals of successful occlusion of affected vessels, cessation of haemorrhage and resolution of fungal plaque without any other treatment in about 30-60 days, this may not occur in all cases. However, the involvement of cranial nerve deficits with neurological signs can persist. Horses with grade III laryngeal hemiplegia may recover, but horses with grade IV laryngeal hemiplegia may need a laryngoplasty. Dysphagic horses may recover over time.

1.4 Imaging of the Carotid Arterial Tree

1.4.1 Angiography

Angiography is a technique to visualise blood vessels by the injection of a positive contrast material into a vessel during radiography, which opacifies the target vessels (Armstrong et al., 2009). It is used commonly for the diagnosis of cardiovascular, cerebrovascular and peripheral vascular disease. The radiographic image of the lumen of the blood vessel is called an angiograph or more commonly an angiogram.

The technique of angiography was first developed and introduced in 1927 by a Portuguese physician and neurologist, Egas Moniz (Antunes, 1974). Even though the images are considered extremely primitive by today's standard, it took Moniz nine attempts on human patients to obtain a successful study that confirmed a clinical diagnosis (Antunes, 1974).

There are different types of angiography based on the underlying technologies used and these include catheter angiography, subtraction and digital subtraction angiography, computed tomography angiography and magnetic resonance angiography. Catheter angiography is the oldest method. This method involved the introduction of a catheter into a blood vessel feeding, or draining to, a region of interest. Once the catheter was established in the vessel, contrast material was injected to highlight the lumen and conventional radiographs obtained. One of the problems of interpretation of smaller vessels and their course was, and is, that superimposition of tissues of higher or lower attenuation could obscure the vessels and any lesions present. In an attempt to overcome this problem, subtraction angiography was developed where a scout film was obtained and processed as a *reversed* film (mask image). The subsequent contrast film was overlain with the reversed film. The two films had a third unexposed film laid on top and a strong uniform light was transmitted through the reversed and contrast films. Once processed, the third film now only showed the contrast in the vessels as the other opacities were cancelled out (Clemmons, 1976, Ort et al., 1977).

Whilst producing very interpretable films, these subtraction techniques initially produced single images and could not be obtained in real-time. Often multiple images to actually follow the contrast as it was injected were desired and rapid film changers were used (Clemmons, 1976). By altering the settings, a predetermined number of films could be obtained at predetermined intervals. The other method was to link a fluoroscopy unit to a cine-film camera (cine-fluoroscopy). Unfortunately, although the latter produced a movie of the contrast injection, the results were not available in real-time as the cine-film had to be sent for development and processing (Ort et al., 1977). The invention of the video camera and recorder did allow movies to be acquired and viewed in real-time (videofluoroscopy) (Shinozaki et al., 1970).

Over time, the development and availability of reasonably sized powerful computers allowed the introduction of digital subtraction angiography. Conventional subtraction angiography in carotid angiography using cut-film technique and plate changer became outmoded (Dean, 1996).

Further advances related to the use of catheter angiography was the addition of rotational angiography with 3D image reconstruction in human (Bosanac et al., 1998, Heautot et al., 1998, Grass et al., 1999, Elgersma et al., 1999, Anxionnat et al., 2001, Hochmuth et al., 2002, Hirai et al., 2003, Hyde et al., 2004, Pedicelli et al., 2007, McKinney et al., 2008, Van Rooij et al., 2008). Rotational angiographic technique, either with subtracted image (3D digital subtraction angiography) or non subtracted image (3D rotational angiography) has started to replace intra arterial 2D digital subtraction angiography technique because this technique only provides a limited number of views.

The 3D digital subtraction angiography is now considered a gold standard for cerebral imaging, particularly in detecting cerebral aneurysms (Bosanac et al., 1998, Anxionnat et al., 2001). It requires a rotating C-arm while acquiring data. Subtraction mask images were acquired at the initial rotational projections. After rotational projections were completed, 3D digital subtraction images were reconstructed from rotational sequences (Anxionnat et al., 2001, Van Rooij et al., 2008). With multiplanar data acquisition, it allows the assessment of significant vascular disease in multiple projections. A more recent modality of 3D rotational angiography was claimed to be the new gold standard in cerebral imaging without the need for preceding mask images for subtraction image (Van Rooij et al., 2008).

Non invasive advances in imaging such as the magnetic resonance angiography and computed tomography angiography have started to be considered to replace the role of catheter angiography because the technique of catheter angiography are invasive (require a catheter to be inserted into a vessel), time consuming and may not suitable for critically ill patients (Bederson et al., 2009).

Computed tomography angiography (CTA) is a non invasive volumetric imaging technique that uses a rapid intravenous injection of iodinated contrast with image acquisition during arterial filling phase in the region of interest. Image acquisition is rapid and CTA data can be viewed from unlimited projections in both 2D and 3D modes. This technique can be used to supplement information obtained by catheter angiography. Over the past 10-12 years, computed tomography has evolved from single section computed tomography, to four multi section, to 16 multi section and currently to 64 multi section computed tomography (McKinney et al., 2008, Menke et al., 2011). The trend is toward 128 and more detector rows (Menke et al., 2011). Multi detector computed tomography is generally known to be more accurate than single detector computed tomography.

Magnetic resonance angiography uses flow-compensated 3D gradient echo sequences and post processing software to compute images of the blood vessels within the 3D data set (Schuierer et al., 1992, Anzalone et al., 1995). Magnetic resonance angiography does not require iodinated contrast and ionizing radiation, thus maybe helpful in the evaluation of pregnant patients. Primary advantage of magnetic resonance angiography is that it can provide thin (sub mm thickness) source image that can be viewed using 2D and 3D modes (Kouskouras et al., 2004).

1.4.2 Other methods

Other modality that can be use for imaging of carotid and cerebral artery is Doppler ultrasonography. It is used to investigate blood flow velocity, pattern and amplitude and it is also a common imaging examination to aid in the diagnosis of carotid disease in human (Grant et al., 2003). Ultrasonography technique is safe, quick and inexpensive.

1.5 Aim of Study

Due to increasing clinical interest and the potentially dramatic course of guttural pouch mycosis related to surgical treatment options, more studies are needed, specifically investigating the anatomy of the arteries associated with the guttural pouch in Equidae without overt guttural pouch disease. This study will focus on the anatomy of the carotid trifurcation and the course of the internal carotid artery in Equidae (horse, donkey and zebra), using rotational angiography and arterial latex casting techniques.

2 ANGIOGRAPHIC VARIATION OF THE CAROTID TRIFURCATION AND THE INTERNAL CAROTID ARTERY IN HORSES

2.1 General Introduction

As previously mentioned, angiography is an imaging technique to visualise blood vessels. Apart from its use to observe the carotid and cerebral vessels, angiography has also been used to study the vasculature of the distal limb of a horse (Scott et al., 1976, Rosenstein et al., 2000).

2.1.1 Carotid Angiography in Equine

Carotid and cerebral vascular imaging of horses is performed generally using conventional angiographic techniques where the horse is positioned in lateral recumbency with the head on the X-ray cassette or plate changer (Colles and Cook, 1983) or alternatively using an image intensifier (fluoroscope) (Lévéille et al., 2000). Several radiographic views are taken by changing the position of the X-ray generator manually. A percutaneous technique (Cook, 1973) or a cutdown technique (Colles and Cook, 1983) can be used for the catheterisation of the common carotid artery. For carotid angiography, the lateral view is much preferred compared to a dorsoventral angiogram, as the latter is of limited diagnostic value because the carotid tree is obscured by the superimposed mandibles (Colles and Cook, 1983). As for cerebral angiography, both lateral and dorsoventral view are required (Colles and Cook, 1983). During surgical treatment of horses with guttural pouch mycosis, carotid angiography has been shown to aid the identification of the correct vessel for occlusion (Macdonald et al., 1999), and as an aid for surgeons in the occlusion of appropriate arteries.

Based on several angiographic studies conducted by Colles and Cook (1983), there was no evidence of significant adverse side effects to carotid or cerebral angiography in horses. The only complication reported in carotid and cerebral angiography in horses was the formation of a thrombus during the cannulation of an artery. However, it has been suggested that using a smaller cannula with a pressure injector may prevent thrombosis formation in the blood vessel (Colles and Cook, 1983).

Angiographic interpretation was found to be difficult if the vessel failed to fill with the contrast material, especially the internal carotid artery and occipital artery (Colles and Cook, 1983, Macdonald et al., 1999). This problem may have been due to several causes; inadequate volume of contrast medium, slow injection of contrast medium, spasm of the artery, thrombosis of vessels, or external pressure on the vessel wall (Colles and Cook, 1983).

The common or standard gross anatomy of the internal carotid artery has been described, and this must be understood to recognise and distinguish the various vessels seen angiographically. The extracranial pathway of the internal carotid artery started from the carotid trifurcation where the internal carotid artery originates caudal and ventral to the occipital artery and runs on the dorsal surface of the medial compartment of the guttural pouch. Then the internal carotid artery pierces the foramen lacerum to continue its pathway intracranially. It passes through the ventral petrosal sinus and enters the venous cavernous sinus where the internal carotid artery forms a sigmoid flexure. After the sigmoid flexure, the internal carotid artery gives rise to the caudal intercarotid and caudal communicating arteries. Then the internal carotid artery continues for a short distance rostrally to terminate as the rostral and middle cerebral arteries (Nanda, 1975, Nanda and Getty, 1975).

The internal carotid artery contributes to the formation of the cerebral arterial circle as the caudal communicating artery joins the basilar artery and contributes to the formation of the lateral and caudolateral quadrants cerebral arterial circle. As for the rostrolateral quadrants of the cerebral arterial circle, these are formed by the union of the rostral cerebral artery with the contralateral.

Angiographic anatomy of the common pattern of the internal carotid artery of horses was described as an un-branched vessel for its course along the lining of the guttural pouch (Colles and Cook, 1983). Consequently, the common angiographic appearance of the internal carotid artery should be that of a curving vessel that does not branch before it enters the cranium via the foramen lacerum, whereupon it shows a marked sigmoid flexure. Immediately after this flexure, the internal carotid artery connects with the contralateral side via the intercarotid artery and forms a part of the cerebral arterial circle (circle of Willis) (Colles and Cook, 1983).

An aberrant branch that arises from the internal carotid artery has been reported in a horse that had severe epistaxis as a result of guttural pouch mycosis (Freeman et al., 1993). In an angiographic study conducted by Colles and Cook (1983), five horses out of thirty seven were found to have bifurcated internal carotid artery on one side of the head. Three of these five horses demonstrated an aneurysm on what they concluded was an abnormal branch of the internal carotid artery, rather than the internal carotid where 15 horses were found to have aneurysms. These three horses were also reported to be affected by guttural pouch mycosis. Greet (1987) also described aneurysm formation (based on angiography) in eight out of ten horses that were affected with guttural pouch mycosis. A more recent publication (Lévéille et al., 2000), reported that two horses, which presented with guttural pouch mycosis, were found on angiography to have an aneurysm on the rostral segment of the internal carotid artery. As far as can be determined only Colles and Cook (1983) appear to have reported multiple aneurysms in individual horses (4/18).

Four healthy horses with unilateral aberrant branching of the internal carotid artery, on the basis of endoscopic investigation have also been reported. Post mortem examination of one of these horses showed that the abnormal branch passed through the caudal portion of the foramen lacerum and united with the basilar artery (Colles and Cook, 1983). This finding was corroborated (Freeman et al., 1993), where the aberrant branch of internal carotid artery joined the basilar artery beneath the pons. This is the usual site of union between the basilar and caroticobasilar arteries (Nanda and Getty, 1975, Freeman et al., 1993). Typically, the caroticobasilar artery is given off from the second curve of the sigmoid flexure of the internal carotid artery and unites with the basilar artery beneath the pons. It is believed that this aberrant branch of the internal carotid artery was an abnormal form of the caroticobasilar artery (Freeman et al., 1993).

2.1.2 Embryonic Development of the Internal Carotid Artery

Knowledge of the embryonic development of the internal carotid artery in early foetal life provides a basis for understanding anatomic variations, particularly aberrant branches. The formation of the embryological aortic arches is the initial point in the genesis of the great arteries and their offshoots.

The branchial arches (also known as the pharyngeal arches) are an embryologic entity that create the gills of fish, and were described in the human foetus as the embryological precursor to multiple structures of the head and neck (Congdon, 1922). Even though the development of the branchial arches resembles the formation of gills in fish and amphibians, in the human embryo real gills (branchia) are never formed, and thus they are more appropriately termed pharyngeal, rather than branchial arches (Sadler, 1995, Larsen, 2001). Pharyngeal arches are covered externally by the ectoderm lined pharyngeal clefts, and internally by endoderm lined pharyngeal pouches. Each arch has its own cartilage, nerve, muscle and artery. The embryonic development of the pharyngeal system produces six pairs of embryonic aortic arches (also known as branchial/pharyngeal arch arteries), but the development of these arches are not all complete or present at any given moment during embryonic development (Congdon, 1922).

The embryonic development has been described extensively in humans. Early embryonic studies in man were performed by Congdon (1922) and Padget (1948) and re-interpretations to simplify the understanding of human embryonic development are based largely on their excellent work (Barry, 1951, Silbergleit et al., 2000, Larsen, 2001, Okohara et al., 2002). Thus, the general embryologic review of the aortic arches presented here is, perforce, largely based on the work in man.

In the early embryo, when the aortic arches are first forming, the blood is pumped from the heart into an undivided truncus arteriosus, which ends in a dilatation, termed the aortic sac. In general, the aortic arches come from this sac. During development, the truncus arteriosus divides into aortic and pulmonary channels. The aortic sac extends laterally to the right and left so that aortic arches on either side appear to arise from horns (Congdon, 1922). Other workers use the term ***ventral aortic root*** to represent the extension of the aortic sac onto the left and right side (Barry, 1951, Vitums, 1951, Vitums, 1969).

In man, the first arch is formed between day 22 and day 24 (embryos averaging 1.3mm in length from crown to rump) and gives rise to a mandibular artery that later regresses just as the fourth arch become recognisable (Congdon, 1922). The second aortic arch arises by day 26 (embryo is now approximately 3-4mm in length from crown to rump) and grows to become the hyoid artery that gives rise to the stapedial artery, which passes through the ring of stapes. The mandibular and hyoid arteries become branches of the third arch when the first and second arches disappear. On day 28, the third and fourth arches appear (4mm embryo length from crown to rump). The third arch grows to form the common carotid arteries and the proximal portion of the internal carotid arteries. The third aortic arch goes on to combine with the distal segments of the paired dorsal aortae to complete the full length of the internal carotid arteries (Congdon, 1922). Later, the embryonic internal carotid artery uncoils as the paired dorsal aortae descend into the chest so that the internal carotid arteries are able to become straight vessels in the neck (Okohara et al., 2002). Then, the right and left external carotid arteries sprout from the common carotids (Larsen, 2001). The left fourth aortic arch retains its connection to the dorsal aortae and contributes to the adult aortic arch, while the right side forms the proximal portion of the right subclavian artery. The embryology of the lower aortic arches (aortic arches fifth and six) is not important to the development of the internal carotid artery so is considered outwith the scope of this review.

Embryonic development of the aortic arches in the horse was described by Vitums (1951, 1969). Six pairs of aortic arches were observed in the first period of embryonic development where the aortic arches originate from the ventral aortic root. The first two pairs of aortic arches were noted to regress very early, and at a later stage of embryonic development (when the truncus arteriosus divides into the aortic and pulmonary channels) the fifth aortic arches appeared in a vestigial form. At about 21 days of gestation (equine embryos averaging 5mm in length from crown to rump) the first and second aortic arches originate from the ventral aortic root. At this stage, the third aortic arch was just appearing. The third arch will grow to form the proximal portion of the right and left internal carotid arteries. As for the distal portion of the internal carotid arteries, these are derived from the cranial extensions of the dorsal aortae. This finding in the equine embryo by Vitums (1969) is in agreement with the observation in human embryo by Barry (1951) but disagrees with the conclusion in the human embryo drawn by Congdon (1922) (where in the human embryo it was described that the third aortic arch grows to combine with the paired dorsal aortae).

Vitums (1969) further described that at about 34-35 days of gestation (embryos averaging 14-15.5mm in length from crown to rump) the segments of the aortic arch system in the horse are incorporated in the formation of the definitive adult aortic arch where three vessels; the innominate artery (which later will be known as brachiocephalic artery), the left common carotid artery and the left subclavian artery appear. This arrangement of vessels was regarded as the primitive mammalian pattern (Vitums, 1969). Then at about 36-37 days of gestation (embryos averaging 14.5-16.5mm in length from crown to rump), the proximal part of the left common carotid artery and the innominate artery (caudal part) join together to form a common vessel known as the brachiocephalic artery. The right common carotid artery originates from the innominate artery and runs craniad along the trachea.

It should be mentioned here that in human, aging of an embryo was based on information of time of ovulation, post-coital staging, menstrual age as well as the size of the embryo (Nishimura et al., 1974, Skidmore, 1976). However, in the work described by Vitums (1969) he stressed that the estimated aging of equine embryos used in his study was mainly determined by the crown rump length and the general development of the embryo compared with similar developmental stages reported in previous work (Ewart, 1915, Vitums, 1951).

Turning to aberrant branches of the internal carotid artery, these have also been reported in human (Altman, 1947, Paullus et al., 1977, Silbergleit et al., 2000, Okohara et al., 2002). Two aberrant branches of the internal carotid arteries have been reported to arise from the petrous portion of this artery; (i) Persistent stapedial artery and (ii) Vidian artery. Petrous aberrant branches of the internal carotid artery are important during occlusion of the internal carotid artery because the aberrant branches provide a channel for retrograde blood flow into this artery.

In relation to the presence of an aberrant branch of internal carotid artery in the adult human, the persistent stapedial artery and the vidian artery development have been described. The stapedial artery is present at four to five weeks of normal foetal development (crown to rump length 4-8mm) where it arises from the hyoid artery near its origin from the proximal internal carotid artery (third aortic arch). At a stage during embryonic development (when the hyoid and mandibular became branches of the third aortic arch) the stapedial artery was the parent vessel for the middle meningeal artery and part of the external carotid artery. Later, the stapedial artery involutes, the middle meningeal and external carotid arteries lose their connection with the petrous part of the internal carotid artery and are instead fed by the internal maxillary artery (Padget, 1948, Paullus et al., 1977). However, when the stapedial artery persists into postnatal life, the middle meningeal artery would be supplied by the persistent stapedial artery (Padget, 1948, Silbergleit et al., 2000). Clinically, the persistent stapedial artery presents as a pulsatile middle ear mass, or is found incidentally during middle ear surgery, or as an incidental finding as a result of diagnostic imaging (Silbergleit et al., 2000). The presence of this artery is also known to complicate stapedectomy and cholesteatoma resection, and prevent cochlea implantation (Silbergleit et al., 2000).

The vidian artery (the artery of the pterygoid canal) usually arises from the external carotid artery, but it may also originate from the petrous part of internal carotid artery and pass into pterygoid canal anastomosing with the maxillary artery.

During embryonic development, if the mandibular artery regresses normally, the vidian artery will arise from the maxillary artery. However, if the mandibular artery fails to regress, the vidian artery will arise directly from the petrous portion of internal carotid artery. The importance of this vessel arises in patients with intractable epistaxis. During maxillary artery ligation, retrograde filling of the distal maxillary and sphenopalatine arteries may occur if the vidian artery arising from the internal carotid artery is not obliterated (Paullus et al., 1977, Okohara et al., 2002).

An understanding of embryonic development of the human is well established. In relation to the presence of aberrant branches of the internal carotid artery, the embryonic development is also well documented in man. However, in the horse the literature on embryonic development is limited. More embryological studies of the internal carotid artery in Equidae are warranted in order to relate the embryonic development of the internal carotid artery to variations in branching, including aberrant vessels.

A study was designed with two objectives: (i) to define and record the anatomy of the carotid trifurcation and the internal carotid artery in horses using 3D angiographic imaging, and (ii) to determine the variation of the carotid trifurcation and the internal carotid artery between individual horses.

2.2 Materials and Methods

The head and necks of 50 horse cadavers were accumulated over time. Selection of heads included horses of mixed breed, age, sex and use presented to the post mortem room at the University of Glasgow, School of Veterinary Medicine for reasons unrelated to disease of the guttural pouch. Horses were either euthanised or died due to natural causes. Signalment data were not recorded during collection of the specimens. The specimens came from variety of sources where data would be incomplete or unavailable. Thus, any resulting data set would be flawed due to its inadequacy. However, no specimens originated from foals or foetuses.

Ethical approval for the study was granted by the School of Veterinary Medicine Ethics and Welfare Committee and consent was obtained for the use of the cadaver material.

2.2.1 Specimen Preparation

The specimen used in this study were not injected with heparin prior to death, thus blood clotting in the vessels at post mortem was to be expected. Upon arrival of the horse specimen, the head and necks were disarticulated from the body at the level of the 3rd and 4th cervical vertebrae ensuring that the guttural pouch and the carotid trifurcation remained intact, and to allow drainage of non clotted blood. The common carotid arteries were identified from the disarticulated region of the neck, thus making identification and catheterisation of these arteries much easier and straight forward. Then, both common carotid arteries were catheterised by advancing a 16Fr male Foley catheter into each common carotid artery for about 5-10cm. The balloon on the tip of the catheter was inflated with 1-2 ml of water and a ligature suture was placed caudal to the balloon to prevent the catheter from slipping out of the artery. These catheters were left in place for both the angiographic procedure and arterial latex casting.

The arterial system were flushed with water using a manual garden pump via a catheter placed in the common carotid artery until no resistance was met and water could be seen flowing from the contralateral common carotid artery (via the Foley catheter) to ensure that all the clotted blood in the arteries were removed. Then, the heads were stored in the freezer at -20ºC, until the procedures were to be performed. The heads were thawed for 3-4 days before angiographic studies were commenced. Prior to angiography, the patency of the arterial system was verified by flushing warm water into the common carotid artery until flow could be seen on the contralateral common carotid artery.

2.2.2 Carotid and Cerebral Vascular Angiography Using Conventional Method (Manual Setting)

Conventional method of angiography of the carotid trifurcation and the internal carotid was carried out in the first seven horse specimens using a Ziehm Vario 3D mobile fluoroscopic machine equipped with a C-arm unit by manual setting the machine (Figure 2-1).

Prior to angiography, the head was placed in left lateral recumbency on a board with two stands to support the weight of the specimen. To extend the guttural pouch, the head was pulled cranially from the neck.

The stand used for this experimental work was purposely designed to be used with the C-arm unit. Utilising this stand, the specimen was positioned between the X-ray generator and the image intensifier (Figure 2-2). Then, a laser positioning beam was directed at the centre of the region cranial to the wing of atlas, ventral to the ear and caudal to the vertical ramus of mandible. The laser positioning device aided in aligning and positioning of the C-arm to the exact region of interest. Then, a plain radiograph (scout radiograph) was taken to ensure correct positioning of the C-arm over the region of the guttural pouch.

After correct positioning of the specimen, approximately, 25-30ml of contrast material (Barium sulphate[1]) was injected to fill the left side of the carotid tree to the level of the internal carotid artery in the cranium. A further 25-30ml contrast material was injected to allow filling into the cerebral vessels and the contralateral carotid arterial tree. After injection of contrast, the Foley catheters on both sides were clamped to prevent leakage of the contrast agent during image acquisition.

Angiographic images of the carotid arterial tree were obtained immediately after the ipsilateral injection of the contrast material. Several lateral, oblique and dorsoventral views of the carotid and cerebral vessels were taken by manually adjusting the angulation of the C-arm.

[1] Baritop® 100, Sakai Chemical Industry Company Ltd

However, sometimes the contrast material did not flow readily into the contralateral side. If such a situation arose contrast material was injected directly into the contralateral common carotid artery, and gas could accumulate along the path of the carotid arterial tree. Injection of contrast directly into right side proved to be easier than persisting with additional contrast injection from the left. If gas was seen to accumulate along the path of the arterial tree, more contrast material (another 25-30ml) was needed to flush the gas from the important structures. Then, image acquisitions were repeated. At the end of conventional angiographic procedures and image acquisition, the contrast material was flushed out with tap water using the manual garden pump (via the catheter) in order to prepare the specimens for arterial latex casting technique.

Figure 2-1: The Ziehm Vario 3D fluoroscopic machine.

Figure 2-2: Setup of fluoroscopic machine and the specimen.

2.2.3 Carotid and Cerebral Vascular Angiography Using Rotational Angiography

Rotational method of angiography of the carotid trifurcation and the internal carotid was carried out in 43 horse specimens using a Ziehm Vario 3D mobile fluoroscopic machine equipped with a C-arm unit. Prior to angiography, the head was placed in left lateral recumbency on a board with two stands to support the weight of the specimen. To extend the guttural pouch, the head was pulled cranially from the neck.

The same stands for the previous angiographic work were used with the C-arm unit. Using the stands, the specimen was positioned between the X-ray generator and the image intensifier. Then, a laser positioning beam was directed at the centre of the region cranial to the wing of atlas, ventral to the ear and caudal to the vertical ramus of mandible. The laser positioning device aided in aligning and positioning of the C-arm on the region of interest. Then, a plain radiograph was taken to ensure the correct positioning of the C-arm at the region of the guttural pouch.

After correct positioning of the specimen, approximately, 25-30 ml of contrast material (Barium sulphate) was injected to fill the left side of the carotid tree to the level of the internal carotid artery in the cranium. Another 25-30 ml of contrast material was injected in to allow filling into the cerebral vessels and the contralateral carotid arterial tree. After injection of contrast, the Foley catheter on both side were clamped to prevent leakage of the contrast agent during image acquisition. Then, three ball bearing markers were placed in a triangular configuration at the right lateral side of the carotid trifurcation to mark or identify the right carotid arterial tree from the left side during rotational angiographic analysis.

Automatic rotational scanning was initiated by activating the Iso-Cine (for Cine-Loop function) and 3D operating modes (for 3D-multiplanar reconstruction). Step by step protocols on Iso-Cine mode of the Ziehm Vario 3D fluoroscopic unit were followed according to the equipment instruction manual (Ziehm, 2007).

In small horse heads, a single automatic scan rotational angiogram was enough to visualise the carotid trifurcation, internal carotid artery and the cerebral vessels with good quality images in a single frame. However, in larger horses, two cycles of automatic scanning were required. The reason to this was the distance of the carotid trifurcation to the cerebral arterial circle was much larger and could not be contained in a single frame. Thus, the first rotational scan was centred for the carotid trifurcation region, and the second centred more craniodorsally to image the internal carotid artery as it contributes to the formation of the cerebral arterial circle. Typically, the laser centring beam for the second set was directed at the level of the petrous temporal bone and ventral to the cranium.

The C-arm movement was motor-driven and could be controlled using a foot switch, which also controlled the exposures. Each scan took approximately two minutes for the C-arm to complete a 136° angle of rotation. With each cycle of automatic scanning, 112 sequences of radiographic images were captured at different angles and these images could be played like a movie using the Cine-Loop function. A Cine-Loop function consisted of multiple or several fluoroscopic images that are acquired in sequence. It could be played like a movie and could also be post edited.

At the end of rotational angiographic procedures and image acquisition, the contrast material was flushed out with tap water using the manual garden pump in order to prepare the specimens for arterial latex casting technique.

2.2.3.1 Three dimensional multiplanar reconstruction

After acquisition of the rotational angiographic images, 3D multiplanar reconstruction (3D-MPR) images of the subject were generated on the fluoroscopic unit computer system. Multi-planar reconstruction (MPR) was launched by pressing the 3D-MPR button after the completion of an automatic scan to produce a 3D representation of the vessels. Once the 3D reconstruction was activated, the 3D volume view, as well as the related slice views, were displayed as four quadrants images. These 3D views are generated by means of an algebraic reconstruction algorithm where the system uses the images of a scan captured with relation to a predefined scan centre to compute the 3D representation of an object.

The object on the 3D volume view could be moved and viewed from all sides using the 6D mouse on the computer attached to the fluoroscopy unit. The axes on each slice view could be shifted or rotated by moving the cursor on one of the axes on the particular quadrants so that observations on different levels of each slice could be appreciated. To reach optimum representation, the contrast and brightness of the 3D-MPR were adjusted. All horses used for 3D imaging also had 3D-MPR images taken as screenshots. Step by step protocols for the 3D-MPR mode of the Ziehm Vario 3D fluoroscopic unit were followed using the equipment instruction manual (Ziehm, 2007).

2.3 Results

2.3.1 Angiographic Variations of the Internal Carotid Artery in Horses

In this study, a common/standard angiogram of the internal carotid artery was determined to be an un-branching curving artery prior to it entering the cranium (Figure 2-3). The borders of the guttural pouches were seen as superimposed radiolucent margins, triangular in shape and located above the pharynx at the caudal region of the skull, ventral to the basisphenoid bone. After entering the cranium, the internal carotid artery formed the S-shaped curve, which is also known as the sigmoid flexure of the internal carotid artery. This artery communicated with the contralateral side via the intercarotid artery (Figure 2-4). Then the internal carotid arteries of both sides continued rostrad to give off the caudal communicating artery, which turned caudal to join the basilar artery resulting in the formation of the lateral and caudolateral quadrants of the cerebral arterial circle. After giving off the caudal communicating artery, the internal carotid arteries continued rostrally for a short distance and terminated at the rostral and middle cerebral arteries. The rostral cerebral artery united with the contralateral artery, and formed the rostrolateral quadrants of the cerebral arterial circle. Sometimes, immediately after the second curve of the sigmoid flexure of the internal carotid artery, a caroticobasilar artery could arise, either unilaterally as shown in Figure 2-5 or bilaterally as shown in Figure 2-6. This artery joined the basilar artery at the base of the pons and was regarded as a normal finding.

The anatomy of the internal carotid artery in horses investigated in this study showed some variations from the general published description of the anatomy of this structure (Furuhata, 1964, Nanda, 1975, Colles and Cook, 1983, Orr et al., 1983). Angiography of the carotid trifurcation and internal carotid artery of both sides was performed on 50 horses and a 100 individual angiograms of the carotid arterial tree were generated. Of 100 angiograms, 83 were considered to follow the common or standard anatomical pattern (based on published descriptions of this structure). There were 17 angiograms observed with anatomical variations. A list of carotid angiographic findings in the horse specimens is shown in Table 2-1.

The first variation demonstrated on angiography was that the internal carotid and the occipital arteries arose as a common trunk. Five out of 17 angiograms were found with this variation. Three of these five angiograms were of the right side and the other two of the left side. In these angiograms, a shared trunk was identified running for a variable length from the common carotid artery termination before the vessels separated as individual arteries (Figure 2-7). However, the distance of the origin of the trunk from the common carotid artery to the point where the trunk separated as occipital artery and internal carotid artery individually was not measured or recorded. In these angiograms, the common carotid artery termination was bifurcated instead of the normal trifurcated form.

An aberrant branch of the extra-cranial internal carotid artery was observed in the remaining 12 angiograms that had variations. Of these 12 angiograms, four had an aberrant branch that united with the basilar artery (Figure 2-8). Three of the variations were observed on the left side and only one was observed on the right side.

Another angiographic variation observed was that the aberrant branch of the extra-cranial internal carotid artery did not unite with the basilar artery; instead the aberrant branch ramified into the surrounding tissue and was not connected to any other vessels (Figure 2-9 and Figure 2-10). Three out of 12 angiograms with an aberrant branch of the internal carotid artery demonstrated this type of variation.

The aberrant branch of the extra-cranial internal carotid artery was also observed to give rise to several smaller satellite branches, and was recognised in 5/12 angiograms shown to have branching of the internal carotid artery. On the basis of the angiograms, it was not possible to definitively conclude whether these smaller branches were connected to the basilar artery.

However, in one angiogram of an aberrant branch of the left internal carotid artery that gave rise to three smaller satellite branches, it was found that two of these branches travelled cranially and one was found to be connected to the basilar artery. The other cranial branch did not appear to be connected to any vessel. One smaller branch from the aberrant branch of internal carotid artery extended caudally and was deemed to be connected to the caudal branch of the ipsilateral occipital artery (Figure 2-11). This was the only angiogram with this peculiarity. In addition, the right occipital and internal carotid arteries of this horse shared a common trunk (Figure 2-12).

As a whole, bilateral variations of the carotid arterial tree were observed in two horses, and unilateral variations were observed in 13 horses. For horses that had unilateral variation of the carotid arterial tree, six were seen on the left side and seven on the right side.

2.3.2 Angiography of the Intracranial Portion of the Internal Carotid Artery and the Cerebral Arterial Circle

A list of cerebral angiographic findings with regard to the arrangement of the cerebral arterial circle and presence of the caroticobasilar artery in horse specimens is shown in Table 2-2. Out of 50 horses, 26 were found with the common arrangement of the cerebral arterial circle. In another 16 horses, the cerebral angiographic views to observe the pattern of this circle were impaired, either due to technical flaws or the circle was superimposed by the external carotid artery and its branches.

Peculiar arrangements concerning the caudolateral quadrant of the cerebral arterial circle were observed in four horses. In these horses, the communication between the caudal communicating and basilar arteries had various connections forming an arteriolar plexus or a rete interconnecting the caudal communicating, intercarotid and the basilar arteries (Figure 2-13). It should be mentioned here that this observation was based on 2D rotational imaging. Issues of superimposition from other vessels had been taken into consideration and verified at each different angle of the rotational views.

Other irregularities of the basilar artery were seen in three horses. Usually, the basilar artery tapers to pass caudally and connect with the cerebral vertebral artery. However, in the observations made here, the basilar artery was not always straight. Sometimes the course of the basilar artery deviated from the centre of the cerebral arterial circle, either tending more towards the right or the left internal carotid artery (Figure 2-14).

The presence of a caroticobasilar artery could be seen in 17 horses, either unilaterally (10) or bilaterally (7). Seven out of ten with a unilateral caroticobasilar artery were on the left side. In one horse with a right unilateral caroticobasilar artery, a connection from this artery to the intercarotid artery was seen (Figure 2-15).

2.3.3 Other Vascular 'Defects'?

There were several pseudo vascular defects due to technique flaws observed in this series of angiographic studies. The narrowing of a vessel, partial filling and failure to fill a vessel with contrast material were observed and are recorded in Table 2-3. In Figure 2-16, some parts of the internal carotid artery were narrowed, which was believed to be due to inadequate thawing of the specimen. In Figure 2-17 (lateral view) and Figure 2-18 (dorsoventral view) which were from the same side of the same horse, the internal carotid artery narrowed for a short distance just before it entered the cranium at the level of sigmoid flexure. However in another horse, the internal carotid artery was observed to become narrow after it entered the cranial cavity, which was after the sigmoid curve (Figure 2-19).

Partial filling of the occipital arteries can be seen in Figure 2-20, where the origin of the artery did not fill fully with contrast, thus giving the false appearance of the occipital and the internal carotid arteries sharing a common trunk. Further angiographic views of this horse confirmed that the carotid trifurcations were actually of common anatomical pattern. In Figure 2-21, the presence of gas at the origin and along the middle part of the left and right internal carotid arteries created difficulties in identification of individual vessels. In order to eliminate the presence of gas within the arterial lumen, more contrast material was injected. As a result, smaller vessels and rami filled with contrast making it much harder to evaluate the important vessels. Injection of too much contrast also contributed to more artefact formation in the angiograms.

Failure to fill with contrast unrelated to technique flaws was seen particularly in the occipital and the basilar arteries. In three horses failure to fill the occipital artery with contrast material was observed. Figure 2-22 shows an example of complete failure to fill this artery. Failure to fill the basilar artery was observed in five horses. An example of the complete failure to fill the basilar artery is shown in Figure 2-23.

2.3.4 Two Dimensional Angiography

Conventional two dimensional angiographic images (manual setting) of the carotid trifurcation and internal carotid artery were obtained in the first seven horse specimens and were considered a pilot study. In one horse, out-pouching of the internal carotid artery was observed and was at first suspected to be an aneurysm of the artery (Figure 2-24). However, further views with different angulation of the C-arm showed that the 'aneurysm' was in fact an aberrant branch of the internal carotid artery.

One technical issue regarding simultaneous angiography of both carotid arterial trees was the superimposition of the right and left carotid arterial trees, which made the observation and evaluation of the carotid trifurcation and the internal carotid artery more confusing (Figure 2-25). Even several oblique views (2-4 views) of both carotid arterial trees failed to provide diagnostic angiographic images. The fact that this study was conducted using cadavers, contrast material on the initial side needed to be flushed out before another angiogram was taken to prevent overlapping, hence more tedious and time consuming. In the live animal, interventional flushing of contrast would not be an issue as the cardiac output would lead to very rapid clearance of the contrast from the carotid arterial tree and its branches.

2.3.5 Cine-Loop Function

In this study, dynamic movements of the whole carotid trifurcation up to the level of the formation of the cerebral arterial circle were visualised in a 2D angiographic series using Cine-Loop function in the Iso-Cine mode. A list of outcomes on Cine-Loop function is illustrated in Table 2-3 where the image qualities were graded subjectively as good, partial and poor quality. A good quality Cine-Loop reflected a high quality angiographic series of the vessels with complete delineation within the region of the scan centre. Any angiographic series that suffered issues related to technical flaws that occurred on the less important part of the arterial tree were considered to be of partial quality. Poor quality images were angiograms that impaired the observation of the whole carotid trifurcation.

A common /standard anatomical pattern of the carotid trifurcation and the internal carotid artery including the formation of cerebral arterial circle are represented in video 2-1. In video 2-2a, the presence of an aberrant branch of the left internal carotid artery could be appreciated. This aberrant branch was traced and was found to be connected to the basilar artery (video 2-2b). Interestingly in another horse, an aberrant branch of the left internal carotid artery with small satellite branches was traced as shown in video 2-3. One branch from the satellite vessels of this aberrant branch was demonstrated clearly to unite with the caudal branch of the ipsilateral occipital artery. The other two branches from this same aberrant branch could also be observed moving cranially, with one of the branches connected to the basilar artery. In the same video, the right carotid arterial tree could be identified where the right internal carotid artery and the occipital artery of this horse shared a common trunk, thus giving the appearance of the common carotid artery bifurcate, rather than trifurcate. This finding showed that there were bilateral variations of the carotid trifurcation and internal carotid artery in this horse.

Presence of the caroticobasilar artery can be visualised easily with the Cine-Loop video, provided the basilar artery was filled up with contrast material (Videos 2-1 to 2-3).

2.3.6 Three Dimensional with Multi-planar Reconstruction (3D-MPR)

Of 50 heads in this study, 43 underwent bilateral rotational angiography with 3D reconstruction imaging of the carotid trifurcation, the internal carotid artery and the cerebral arterial circle. Following 3D reconstruction of an image, a screenshot of the 3D-MPR images was taken. A list of outcomes of 3D-MPR representation in relation to the Cine-Loop function can be referred in Table 2-3.

The 3D screenshot images appear on the screen as a four quadrant image. The left bottom quadrant indicates the 3D volume view and the other three quadrants show the multi planar/sliced views of the subject. The subject can be sliced in three planes, which are the sagittal, the axial and the coronal planes. Since the fluoroscopy machine was manufactured for human medical purposes, the terminology 'coronal' is associated with human anatomy. For clarity in relation to the horse, the term coronal plane is actually referring to the dorsal plane.

Eight specimens out of 43, suffered failure to launch the 3D reconstruction due to software malfunction. Thus, only 35 horses with 3D-MPR images were produced. Out of all 3D-MPR images on these specimens, only ten were of high quality, where the vessel delineation was complete and all vessels within the range of the scan centre were able to be reconstructed successfully (Table 2-3).

The quality of the 3D-MPR images were dependant on the quality of the angiographic series on the Cine-loop function. Thus, the problems seen on 3D-MPR representations were relative to the issues seen in Cine-Loop function, which include; reduced visibility of small vessels, interruptions along the vessel due to partial or complete failure to fill with contrast, fading quality on reconstructed images and excessive presence of artefacts. Apart from some issues of image quality, screenshots of 3D-MPR on six other specimens were considered satisfactory because reduced visibility of small vessels and interruptions occurring on unimportant regions of the targeted vessel. Another 15 specimens with 3D-MPR screenshots were considered not suitable for diagnostic evaluation.

A 3D screenshot image that highlights a common anatomical pattern of the internal carotid artery and the formation of the cerebral arterial circle is shown in Figure 2-26. A screenshot of the occipital artery and the internal carotid artery sharing a common trunk is shown in Figure 2-27.

Unfortunately, any aberrant branches of the extra-cranial internal carotid artery were difficult to reproduce on 3D-MPR. Bilateral caroticobasilar arteries are demonstrated in the 3D screenshot in Figure 2-28.

2.4 Discussion

Whilst it was recognised that there have been merit in gathering signalment information (age, sex, breed), such information has not been identified as important predisposing factors associated with guttural pouch mycosis (Cook, 1968a, Greet, 1987). The first seven horses were considered a pilot study and problems on manual setting were addressed. Unfortunately, other problems such as artefacts and excessive contrast that subsequently cropped up did not arise during the pilot study.

On the other hand, rotational angiography with 3D imaging (3D-RA) using the Ziehm Vario 3D fluoroscopic machine proved reliable and rapid despite some issues related to 3D imaging. Correct positioning of the specimen and the rotational arm of the machine was crucial to get a good exposure of the carotid trifurcation and the internal carotid arteries. The ideal position would be where the midsagittal plane (nasal septum) is either perpendicular or parallel to the primary beam for orthogonal views of the region/s of areas of interest -the carotid trifurcation and the internal carotid artery. The 2D angiographic series were created by the Cine-Loop function where interpretation of the angiograms was straight forward and anatomical variations could be identified easily.

Based on the angiographic findings, there are five distinct variations of the internal carotid artery of horses compared to the common anatomical pattern of this structure. These variations were identified as follows:

1. The internal carotid artery and occipital artery arise as a common trunk (5/17 angiograms with anatomical variation)
2. Presence of an aberrant branch of the internal carotid artery that unites with the basilar artery (4/17 angiograms with anatomical variation)
3. Presence of an aberrant branch of the internal carotid artery that does not unite with the basilar artery (3/17 angiograms with anatomical variation)
4. An aberrant branch of the internal carotid artery that gives rise to several satellite branches (5/17 angiograms with anatomical variation)
5. An aberrant branch of the internal carotid artery with satellite branch that is connected to the caudal branch of the ipsilateral occipital artery (1/5 angiograms that have aberrant branch of internal carotid artery with satellite vessels).

The presence of a caroticobasilar artery in the horse is considered a common variation, being a constant anastomosis between the internal carotid and basilar arteries (Nanda and Getty, 1975). This connection usually arises from the second curve of the sigmoid flexure of the internal carotid artery and unites with the basilar artery.

One aim of surgical occlusion of the internal carotid artery (in cases of guttural pouch mycosis) is to prevent fatal haemorrhage due to erosion of the artery caused by invasion of the mycotic plaque across the wall of the medial compartment of the guttural pouch - clinically manifested by epistaxis. Crucially, the internal carotid artery is not an end artery, thus to prevent haemorrhage from the internal carotid artery, normograde and retrograde blood flow should be prevented. Occlusion of the affected internal carotid artery at its origin does not reduce the risk of fatal haemorrhage because retrograde blood flow from the cerebral arterial circle maintains arterial pressure distal to the occlusion site. Successful occlusion of the internal carotid artery has been achieved by occluding the vessel rostral to the mycotic lesion (prevent retrograde flow) and also on the cardiac site of the lesion (prevent normograde flow) (Freeman and Donawick, 1980a). Thus the technique of balloon tipped catheter was developed (Freeman and Donawick, 1980a).

However, failure of the balloon tipped catheter occlusion technique has been reported because the balloon tipped catheter entered an aberrant branch of the internal carotid artery and thus retrograde blood flow from the cerebral arterial circle through the internal carotid artery was not prevented (Freeman et al., 1993). Thus fatal haemorrhages could still arise post operatively. It has been suggested that if an aberrant branch of the internal carotid artery was found, it should be occluded at its origin in order to prevent retrograde blood flow into the internal carotid artery, along with occlusion of the actual internal carotid artery rostral to the mycotic lesion(Freeman et al., 1993).

The more recent technique of transarterial coil embolisation (TCE) can selectively and precisely occlude the arterial segment affected by the mycotic plaque under fluoroscopic guidance (Matsuda et al., 1999, Lévéille et al., 2000, Lepage, 2005). This technique is facilitated by angiographic imaging of the affected vessels, identification of any aberrant branches and or specific sites of bleeding (Lévéille et al., 2000).

In another report (Miller et al., 1998), the internal carotid artery pathway was recognised as leading to an aberrant course that travelled more medially with absence of the sigmoid flexure of the artery. The occipital artery on the same side was also absent. These abnormalities caused the balloon tipped catheter to press on the caudal cerebellar arteries, resulting in cerebellar artery vasospasm and necrosis, followed by respiratory failure and death. In such cases, angiography would be an invaluable technique during surgery to identify aberrant vascular anatomy, which might compromise the surgical outcome.

Therefore, angiographic studies of the internal carotid artery in cases of guttural pouch mycosis are helpful for surgeons during guttural pouch surgery. With the aid of fluoroscopy, one could confirm that the correct vessel has been occluded. It would also provide an invaluable piece of information for even experienced surgeons in assessing bizarre arterial anomalies and reduce the risk of post operative haemorrhage.

Bilateral variations of the carotid trifurcation and the internal carotid artery were seen in two horses in this study. Based on these findings, it is clear that there are more anatomical variations of the internal carotid artery of the horse than reported previously (Du Boulay and Verity, 1973, Nanda, 1975, Colles and Cook, 1983).

2.4.1 "Aneurysm" of the Internal Carotid Artery

Based on an apparent normal population (unselected specimens), aneurysmal formations along the arterial vessels were not detected in any of the heads in this study. In one horse, an out-pouching of the internal carotid artery was observed and initially suspected to be an aneurysm of the artery. However, aneurysm formation was ruled out with further angiographic views and increased rotational angle that showed the aneurysm to be an aberrant branch of the internal carotid artery. Colles and Cook (1983) reported that 18 of 25 horses with guttural pouch mycosis had demonstrable aneurysms. Five of these horses had a unilateral bifurcated internal carotid artery (aberrant branch of internal carotid). In three they declared that the aneurysm was located on the aberrant branch rather than on the internal carotid. This poses several questions if the aneurysm reported is genuine. Are they in fact secondary or a consequence of invasion of the guttural pouch with fungal plaque, or are aneurysms exceedingly rare, yet a precipitating factor in the development of guttural pouch mycosis. It is proposed that with increased angiographic views at different angles of the internal carotid artery, one could confirm whether "aneurysm" formation was actually an aberrant branch of the internal carotid. However, another angiographic study (Greet, 1987) revealed that aneurysms occurred at the sigmoid curvature of the internal carotid artery in eight horses affected by guttural pouch mycosis and that these findings supported the theory advanced by Colles and Cook (1983) who suggested that a primary arterial lesion may predispose horses to guttural pouch mycosis. In contrast, other angiographic work, (Lepage et al., 2004), found only a few cases with aneurysm formation of the internal carotid artery, the external carotid artery or the maxillary artery. Indeed, Lepage (2005) disputed the theory of primary arterial lesion, in the form of an aneurysm, predisposing horses to guttural pouch mycosis (Lepage, 2005).

2.4.2 Variant Anastomoses of the Intracranial Portion of the Internal Carotid Artery

One of the most reported eccentric anastomosis related to the intracranial portion of the internal carotid artery in the equine species is the presence of the caroticobasilar artery (Nanda, 1975, Nanda and Getty, 1975, Frackowiak et al., 1997). The presence of caroticobasilar anastomosis, which is equivalent to foetal type primitive trigeminal artery in man, is considered an anomaly and labelled as a variant of the Cerebral Arterial Circle (Wismer, 1989). The clinical presentation of a caroticobasilar artery in man was of a throbbing occipital headache due to vertebrobasilar insufficiency (Wismer, 1989).

However in the equine species, the presence of this small vessel has been reported to be a normal finding and does not affect the horse clinically (Nanda and Getty, 1975). The reason to this is that the communication present in the horse is a weak and primitive type of anastomosis retained from the early embryonic stages. Furthermore in the horse, retention of this weak anastomotic network may not induce regression of trigeminal artery as it does in man (Nanda and Getty, 1975). However, the trigeminal artery was not observed in this study. An observation made here, in one horse was that the right caroticobasilar artery was found to form a communication with the caudal intercarotid artery. This finding is in agreement with a dissection study using vinyl and latex arterial cast (Frackowiak et al., 1997).

The description given for the caudal communicating artery was that the artery turns caudal after coming off the intracranial portion of internal carotid artery, and then joins the basilar artery to form the lateral and caudolateral quadrants of the cerebral arterial circle (Nanda, 1975). In this study, generally the arrangement of the caudal communicating giving rise to the basilar artery followed this pattern. However in some (four horses), it was observed that there were some indirect fine branches at the terminal end of the caudal communicating arteries, and somehow the continuation to the basilar artery was not easy to determine. The union of the distal segment of the caudal communicating artery with the basilar artery is created by a rete or plexus of the terminal branches of the basilar artery as recognised by Sisson (1910). According to Nanda (1975), a rostral cerebellar artery originates from the terminal portion of the basilar artery, of which there can be either two or three on either side. Where a plexus or rete can be seen before the basilar artery joins the caudal communicating artery, the rostral cerebellar artery may leave this plexus in a variable and asymmetrical manner (Nanda, 1975).

The odd arrangement of the caudolateral quadrants of the cerebral arterial circle was also seen and reported by (Gillilan, 1974). He suggested that the caudal communicating artery should not be named as such because of the presence of various fine branches interconnected with the basilar artery, which were arranged in an odd manner similar to the primitive patterns observed in other lower mammals and submammals. Perhaps in view of the results described here, the variations in arrangement of these fine vessels might be regarded as variant anastomoses of the cerebral arterial circle. Based on the observations herein, the rete was seen as various anastomotic fine vessels interconnecting the basilar artery, not only to the caudal communicating but also to the caudal intercarotid arteries.

Du Boulay (1973) claimed that the basilar artery in the horse tapers as it passes caudally; however, Gillilan (1974) stated that the basilar artery in the horse is uniform in size throughout its course. In our findings (three horses), basilar arteries were observed to be non-uniform by tapering in size and may deviate from the mid-line. Unfortunately, a quantitative measurement of the size of basilar artery was not made and this finding was based on angiographic observation along the length of the basilar artery.

2.4.3 Problems with Angiographic Interpretations

A number of features led to difficulties in the interpretation of the angiograms, these included; narrowing of a vessel, complete blockage or partial filling of a vessel with contrast material. Partial filling and complete failure to fill the arterial lumen with contrast material may be due to several reasons that can be associated with angiographic techniques as described earlier by Colles and Cook (1983). Other investigators in the field of post mortem angiography have attempted to overcome this difficulty by perfusing the vascular system with oil or saline before injecting the contrast material (Grabherr et al., 2007).

Inadequate volume or pressure of contrast material injected into the common carotid artery will result in poor filling of the vessels, especially the occipital or the basilar arteries (Colles and Cook, 1983). Leakage of the contrast material also contributes to inadequate pressure during injection. Perhaps this was due to the cadavers used in this study having been disarticulated at the third and fourth levels of the cervical vertebrae, resulting in some leakage of the contrast material through the transected artery and veins. Leakage also contributed to the fading quality of the arterial image. Improper thawing of the cadaver specimen may occlude the vessel either due to internal blockage in the vessel lumen or external pressure on the vessel wall with residual ice or frozen tissue.

Poor injection techniques of the contrast material resulted in the presence of gas in the arterial lumen which made interpretation of some of the results difficult. In order to flush out the gas within the lumen, more contrast material was needed, this caused small vessels and rami to fill with contrast. Another technique to prevent gas bubble in the arteries was to inject contrast material from one side to fill the contralateral side of arterial tree. However, small, unimportant vessels on the injection side were so filled with contrast that they reduced the quality of the angiogram with artefact formation. These may lead to confusion in interpretation and provide distraction from the important portions of the image. Thus in the clinical scenario, misinterpretation may affect decisions relating to occlusion options.

Angiographic appearance of a narrowed arterial lumen either on a section or along the arterial blood vessel may indicate pre-existing arterial disease such as thrombosis. If the narrowing of the vessel occurred extra-cranially, confirmation can be made based on dissection. Narrowing of the internal carotid artery, i.e. after its sigmoid curvature was difficult to be confirm on dissection, as at this level, the internal carotid artery enters the base of the skull and the rest of the artery is located intra-cranially.

In the live animal, a reported problem that lead to difficulty in interpretation of carotid angiograms was spasm of arteries during angiography (Colles and Cook, 1983) and either caused partial or complete narrowing of the vessel lumen. In that report, horses with guttural pouch mycosis had a higher incidence of spasm or failure of filling of the occipital artery compared to those with a healthy guttural pouch. An explanation of the cause of vasospasm on the internal carotid artery was given by Macdonald et.al (1999). According to these workers, the internal carotid artery was located adjacent to the carotid body and carotid sinus which contains baroreceptors and chemoreceptors. Stimulation of these baroreceptors, perhaps during manipulation of the internal carotid artery triggered the arterial spasm (Macdonald et al., 1999).

In this cadaveric study, filling of the basilar artery can be difficult to demonstrate especially in larger horse specimens. With higher volume and pressure of contrast material during injection, it may provide satisfactory filling of the basilar artery.

2.4.4 Geometric Distortion and Magnification

The basic principle in radiography is to place the area to be radiographed as near as possible to the image intensifier in order to achieve a sharp image and reduce the effect of magnification. In principle, magnification effect increases: (i) as the object to film distance is increased and (ii) the focus to film distance is decreased. In these experiments, some degree of magnification of the carotid arterial tree was seen because the object to film distance was increased due to the location of the vessels, embedded deep in the thick neck muscles and soft tissue. Thus, it was impossible to place the subject of interest very close to the image intensifier in order to avoid magnification of the image. Another factor that contributes to increase the distance of the object to the intensifier is the size of the specimen itself in relation to the arch of the C-arm of the fluoroscopy machine. Ideally, the image intensifier should be placed as close as possible to the skin of the specimen, but this is not particularly feasible as the image intensifier cannot be placed too close to the specimen as the C-arm will collide with certain parts of the specimen when the C-arm rotates around the specimen. The larger the size of the specimen, the greater the distance required from the specimen to the image intensifier to prevent collision. Thus, in large horse head specimens, the angiograms were more magnified.

However, the magnification effect was not a big issue for this research study because the main objective of this research was to identify any anatomical variations of the internal carotid artery. Measurement of the length of blood vessels, particularly the length of the internal carotid artery, was not done due to the fact that calibration of the machine was not performed beforehand. Any angiographic measurement done without calibrating the machine will not be true because of the magnification effect due to the reasons stated above.

The fluoroscopy machine used for this study was equipped with an image intensifier with 3D reconstruction technology. One of the less ideal attributes of the image produced by the image intensifier is a warping effect at the periphery of the image, known as pin cushion distortion. This can create errors of 10% to 15% in distance measurement at the peripheral areas compared to the measurements in the central area (Seibert, 2006). This effect has been seen consistently in the angiographic series (as a Cine-loop video) of the carotid arterial tree and the cerebral arterial circle in this study. An “S” distortion can also occur if the electrostatic and magnetic cylindrical focusing gradients interact with the earth’s magnetic field with the use of the image intensifier (Seibert, 2006).

A non-uniform image profile of the output image as a result of the vignetting process was also seen consistently. Vignetting is a process describing the loss of light intensity at the periphery of an image because light scatters away from the output phosphor. A veiling glare can also be observed in the angiographic series played in Cine-Loop function, where a long-range light scattering event reduces image contrast at the region of the glare. However, light loss and light scatter within the image intensifier in this study was considered very minimal and did not impair the image qualities for identification and diagnostic purposes.

2.4.5 Limitations

The 3D views were generated by means of an algebraic reconstruction algorithm. The computer system of the fluoroscope unit uses the images captured in relation to the predefined scan centre to compute a 3D representation of an object. Observation and evaluation of the 3D representation of an object was best viewed on the computer system on the fluoroscopic unit or by using software that was compatible for post processing of DICOM format images. The screenshot images would only provide information at the level of the slice view of the object but the actual 3D volume view cannot be appreciated from all sides.

Visualisation and interpretation issues related to the use of the fluoroscopic unit occurred mainly in the 3D multi-planar reconstruction images. The quality of the 3D-MPR images depends on the quality of the angiographic series on the Cine-loop function. Thus, any low quality images on the Cine-loop will result in a poor reconstruction of the 3D-MPR display. There are various reasons why the 3D-MPR did not perform to expectation and these shall be described.

Apart from vascular defects due to technical flaws, the issue with vessel delineation in 3D-MPR representation was related to the intensity of contrast material in the vessels. Specimens with low contrast intensity as a result of fading of contrast material suffer low quality 3D-MPR images. In this study, the fading quality of the contrast delineation was intensified by leakage of contrast material through the transected blood vessels and muscles as the entire specimens used in this study were disarticulated from the body at the level of third and fourth cervical vertebral joint. Insufficient contrast material in the vessels contributed by partial or complete blockage of blood vessel also impaired the ability to fill up smaller vessels with contrast agent, thus resulted in the failure to visualise fine vessels.

Another factor that influenced the quality of vessel delineation in 3D representation was the location of the vessels from the point of reference of the scan centre. The further the distance of the vessel from the scan centre, the more likely the vessel disappeared during reconstruction of the 3D image. This was true particularly for small vessels that were located at the periphery of the point of reference. This was also an issue in large horses that had a large carotid trifurcation, where the range of the scan centre could only cover a limited area. Thus, very limited visualisation of carotid trifurcation could be produced in 3D.

Another reason for reduced visibility in the 3D-MPR representation, especially of small or narrow vessels, was related to the rendering method during reconstruction of 3D images. Low opacity of smaller vessels was similar to the soft tissues, where during image reconstruction; the system's ability to differentiate between the small vessels and soft tissue structures was reduced. As a result, the vessel visibility or its details in 3D representation were lost.

In conclusion, angiographic observation and evaluation of the internal carotid artery in this study cannot rely solely on the 3D images, but must be accompanied by the Cine-Loop angiographic series to avoid misrepresentation due to limitations of the 3D-MPR display. Despite this, the angiographic work done in this study produced superior image quality, where the maximum potential of this fluoroscopic unit was reached.

Table 2-1: Carotid angiography findings in horse specimens

No.	Right	Left		No.	Right	Left
1	N	N		26	N	N
2	N	Δ		27	N	N
3	N	O		28	N	N
4	N	N		29	Ø	N
5	N	N		30	N	N
6	Δ	N		31	N	N
7	Y	N		32	N	N
8	N	N		33	N	N
9	N	N		34	N	Y
10	N	N		35	N	N
11	N	N		36	N	N
12	N	O		37	N	N
13	N	O		38	Δ	*
14	N	Ø		39	N	N
15	N	N		40	N	N
16	N	N		41	N	N
17	N	N		42	N	N
18	Y	N		43	Y	N
19	Δ	N		44	N	N
20	Ø	Δ		45	N	N
21	O	N		46	N	N
22	N	N		47	N	N
23	N	N		48	N	N
24	N	N		49	N	N
25	N	N		50	N	N

N: Common/standard anatomical pattern of the carotid trifurcation and internal carotid artery (83)

△: Internal carotid artery and occipital artery share a common trunk (5/17)

O: Internal carotid artery has an aberrant branch that connects to basilar artery (4/17)

Ø: Internal carotid artery has an aberrant branch that is not connected to the basilar artery (3/17)

Y: Aberrant branch off the internal carotid artery have satellite vessels (4/17)

***: Aberrant branch off the internal carotid artery connected to the occipital artery (1/17)**

Table 2-2: Cerebral angiographic findings in horse specimens

Horse	Arrangement of cerebral arterial circle	Caroticobasilar artery
1-7	N/A	N/A
8	Common pattern	Absent
9	N/A	N/A
10	Common pattern	Absent
11	Peculiar-rete/plexus like	Absent
12	Common pattern	Absent
13	Peculiar- rete/plexus like	Absent
14	Common pattern	Absent
15	Common pattern	Absent
16	Common pattern	Absent
17	Common pattern	Absent
18	N/A	N/A
19	N/A	N/A
20	Common pattern	Absent
21	N/A	N/A
22	N/A	N/A
23	Common pattern	Bilateral
24	Common pattern*	Left
25	Common pattern	Bilateral
26	Peculiar- rete/plexus like	Bilateral
27	N/A	N/A
28	Common pattern*	Bilateral
29	N/A	N/A
30	Common pattern	Absent
31	Common pattern	Absent
32	Common pattern	Left
33	Common pattern	Absent
34	Common pattern	Absent
35	Common pattern	Absent
36	Common pattern	Left
37	Common pattern	Absent
38	Common pattern	Left
39	Common pattern	Absent
40	Common pattern	Left
41	Peculiar connection*	Right*
42	Common pattern	Bilateral
43	Common pattern	Left
44	Common pattern *	Left
45	N/A	N/A
46	Common pattern	Right
47	Peculiar- rete/plexus like	Bilateral
48	Common pattern	Bilateral
49	Common pattern	Right
50	N/A	N/A

Cerebral arterial circle

Common/standard anatomical arrangement of cerebral arterial circle (26)

Common pattern* = Common anatomical arrangement of cerebral arterial circle with irregular course of basilar artery (3)

Peculiar- rete/plexus like: Peculiar arrangement of the cerebral arterial circle; rete/plexus like (4)

Peculiar connection* = a connection from the caroticobasilar artery to the intercarotid artery was observed (1)

N/A: Not able to be appreciated (16)

Caroticobasilar artery

Absent (17)

Bilateral (7)

Left (7)

Right (3)

N/A: Not able to be appreciated (16)

*** = caroticobasilar artery on this side has a connection to the intercarotid artery**

Table 2-3: List of imaging quality using Cine-Loop and 3D-MPR in horse specimens

Horse	Cine-Loop		3D-MPR		Comments (based on Cine-Loop)
	Carotid	Cerebral	Carotid	Cerebral	
1-7	NA	NA	NA	NA	Manual 2D imaging performed
8	±	+	NA	NA	Both OA partially filled with contrast
9	X	X	NA	NA	Too much artefacts
10	+	+	NA	NA	-
11	±	+	NA	NA	-
12	+	+	NA	NA	-
13	+	+	NA	NA	Right ICA narrowed after the sigmoid flexure
14	+	+	NA	NA	Right ICA after the sigmoid flexure
15	+	+	NA	NA	Right ICA narrowed before the sigmoid flexure. Basilar artery not fill with contrast
16	+	+	X	+	BA not fill with contrast
17	+	+	X	X	Left ICA not fill with contrast
18	±	±	X	X	Right ICA partially filled with contrast. BA not fill with contrast
19	X	X	X	X	Leakage of contrast through transected right ICA
20	+	+	±	±	BA not fill with contrast
21	±	±	X	X	Gas in the left OA and both ICA, including aberrant branch of right ICA
22	X	X	X	X	Both ICA filled halfway with too much contrast on the other unimportant vessels
23	+	+	+	+	-
24	+	+	+	+	-
25	+	+	±	±	-
26	±	+	±	±	Right OA failed to fill with contrast
27	X	X	X	X	Partial filling of both ICA due to gas. Too much contrast on the other unimportant vessels
28	X	+	X	X	Right OA failed to fill with contrast
29	±	X	X	X	Several narrowed regions along the left ICA. BA not fill with contrast
30	+	+	+	+	-
31	+	+	+	+	-
32	+	+	+	+	-
33	±	±	±	±	-
34	+	+	+	+	-
35	X	X	X	X	Gas in both OA.
36	+	+	X	X	-
37	X	X	X	X	Presence of gas along both ICA

Horse	Cine-Loop		3D-MPR		Comments
	Carotid	Cerebral	Carotid	Cerebral	
38	±	+	±	±	-
39	+	±	±	±	-
40	±	±	X	X	Too much contrast
41	X	±	X	X	Both OA partially filled with contrast due to gas
42	+	+	+	+	-
43	+	+	+	+	-
44	+	+	+	+	-
45	X	X	X	X	Left OA and ICA failed to fill with contrast- improper thawing
46	±	±	X	X	-
47	+	+	±	±	-
48	+	+	+	+	-
49	+	+	+	+	-
50	±	X	X	X	Gas in the left ICA

+ = Good quality

± = Partial quality

X = Poor quality

NA = Not activated/Not launched

ICA= Internal carotid artery

OA= Occipital artery

BA= Basilar artery

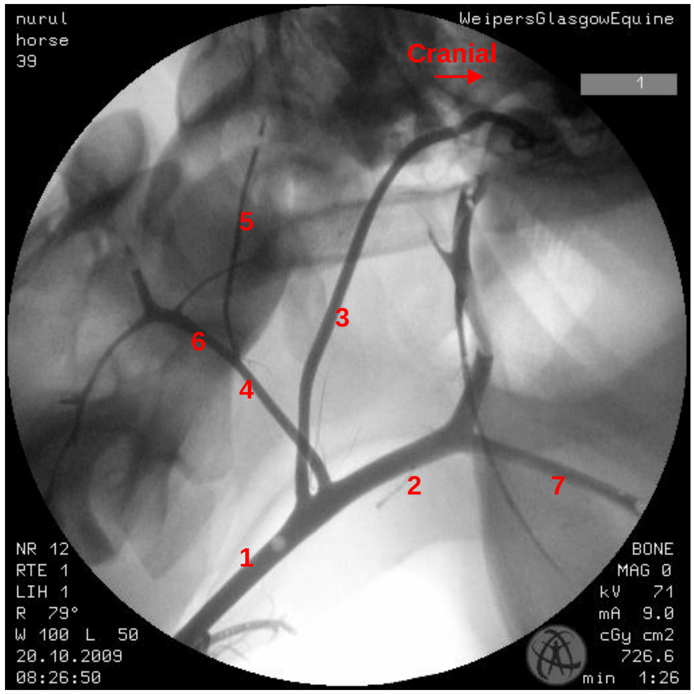

Figure 2-3: Lateral angiogram of the common pattern of the carotid trifurcation and the internal carotid artery of a horse.
1 common carotid artery; 2 external carotid artery; 3 internal carotid artery; 4 occipital artery; 5 cranial branch of occipital artery; 6 caudal branch of occipital artery; 7 linguofacial trunk (x 1/3).

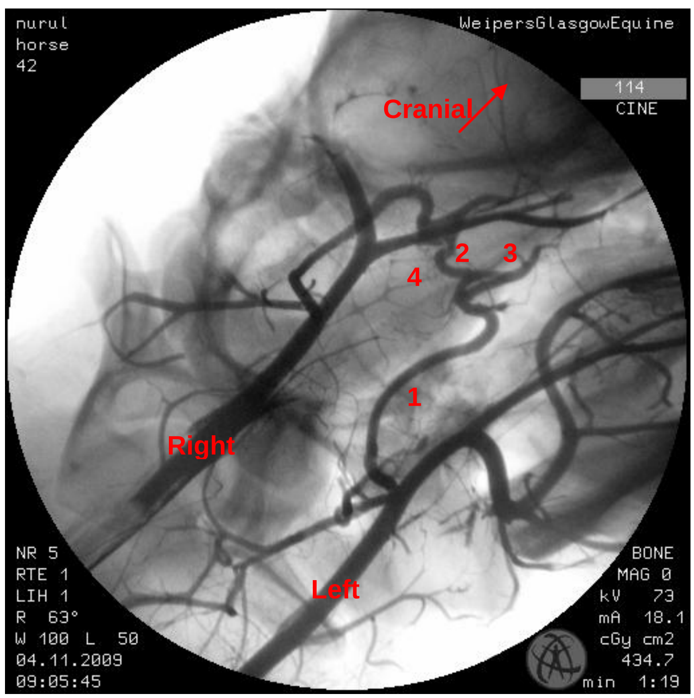

Figure 2-4: Dorsoventral angiogram of the common pattern of the distal internal carotid artery that contributes to the formation of the cerebral arterial circle of a horse.
1 internal carotid artery; 2 intercarotid artery; 3 caudal communicating artery; 4 basilar artery (x 1/3).

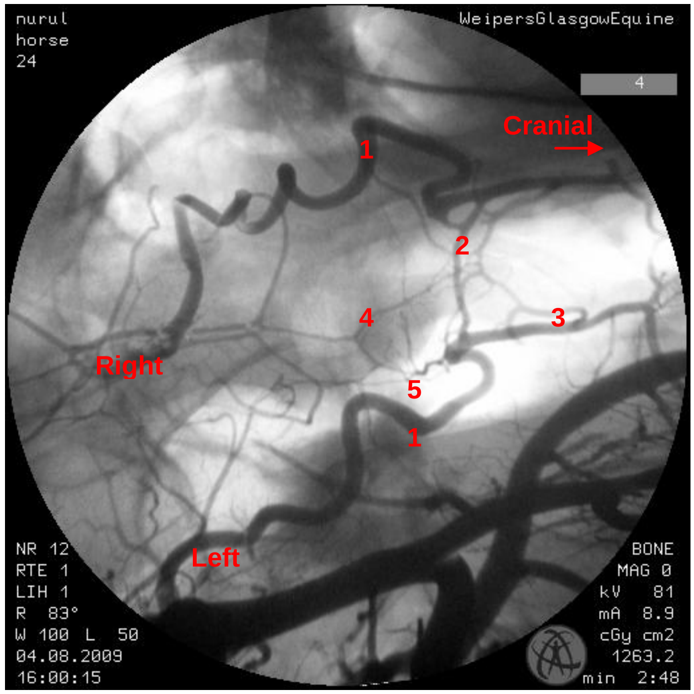

Figure 2-5: Dorsoventral angiogram of the distal internal carotid artery and the cerebral arterial circle of a horse. There is a caroticobasilar artery on the left side. Note the both internal carotid arteries are more tortuous than normal.
1 internal carotid artery; 2 intercarotid artery; 3 caudal communicating artery; 4 basilar artery; 5 caroticobasilar artery (x 1/3).

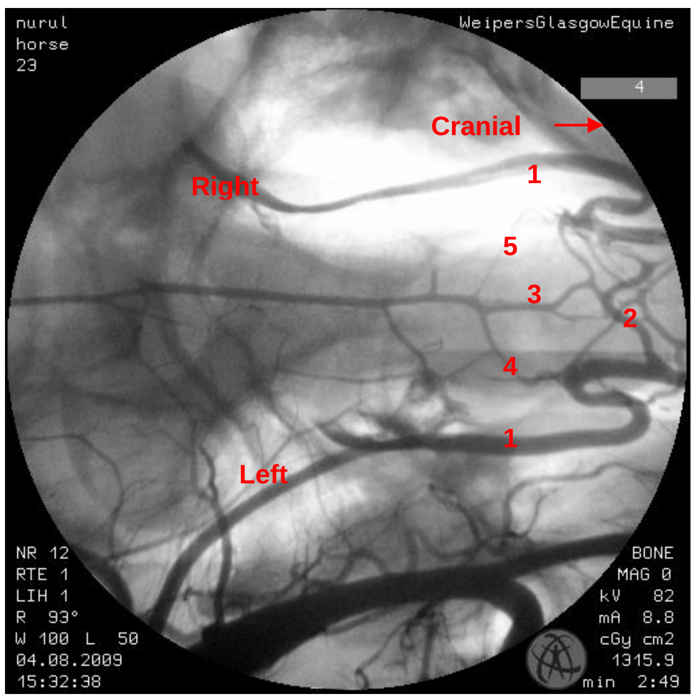

Figure 2-6: Dorsoventral angiogram of the distal internal carotid artery and the cerebral arterial circle of a horse. Note the presence of bilateral caroticobasilar arteries.
1 internal carotid artery; 2 intercarotid artery; 3 basilar artery; 4 left caroticobasilar artery; 5 right caroticobasilar artery (x 1/3).

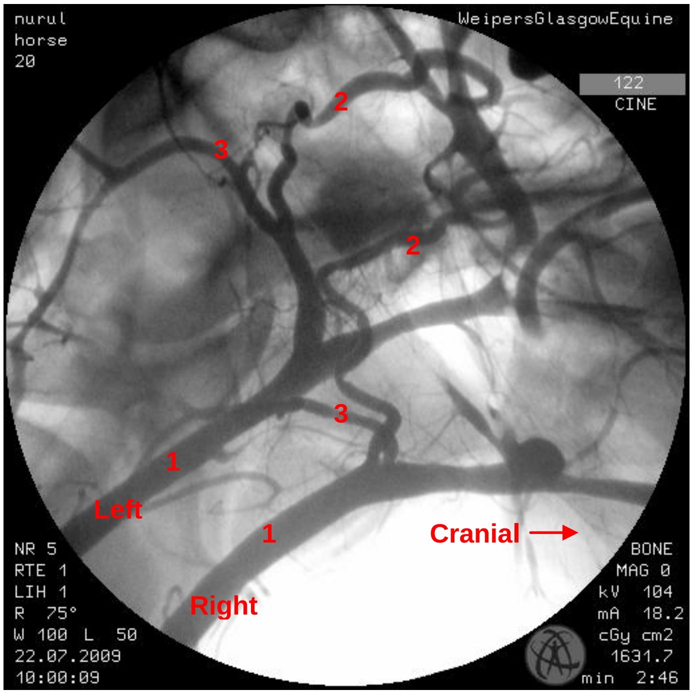

Figure 2-7: Oblique angiographic view of the carotid trifurcation and the internal carotid artery of a horse showing variation from the common pattern of these structures. The left occipital artery and internal carotid artery share a common trunk.
1 common carotid artery; 2 internal carotid artery; 3 occipital artery (x 1/3).

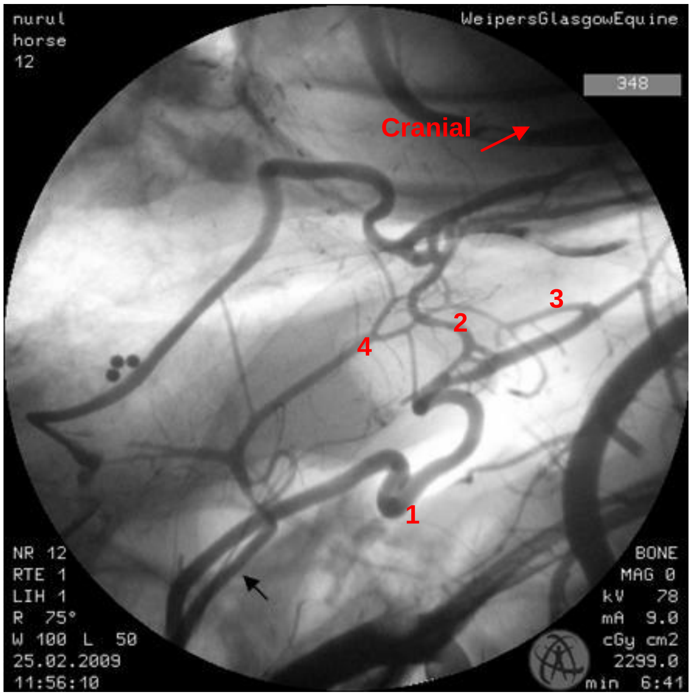

Figure 2-8: Dorsoventral angiogram of the distal internal carotid artery & cerebral arterial circle of a horse showing variation from the common pattern of these structures. Note the presence of an aberrant branch of the left internal carotid artery which unites with the basilar artery (black arrow). Ball bearing markers indicate the right side of carotid arterial tree. 1 internal carotid artery; 2 intercarotid artery; 3 caudal communicating artery; 4 basilar artery (x 1/3).

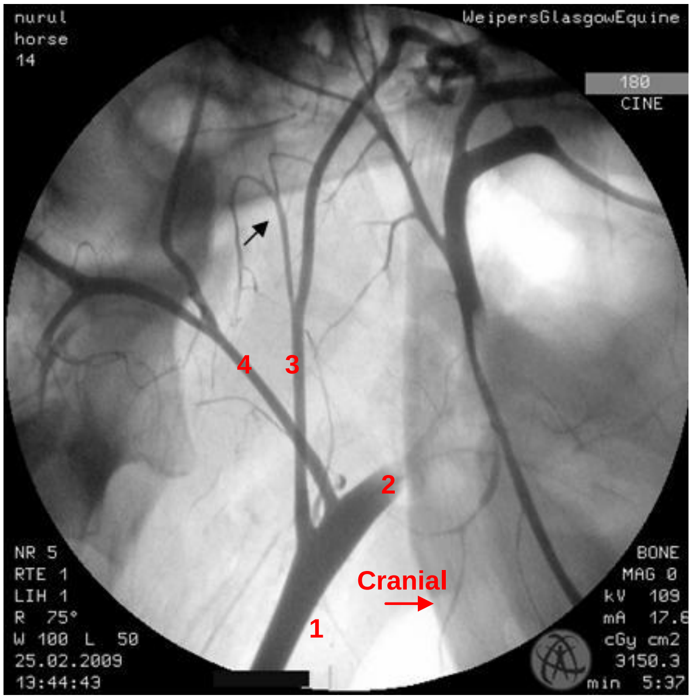

Figure 2-9: Lateral angiogram of the left carotid trifurcation and the internal carotid artery of a horse shows variation from the common pattern of these structures.
Note the aberrant branch of the left internal carotid artery which gives rise to another smaller branch (black arrow). 1 common carotid artery; 2 external carotid artery; 3 internal carotid artery; 4 occipital artery (x 1/3).

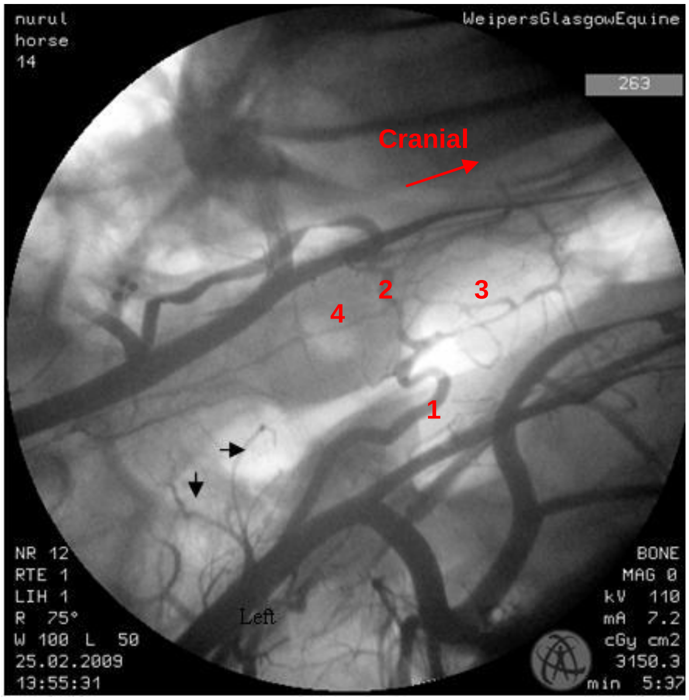

Figure 2-10: Dorsoventral angiogram of the distal internal carotid artery of the same horse as above, which shows variation from the common pattern of this structure.
The aberrant branches of the left internal carotid artery did not unite with the basilar artery (black arrows). Ball bearing markers indicate the right side. 1 internal carotid artery; 2 intercarotid artery; 3 caudal communicating artery; 4 basilar artery (x 1/3).

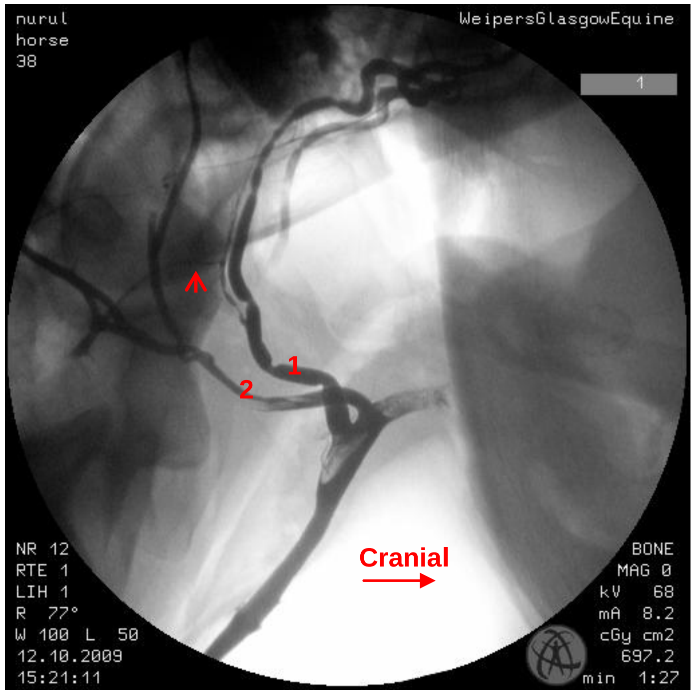

Figure 2-11: Lateral angiogram of left carotid arterial tree of a horse shows variation from the common pattern of this structure. The left internal carotid artery has an aberrant branch (red open arrow) that unites with the caudal branch of the occipital artery of the same side. 1 internal carotid artery; 2 occipital artery (x 1/3).

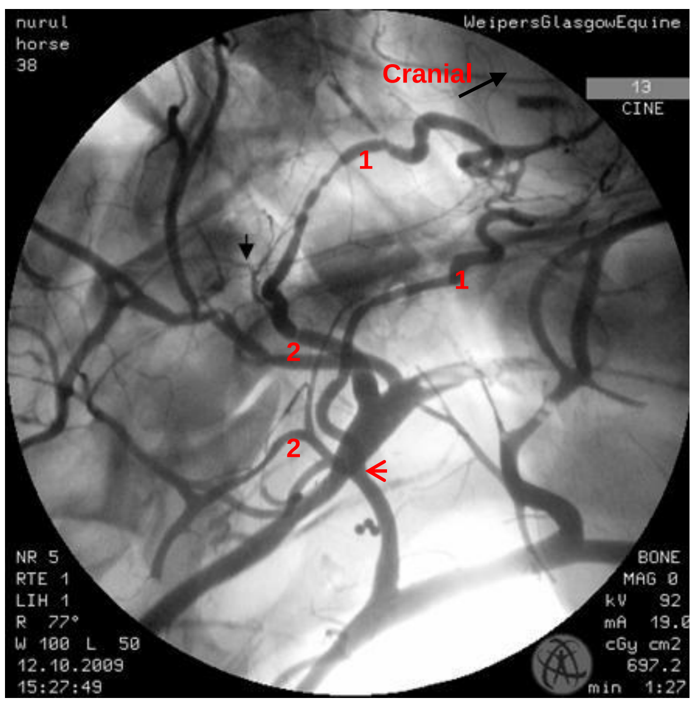

Figure 2-12: Oblique angiographic view of both side carotid arterial trees of a horse. The right and left internal carotid artery show variation from the common pattern of this structure. On the right, the internal carotid artery shares a common trunk with the occipital artery. However, the point of separation (red open arrow) from the common trunk is superimposed by the contralateral common carotid artery. The left internal carotid artery has an aberrant branch that unites with the caudal branch of occipital artery of the same side (black arrow). Ball bearing markers indicate the right side of carotid arterial tree. 1 internal carotid artery; 2 occipital artery (x 1/3).

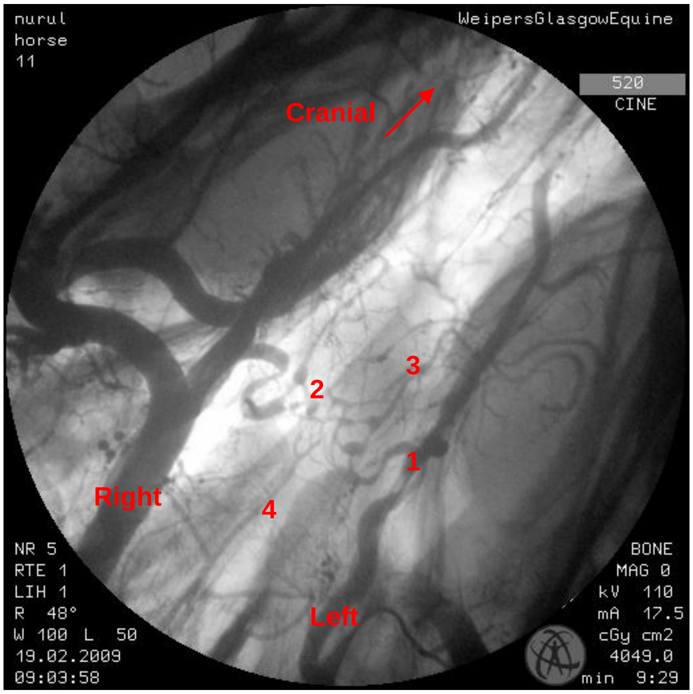

Figure 2-13: Dorsoventral angiogram of the cerebral arterial circle of a horse shows variation from the common pattern of this structure. Note the peculiar arrangement of the caudolateral quadrants of the cerebral arterial circle where rete or plexus like connections interconnecting the caudal communicating, intercarotid and basilar arteries can be observed.
1 internal carotid artery; 2 intercarotid artery; 3 caudal communicating artery; 4 basilar artery (x 1/3).

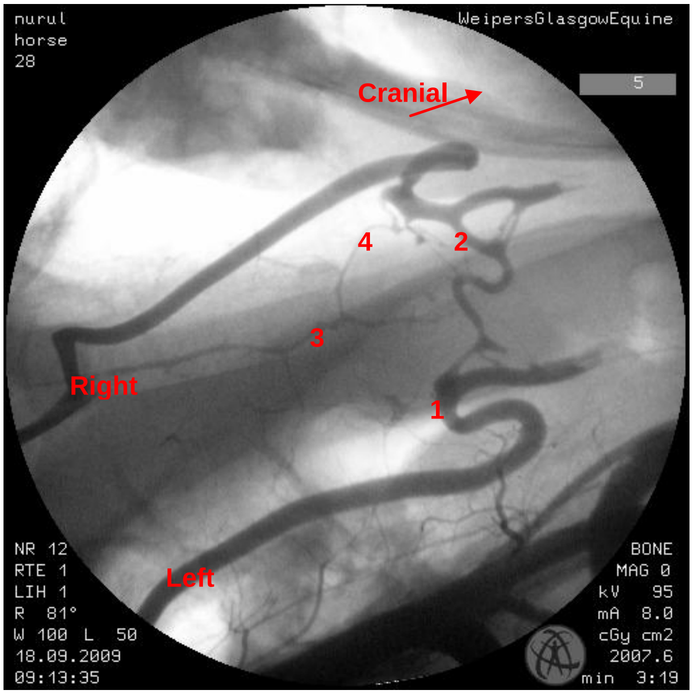

Figure 2-14: Dorsoventral angiogram (slight obliquity) of the cerebral arterial circle of a horse. The basilar artery was not straight and leaning to the right side.
Note that the intercarotid artery was more tortuous than the common pattern of this structure. 1 internal carotid artery; 2 intercarotid artery; 3 basilar artery; 4 caroticobasilar artery (x 1/3).

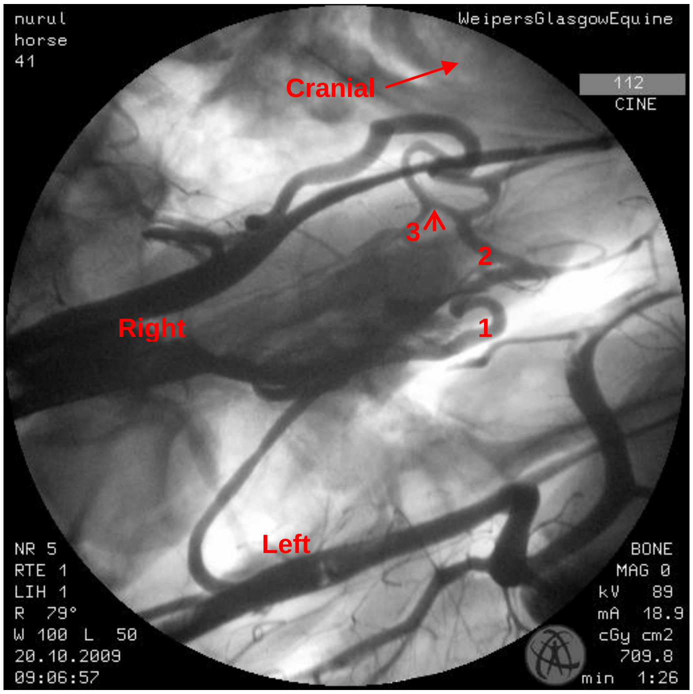

Figure 2-15: Oblique angiogram of the internal carotid arteries and the cerebral arterial circle of a horse. There is a connection from the right caroticobasilar artery to the intercarotid artery (red open arrow).
1 internal carotid artery; 2 intercarotid artery; 3 caroticobasilar artery (x 1/3).

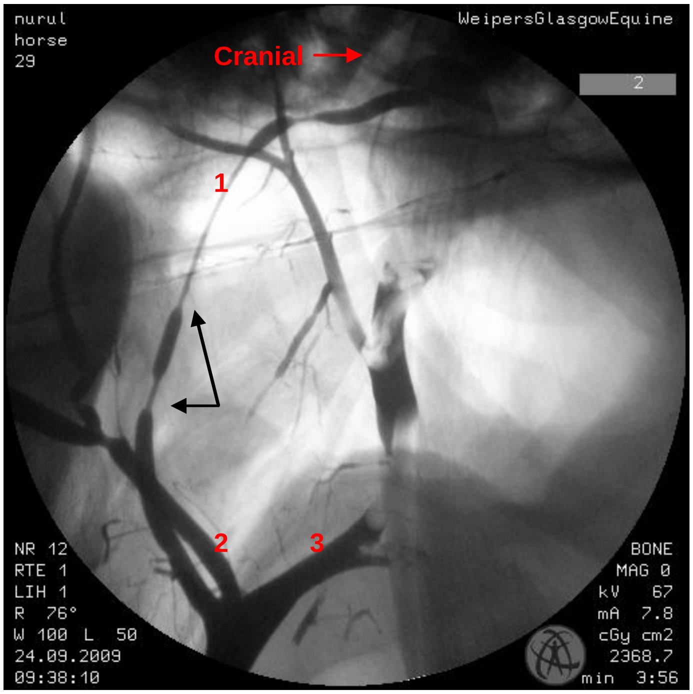

Figure 2-16: Lateral angiogram of the left carotid arterial tree of a horse with interrupted narrowing along the internal carotid artery (black arrows), due to inadequate thawing of the frozen specimen prior to angiography.
1 internal carotid artery; 2 occipital artery; 3 external carotid artery (x 1/3).

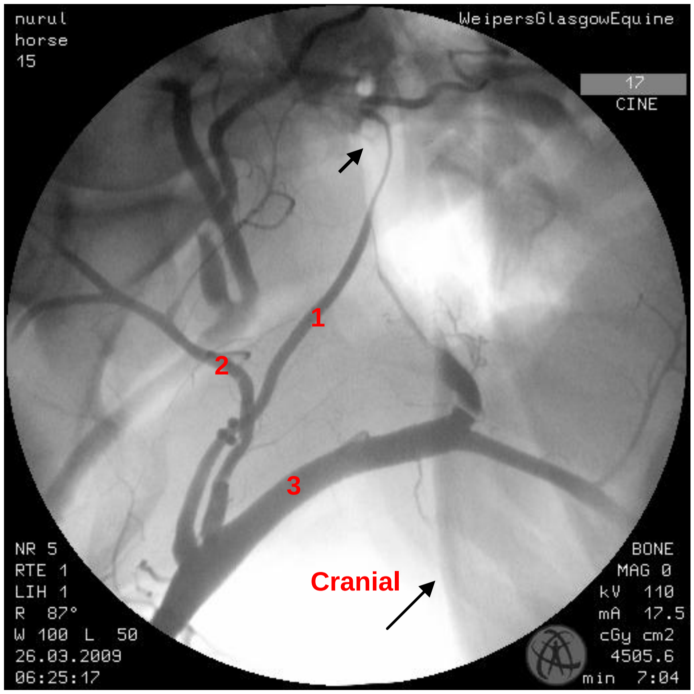

Figure 2-17: Lateral angiogram (slight obliquity) of the right carotid arterial tree of a horse with narrowing of the internal carotid artery (black arrow) due to inadequate thawing of the frozen specimen prior to angiography.
Ball bearing markers indicate the right side of the carotid arterial tree (overlapped with internal carotid artery). 1 internal carotid artery; 2 occipital artery; 3 external carotid artery (x 1/3).

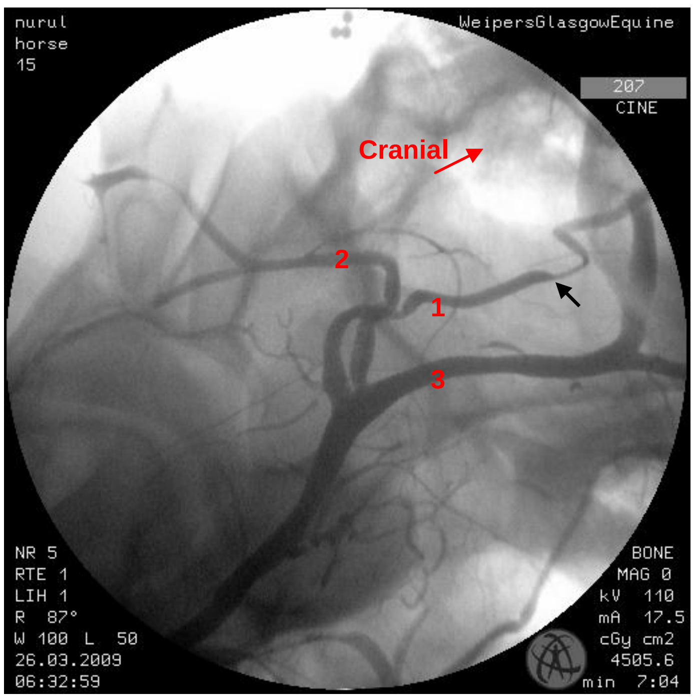

Figure 2-18: Oblique angiographic view of the left carotid arterial tree of the same horse as above. Note the narrowing of the internal carotid artery seen from a different angle (black arrow).
1 internal carotid artery; 2 occipital artery; 3 external carotid artery (x 1/3).

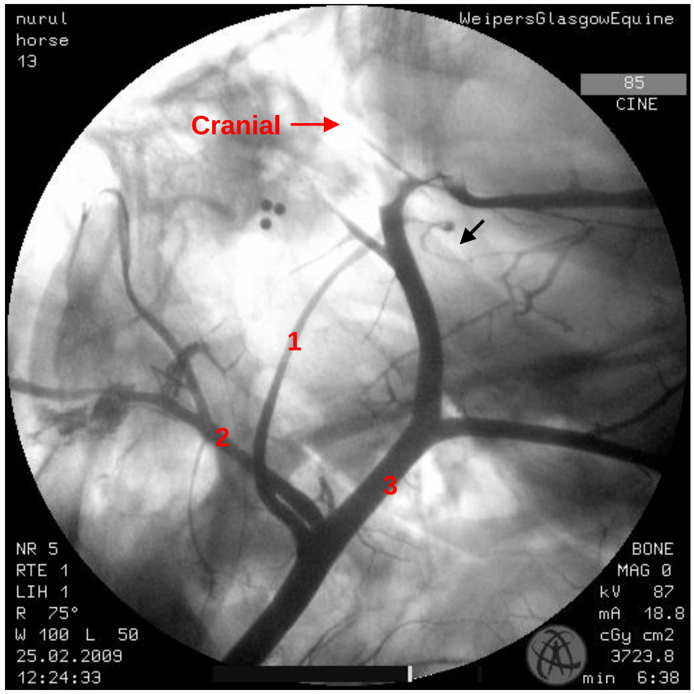

Figure 2-19: Lateral angiogram of the right carotid arterial tree of a horse with narrowing of the internal carotid artery after the sigmoid curvature (black arrow).
Ball bearing markers indicate the right side of carotid arterial tree. 1 internal carotid artery; 2 occipital artery; 3 external carotid artery (x 1/3).

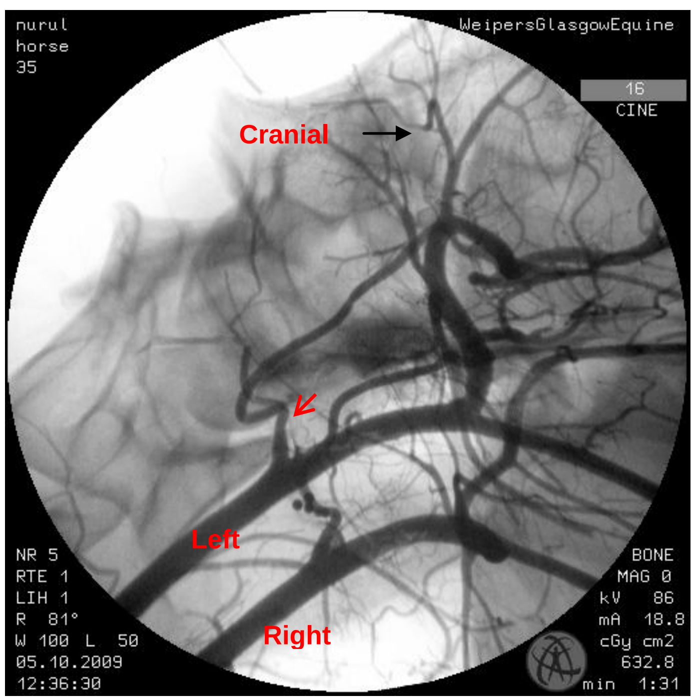

Figure 2-20: Oblique angiographic view of both carotid arterial trees of a horse. Partial filling of the left occipital artery with contrast material is due to gas. This resulted in confusion over angiographic interpretation (red open arrow) (x 1/3).

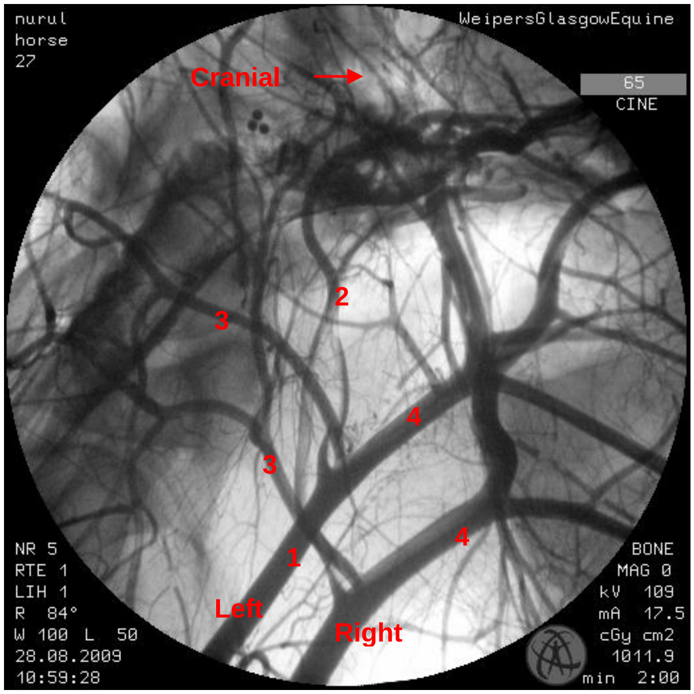

Figure 2-21: Oblique angiographic view of both carotid arterial trees of a horse. Gas has accumulated along the internal carotid arteries of both sides.
1 common carotid artery; 2 internal carotid artery; 3 occipital artery; 4 external carotid artery (x 1/3).

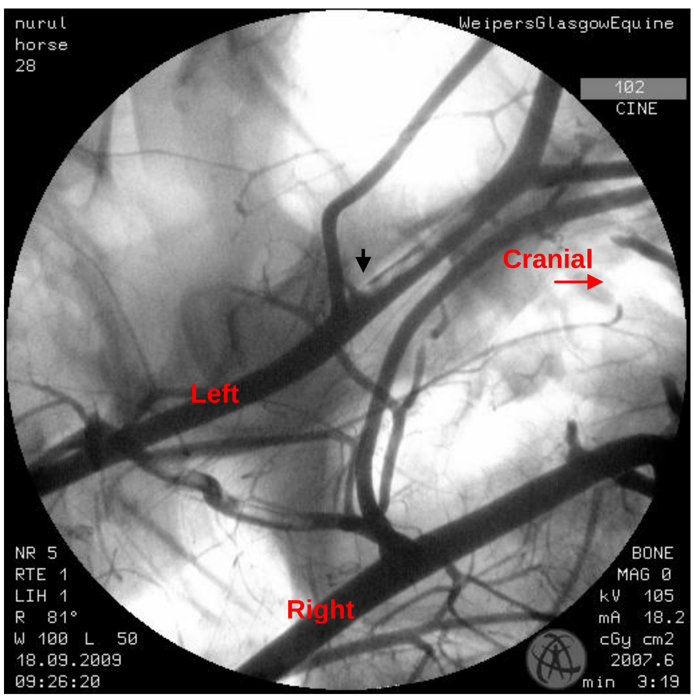

Figure 2-22: Oblique angiographic view of both carotid arterial trees of a horse. Complete failure of the right occipital artery to fill with contrast. Black arrow indicates the location of origin of occipital artery (x 1/3).

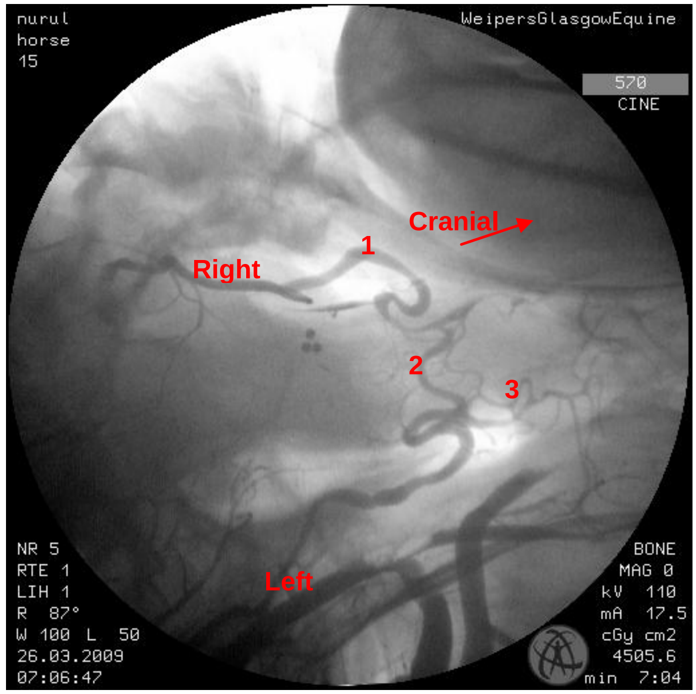

Figure 2-23: Dorsoventral angiogram of the distal internal carotid artery and cerebral arterial circle of a horse. In this angiogram, the basilar artery has not filled with contrast.
Ball bearing markers indicate the right side of carotid arterial tree. 1 internal carotid artery; 2 intercarotid artery; 3 caudal communicating artery (x 1/3).

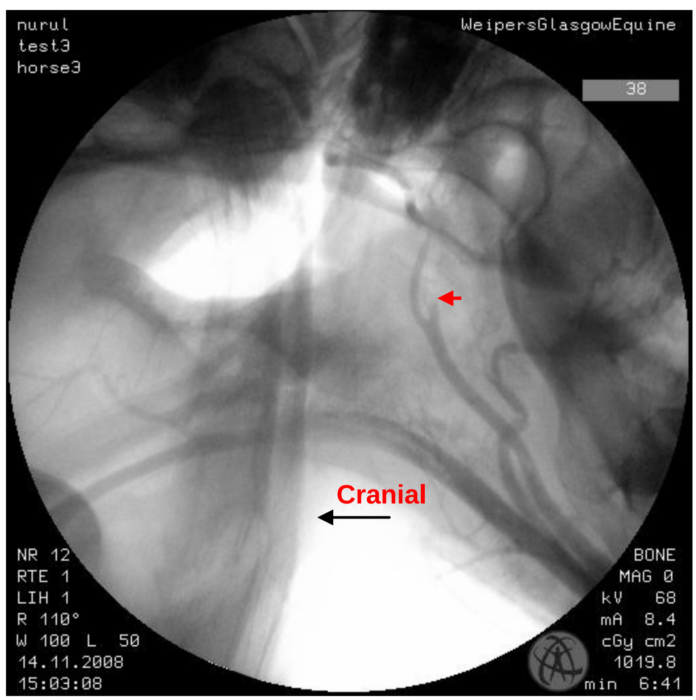

Figure 2-24: Lateral angiographic view of the left internal carotid artery of a horse shows variation from the common pattern of this structure. Seeming out-pouching of the internal carotid artery was actually an aberrant branch of this artery (red arrow) (x 1/3).

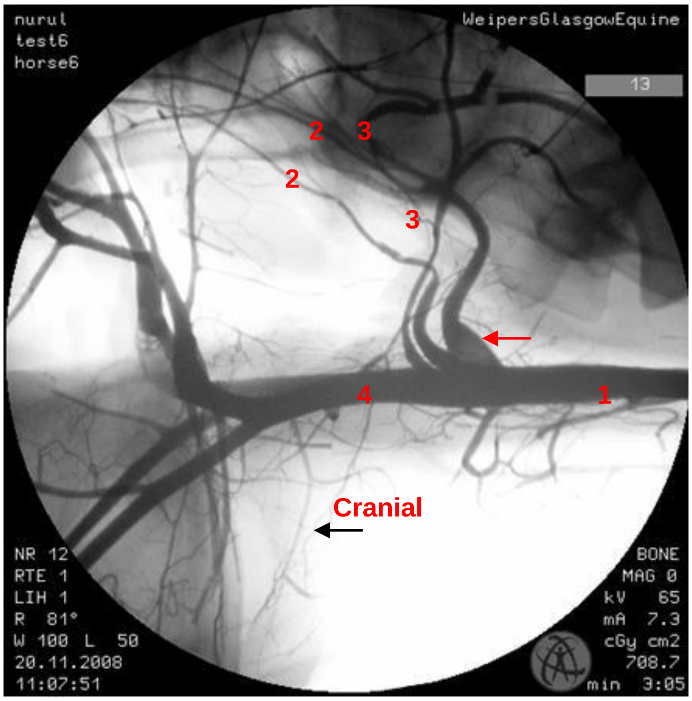

Figure 2-25: Lateral angiogram of the carotid arterial tree of a horse. The right internal carotid shows variation from the common pattern of this structure where the internal carotid artery and occipital artery share a common trunk.
The origin of this trunk from the common carotid artery was quite broad (red arrow). Angiographic observation of the carotid trifurcation was difficult to determine due to superimposition of the left and right carotid arterial tree. 1 common carotid artery; 2 internal artery; 3 occipital artery; 4 external carotid artery (x 1/3).

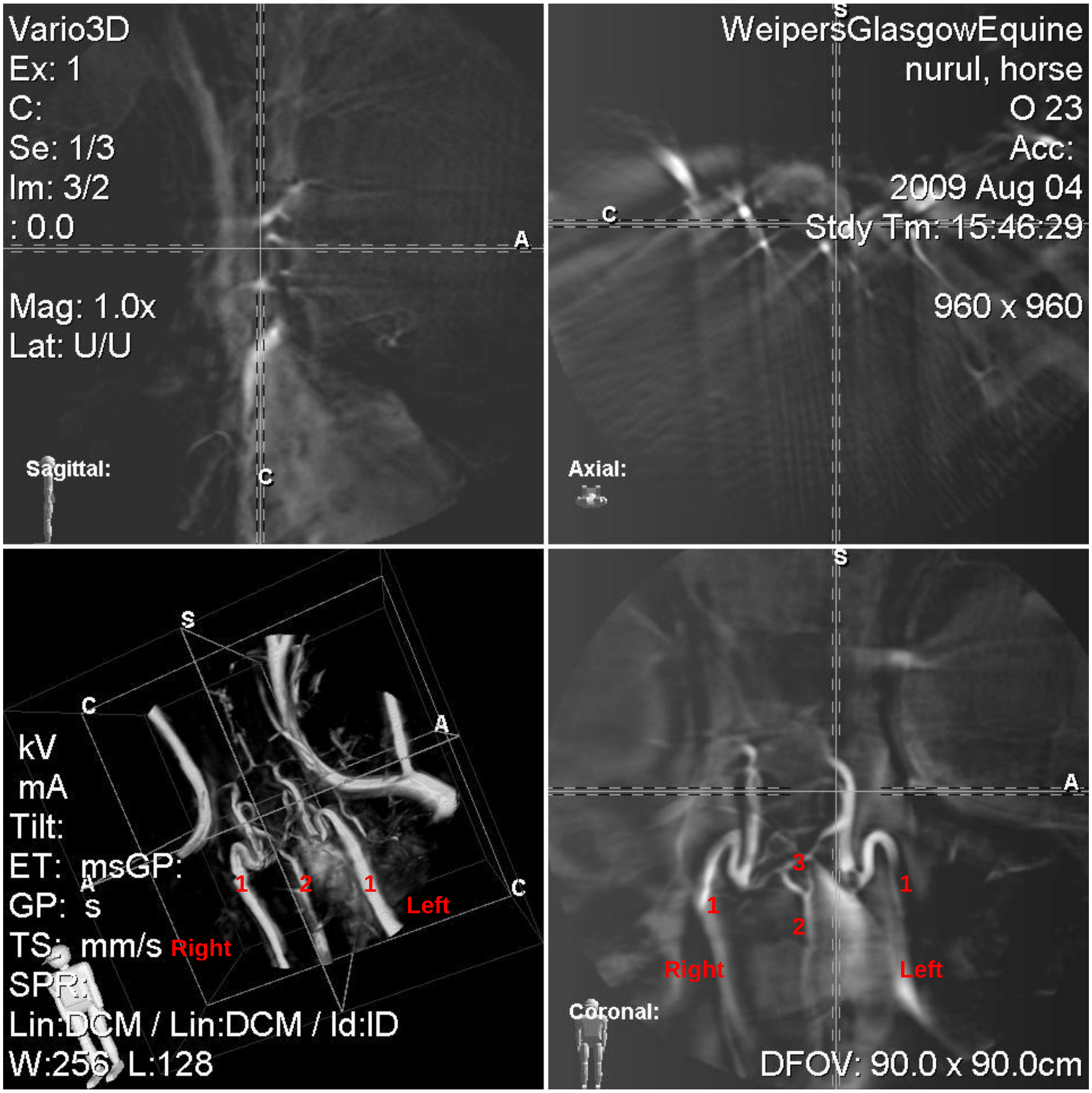

Figure 2-26: A 3D screenshot image that highlights a common pattern of the internal carotid artery and the formation of the cerebral arterial circle of a horse on the 3D volume view (left bottom quadrant) and the coronal slice view (right bottom quadrant).
The orientation on each quadrant is determined by the position of a cartoon man at the left side of the quadrants. The 3D volume view presentation is best viewed on software that supports this program. A axial; C coronal; S sagittal; 1 internal carotid artery; 2 basilar artery; 3 intercarotid artery.

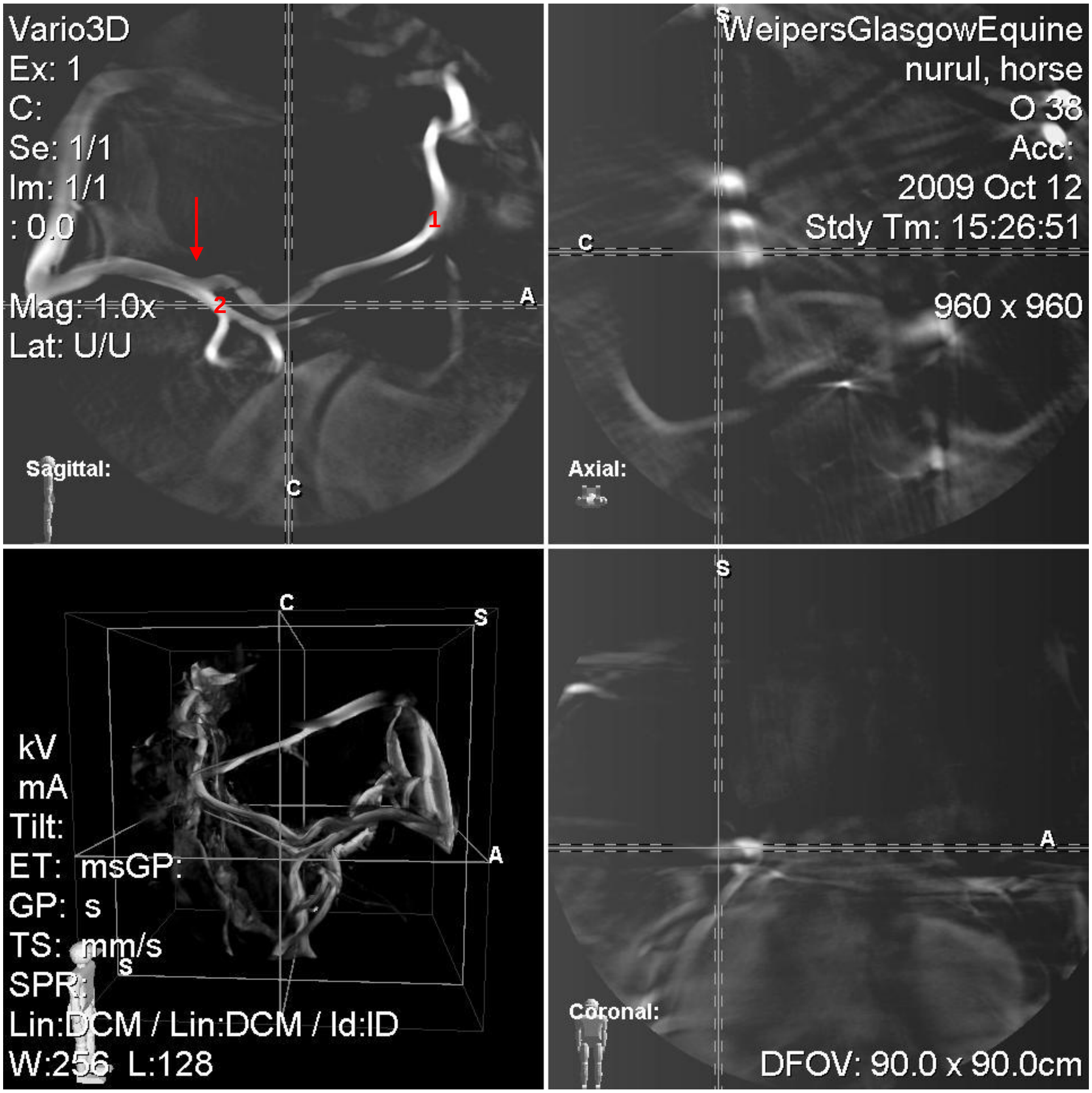

Figure 2-27: A 3D screenshot image of a horse that highlights the right internal carotid artery and the occipital artery sharing a common trunk from the common carotid artery.
The sagittal section provides the best plane to observe this anatomical variation (arrow). Position of the subject on the 3D volume view on this screenshot image impaired the ability to observe this variation. A axial; C coronal; S sagittal; 1 internal carotid artery; 2 occipital artery.

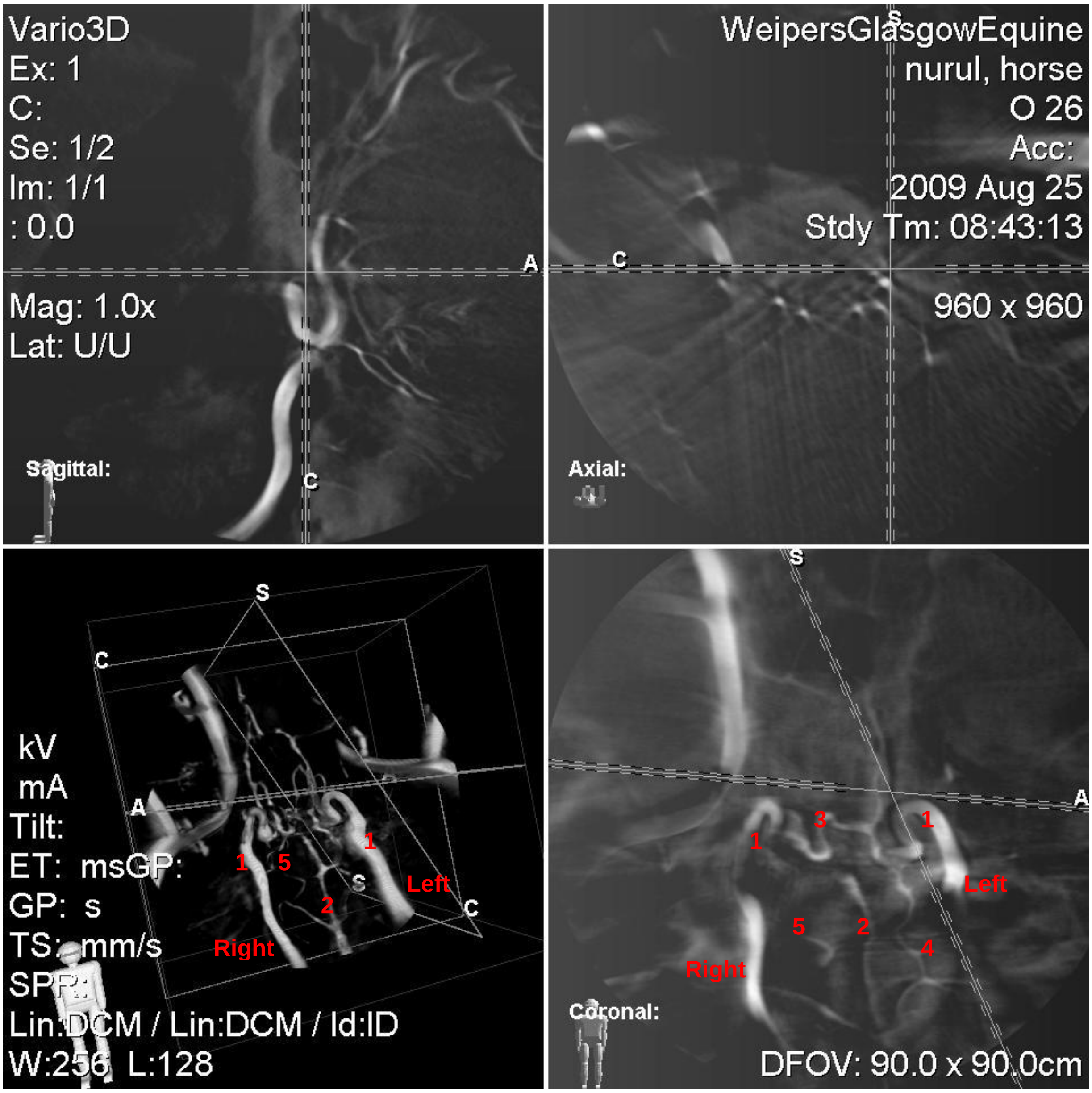

Figure 2-28: A 3D screenshot image of a horse that highlights bilateral presence of caroticobasilar artery (arrow on coronal slice).
Coronal plane showed the best image quality to observe this artery. A axial; C coronal; S sagittal; 1 internal carotid artery; 2 basilar artery; 3 intercarotid artery; 4 left caroticobasilar artery; 5 right caroticobasilar artery.

3 ANGIOGRAPHIC VARIATIONS OF THE CAROTID TRIFURCATION AND THE INTERNAL CAROTID ARTERY IN DONKEYS

3.1 Introduction

The angiographic appearance of the carotid trifurcation and the internal carotid artery of donkeys has been reported to be of a similar pattern to those of the horse (Colles and Cook, 1983). However, one major difference found was that the common carotid artery may terminate as four branches instead of three, where the linguofacial trunk (external maxillary artery) arises directly from the common carotid artery and not as a branch of the external carotid artery. Another difference noted was that the occipital artery of donkeys was larger than in horses (Colles and Cook, 1983).

There is a paucity of published literature relating to the internal carotid artery and the cerebral arterial circle of donkeys. However, in one report (Ozgel and Dursun, 2007) it was argued that the internal carotid artery intracranially bifurcates into caudal communicating and rostral cerebral arteries, with the middle cerebral artery branching from the rostral cerebral artery and not from the internal carotid artery. Contrary to what has been described in the horse, the internal carotid artery was considered to give off the caudal communicating artery and continue for a short distance rostrally to terminate as the rostral and middle cerebral arteries (Nanda, 1975). In other words, the rostral cerebral artery starts after the origin of the middle cerebral artery.

In addition, in one donkey a rostral intercarotid artery was observed in the cerebral arterial circle (Ozgel and Dursun, 2007). This was described as a thin vessel originating from the extension of the internal carotid artery (or should be called rostral cerebral artery) at the level where the internal carotid artery gives off the caudal communicating artery. The rostral intercarotid artery formed a connection to the contralateral vessel.

This study was carried out with two objectives: (i) to define and record the anatomy of the carotid trifurcation and the internal carotid artery in donkeys using 3D rotational angiographic imaging, and (ii) to determine the variation of the carotid trifurcation and the internal carotid artery between individual donkey.

3.2 Material and Methods

The head and neck of 26 donkeys were accumulated. There were no selection criteria; i.e. all available donkeys regardless of breed, age, sex and working purposes were studied. Donkeys were either euthanised or had died of natural causes. Signalment data were not recorded during collection of the specimens. However, no specimens originated from foals or foetuses. The donkeys' heads were donated by The Donkey Sanctuary and were transported from Devon to Glasgow. Ethical approval for the study had been granted by the Faculty of Veterinary Medicine Ethics and Welfare Committee and consent was obtained for use of the cadaver material.

3.2.1 Specimen Preparation

The donkey specimens used in this study were not injected with heparin prior to death, thus blood clotting in the vessels at post mortem was expected. With courtesy of the staff of the donkey sanctuary, the head and necks of the specimens were disarticulated from the body at the level of the 3rd and 4th cervical vertebrae ensuring that the guttural pouch and the carotid trifurcation remained intact. However, the muscles surrounding the cervical vertebrae were stripped off to allow identification of the point of disarticulation of the neck from the body. Specimens were collected and kept frozen at -20°C until they were ready to be transported to Glasgow. Information regarding time interval from death to freezing was unavailable.

The specimens were transported (from frozen) using a non refrigerated vehicle and some degree of thawing had occurred during transportation. Upon arrival of the specimens to the School of Veterinary Medicine, University of Glasgow, the donkey specimens were immediately stored in the freezer at -20°C, until the procedures were to be performed. The donkey specimens were thawed for 3-4 days. Then, both common carotid arteries were catheterised by advancing a 16Fr male Foley catheter into each common carotid artery for about 5-10 cm. The balloon on the tip of the catheter was inflated with 1-2 ml of water and a ligating suture placed caudal to the balloon to prevent the catheter from slipping out of the artery. These catheters were left in place for both angiographic procedure and subsequent arterial latex casting.

The arterial system was flushed with warm water using a manual garden pump via the catheter until no resistance was met and water could be seen flowing from the contralateral common carotid artery. This was an attempt to ensure that clotted blood and ice formation in the arteries were removed. Prior to angiography, the arterial system was flushed again to verify the patency of the arterial system.

3.2.2 Carotid and Cerebral Vascular Angiography Using Rotational Method

Rotational angiography of the carotid trifurcation and the internal carotid artery in donkey specimens was carried out using a Ziehm Vario 3D mobile fluoroscopic machine equipped with a C-arm unit (Figure 2-1) with minor alterations to the rotational angiographic method described in Chapter 2. The head was placed in left lateral recumbency on a board with two stands to support the weight of the specimen. To extend the guttural pouch, the head was pulled cranially from the neck.

The stand used for this experimental work was purposely designed to be used with the C-arm unit. Using this stand, the specimen was positioned between the X-ray generator and the image intensifier. The freely selectable positions of the scan centre allowed adjustment and defining of a scan centre in certain ranges without having to move the specimen. A laser positioning device aided in aligning and positioning of the C-arm on the exact region of interest.

Then, approximately, 15- 20ml of contrast material (Barium sulphate) was injected into the left common carotid artery to fill the carotid arterial tree to the level of internal carotid artery in the cranium. A further 15-20ml of contrast material was injected to allow filling of the cerebral vessels and the contralateral carotid arterial tree. After injection of contrast, the Foley catheters on both sides were clamped to prevent leakage of the contrast agent during image acquisition. Then, three ball bearing markers were placed in a triangular configuration at the right lateral side of the carotid trifurcation to mark or identify the right carotid arterial tree from the left side during rotational angiographic analysis.

A radiograph was taken prior to rotational scanning to ensure the scan centre was positioned at the centre of the internal carotid artery, between the carotid trifurcation and the caudal rostral quadrant of the cerebral arterial circle.

Then, automatic rotational scanning was initiated by activating the Iso-Cine and 3D operating modes. Step by step protocols on the Iso-Cine mode of the Ziehm Vario 3D fluoroscopic unit were followed as per the equipment instruction manual (Ziehm, 2007). Due to the smaller size of the donkey head compared to the horse, a single cycle of automatic scanning was enough to visualise both the carotid trifurcations and the internal carotid arteries in a single screen.

Each scan took approximately two minutes for the C-arm to complete a 136° angle of rotation. With each cycle of automatic scanning, 112 sequences of radiographic images were captured at different angles and these images could be played like a movie in the Cine-Loop function. A Cine-Loop function consists of multiple or several fluoroscopic images that are acquired in sequence. As well as being able to be played like a movie, they can also be post edited later.

3.2.2.1 Three dimensional multiplanar reconstruction image

After acquisition of the rotational angiographic images, the 3D multiplanar reconstruction (3D-MPR) images of the subject were generated on the fluoroscopic unit computer system. Multi-planar reconstruction (MPR) was launched by pressing the 3D-MPR button after the completion of an automatic scan to produce a 3D representation of the vessels on all the donkey specimens. All donkeys which had 3D imaging done had 3D-MPR images taken as screenshots. Step by step protocol on 3D-MPR mode on the Ziehm Vario 3D fluoroscopic unit were followed (Ziehm, 2007).

3.3 Results

3.3.1 Angiographic Variations of the Internal Carotid Artery

A common/standard anatomical pattern of the internal carotid artery and its pathway in donkeys are similar to that observed in the horse (Figure 3-1). Rotational angiography of bilateral carotid trifurcation and internal carotid artery was performed on 26 donkeys, producing 52 angiograms. Thirty nine angiograms demonstrated a common pattern and 13 had variations. A list of carotid angiographic findings in donkey specimens is shown in Table 3-1.

The angiographic dissimilarities seen involved variations at the termination of the common carotid artery. Sharing of a common trunk with the occipital and the internal carotid arteries was observed unilaterally in one donkey (Figure 3-2). Five angiograms demonstrated the linguofacial trunk originating from the common carotid artery (Figure 3-3). In five other angiograms, it appeared that the linguofacial trunk shared a common origin with the external carotid artery (Figure 3-4).

Another interesting finding in two angiograms was that the internal carotid artery originated much more caudal to the occipital artery (Figure 3-5), compared to the common anatomical pattern. The distance of the origin of the internal carotid artery to the termination of the common carotid artery was neither measured nor recorded during angiography, but was measured during dissection. An aberrant branch of the internal carotid artery was not seen in these donkeys as observed in horses.

As a whole, bilateral variations were seen in one donkey, and unilateral variation in 11 donkeys. Out of 13 angiograms with variations, it was noted that nine variations were on the left side and four on the right.

3.3.2 Angiography of the Intracranial Portion of the Internal Carotid Artery and the Cerebral Arterial Circle

A list of cerebral angiographic findings with regards to the arrangement of the cerebral arterial circle and the presence of caroticobasilar artery in donkey specimens is shown in Table 3-2. With regard to the cerebral arterial circle, irregularities concerning the basilar artery were seen in two donkeys where the pathway was not straight (Figure 3-6).

The presence of the caroticobasilar arteries could be appreciated in 20 donkeys, either unilaterally (10) or bilaterally (10). Figure 3-6 shows an example of unilateral presence of this artery and Figure 3-7 shows a bilateral presence. However, several eccentric connections were seen in addition to this artery in certain donkeys. In two donkeys, a small vessel originating from the second curve of the sigmoid flexure of the left internal carotid artery was seen to be connected to the caudal intercarotid artery (Figure 3-8). In another donkey, an eccentric connection was seen on the left side where a vessel originating from the second curve of the sigmoid flexure was observed to join the caudal communicating artery before that artery joined the basilar artery to form the caudolateral quadrants of the cerebral arterial circle (Figure 3-9).

On the other hand, in one donkey, it was thought that the caudal intercarotid artery was absent but its presence was confirmed with repeated views of Cine-Loop function (Figure 3-10).

3.3.3 Cine-Loop Function

Dynamic movements of the carotid arterial tree up to the level of the cerebral arterial circle in donkeys were observed in 2D angiographic series using the Cine-Loop function in the Iso-Cine mode.

A list of outcomes on Cine-Loop function and 3D-MPR representation can be referred to in Table 3-3, where the image qualities were graded subjectively into good, partial and poor quality. A good quality Cine-Loop reflected a high quality angiographic series of the vessels with complete delineation within the region of the scan centre. Any angiographic series that suffered issues related to technical flaws that occurred on less important regions of the targeted vessel would be considered to be of partial quality. Poor quality images were defined as angiograms that impaired the observation of the whole carotid trifurcation. In the donkey specimens, good quality Cine-Loop could be appreciated in 13 donkeys, eight were considered partial, and another five were of poor quality.

A common/standard anatomical pattern of the carotid trifurcation and internal carotid artery, including the formation of the cerebral arterial circle are illustrated in video 3-1. Sharing of a common trunk by the occipital and the internal carotid arteries can be evidenced in video 3-2. Variation at the termination of the common carotid artery can be seen in video 3-3 and 3-4, where the origin of the linguofacial trunk differs.

In video 3-5, it was observed that the linguofacial trunk originating from the common carotid artery (rather than originating from the external carotid) and the internal carotid originated more caudal from the carotid termination. This variation was difficult to appreciate from the accepted common anatomical pattern of this structure.

In one donkey, the caudal intercarotid artery was very small and tortuous, thus difficult to identify, and even thought to be absent. The presence of this artery at the level of the cerebral arterial circle in this donkey was confirmed and was best detected and viewed using Cine-Loop function (video 3-6).

3.3.4 Three Dimensional with Multi-Planar Reconstruction (3D-MPR)

All 26 donkey heads underwent bilateral rotational angiography with 3D reconstruction imaging of the carotid trifurcation, the internal carotid artery and the cerebral arterial circle. Issues regarding 3D-MPR quality were observed to be similar to those described in the horse in the previous chapter (2), where the 3D-MPR images quality depends on the quality of the angiographic series on the Cine-Loop function. Following 3D reconstruction of an image, a screenshot of the 3D-MPR images were generated.

Seven specimens demonstrated good quality 3D-MPR, where all the vessels within the range of the scan centre were able to be reconstructed successfully. Four others were considered satisfactory or regarded as partial quality because reduced visibility of small vessels and interruptions occurred on unimportant regions of the targeted vessel. Another 12 were classified as poor quality images due to poor reconstruction quality. Failure to launch 3D operating mode due to technical issues occurred in three donkey specimens. The outcomes of the Cine-Loop function and 3D-MPR representation in all the donkey specimens can be referred to in Table 3-3.

A 3D screenshot of the common anatomical pattern of the carotid trifurcation, the internal carotid artery and the cerebral arterial circle are shown in Figure 3-11. A screenshot of the occipital artery and the internal carotid artery sharing a common trunk is shown in Figure 3-12. The difference in the origin of the linguofacial trunk can be appreciated in the 3D-MPR (Figure 3-13 and Figure 3-14), although it was fairly limited compared to the Cine-Loop function. A 3D screenshot of an internal carotid artery originating much more caudal to the carotid termination was not of very good quality because the image was sliced more proximal than the exact origin of the internal carotid artery (Figure 3-15).

3.4 Discussion

3.4.1 Similarities of Issues with Rotational Angiography of the Horse

In the previous chapter, issues regarding angiographic interpretation have been described and discussed. Not surprisingly, the same problems that created challenges in terms of interpretation in the horse were also seen in the angiograms from the donkeys, despite the smaller head size. Cine-Loop function in rotational angiography of the carotid arterial tree and the cerebral arterial circle in donkeys produced superior quality angiograms. As the size of donkey heads were much smaller than the horse specimens, the whole carotid trifurcation up to the level of cerebral arterial circle could be viewed in a single frame of the Cine-Loop function. However, issues with the 3D-MPR were also seen in the donkeys as in the horses.

3.4.2 Quality of Specimens

Autolytic post mortem changes were seen in most of the donkey specimens received. These post mortem changes most likely arose as a result of the distance and length of time taken to transport the specimens. Decomposition of tissue was perhaps made worse as the muscles surrounding the cervical vertebrae were stripped from the neck to the base of the skull for the purpose of identification of the joint of the third and fourth cervical vertebrae. Furthermore, the arteries of decomposed cadaveric material appeared misshapen, making identification of the individual arteries harder. Angiographic contrast quality also deteriorated with poor quality cadaver material as the contrast materials leaked through the sloughed muscles and the cervical joints.

The donkey specimens were kept in the freezer at -20ºC for quite some time. Because of this, some of the donkey necks were flexed and appeared to be bent awkwardly even after they had been fully thawed. This created problems in orientation and positioning of the specimen during angiography. Technically, the angiography rotation moves from the lateromedial to dorsoventral view. However, the flexed head and neck of the specimens caused the angiographic view to be orientated caudal to cranial.

In some donkeys, the necks were disarticulated very close to the termination of the common carotid artery. Due to the very short common carotid artery before the carotid trifurcation, it was difficult to secure the Foley catheter as satisfactorily as would have been liked along the carotid artery. Insecure placement of the catheter caused backflow of contrast material from the artery. Sometimes, because of the pressure applied while injecting the contrast, the catheter itself could be displaced from the artery. In donkeys that were presented with a short common carotid artery, the Foley catheter had to be inserted within the carotid trifurcation and this resulted in some degree of dilatation at the carotid bulb, which became more difficult to secure. In order to prevent the catheter slipping out, a ligature incorporating the vessel and fluid filled balloon catheter was placed.

3.4.3 Importance of Findings

Based on the angiographic findings, the carotid trifurcation of the donkeys (39/52 angiograms) showed a similar pattern to those found in horses. The variations of this structure in the donkeys (13/52) were listed as follow:

1. Internal carotid artery and occipital artery share a common trunk (1/13)
2. Linguofacial trunk seen as a branch of the common carotid artery, rather than from the external carotid artery (5/13 angiograms with anatomical variation)
3. Linguofacial trunk actually share a common trunk of origin with the external carotid artery (5/13)
4. The internal carotid artery originated more caudal from the common carotid artery termination (2/13)

Earlier carotid angiographic observations of a donkey, described the origin of linguofacial trunk as from the common carotid artery and not as a branch of the external carotid artery as is the case in the horse (Colles and Cook, 1983).

However, this observation was based on a single donkey, thus this finding cannot be regarded as conclusive. Based on our findings regarding the linguofacial trunk, its anatomical arrangement may create confusion in terms of where exactly the linguofacial trunk originates. Perhaps, the length of the external carotid artery was very short before it gave off the linguofacial trunk, which made it appear that the linguofacial trunk shared a common origin with the external carotid artery. It is suggested that in donkeys presented with this type of arrangement, the linguofacial trunk shares a common trunk with the external carotid artery.

A variation of the carotid trifurcation found in the donkey, similar to the variation found in the horse, was that the internal carotid artery and occipital artery shared a common trunk. Interestingly, an aberrant branch of the internal carotid artery was not seen in any of the donkeys studied.

The origin of the internal carotid artery in two angiograms of donkeys was observed to be commencing more caudal than the common anatomical pattern of this structure. Usually, the internal carotid artery always originated very close to the occipital artery. In donkeys that have a linguofacial trunk originating from the common carotid artery and an internal carotid artery originating very caudal to the termination of the common carotid, there may be confusion in identifying the internal carotid artery, given the assumption that the common carotid artery terminates into three branches. One may mistakenly think that the internal carotid artery was absent, or worse, identify the occipital artery as the internal carotid artery.

Apart from the caroticobasilar, another peculiar artery was seen originating from the level of sigmoid flexure of the internal carotid artery and connected to the caudal intercarotid artery (2 donkeys) or to the caudal communicating artery (1 donkey). However, Frackowiak et. al (1997) in a dissection study reported that the caroticobasilar artery may form a communication with the caudal intercarotid artery, and noted this observation was not seen in all horses, Przewalski's horses and in donkeys. After careful evaluation of the two dimensional angiographic series of the cerebral arterial circle in these angiograms, one might speculate that this observation was as a result of superimposition artefact and technical limitations. Due to the complex three dimensional structures of the cerebral arterial circle and its connections, the best way to verify the continuation of these eccentric vessels is by viewing its three dimensional display using the 3D-MPR function. However, due to the fact that the 3D-MPR representations faced some limitations of its own, further investigation on these eccentric vessels could not be carried out accordingly.

It is important for veterinarians to be aware that the variations of the carotid termination of donkeys may differ from those described in the horse. This information would be particularly important in any surgery or treatment involving the carotid arterial tree, especially in cases of guttural pouch mycosis. Even though mycosis of the guttural pouch in the donkeys is believed to be rare or most likely under reported, opportunities for error in identifying which artery to be occluded are apparent. The findings described provide invaluable information for surgeons who may attempt to occlude internal carotid, external carotid or occipital arteries without the aid of image intensification, i.e, to perform a balloon tipped catheter technique as a treatment of guttural pouch mycosis.

Table 3-1: Carotid angiography findings in donkey specimens

Donkey	Right	Left
1	N	N
2	N	O
3	N	Ø
4	O	Ø
5	N	N
6	N	N
7	N	O
8	N	N
9	N	Y
10	O	N
11	O	N
12	N	N
13	N	N
14	N	N
15	N	N
16	N	Δ
17	N	N
18	Y	N
19	N	N
20	N	Ø
21	N	N
22	N	Ø
23	N	N
24	N	N
25	N	Ø
26	N	N

N: Common/standard anatomical pattern of the carotid trifurcation and internal carotid artery

Δ: Internal carotid artery and occipital artery share a common trunk

O: Linguofacial trunk share a common origin with external carotid artery

Ø: Linguofacial trunk arise directly from common carotid artery

Y: Origin of internal carotid artery very caudal to the carotid termination

Table 3-2: Cerebral angiographic findings in donkeys

Donkey	Arrangement of cerebral arterial circle	Caroticobasilar artery
1	Common pattern, basilar a. not straight	Absent
2	Common pattern	Left
3	Common pattern	Bilateral
4	Common pattern	Bilateral
5	N/A	N/A
6	Common pattern	Bilateral
7	Common pattern	N/A
8	Common pattern	Left
9	N/A	N/A
10	Common pattern	Bilateral
11	Common pattern	Left
12	Peculiar connection 1	Left
13	Common pattern	Right
14	Common pattern	Bilateral
15	Peculiar connection 2	Bilateral
16	Common pattern	Left
17	Peculiar connection 2	Bilateral
18	N/A	N/A
19	Common pattern	Left
20	Caudal intercarotid was very small	Bilateral
21	Common pattern	Absent
22	Common pattern	Left
23	Common pattern	Bilateral
24	Common pattern	Left
25	Common pattern	Bilateral
26	Common pattern, basilar a. not straight	Right

Cerebral arterial circle

Peculiar connection 1 = A connection from the second curve of sigmoid flexure of internal carotid artery to the caudal communicating artery (1)

Peculiar connection 2 = A connection from the second curve of sigmoid flexure of internal carotid artery to the intercarotid artery (2)

Common pattern of cerebral arterial circle (17)

Common pattern of cerebral arterial circle but basilar artery was not straight (2)

N/A = Not able to be appreciated (3)

Caroticobasilar artery

Absent (2)

Bilateral (10)

Left (8)

Right (2)

Table 3-3: List of imaging quality using Cine-Loop and 3D-MPR in donkey specimens

Donkey	Cine-Loop (Carotid and cerebral vessels)	3D-MPR (Carotid and cerebral vessels)
1	+	NA
2	+	NA
3	±	X
4	+	+
5	X	X
6	+	±
7	+	+
8	±	X
9	±	±
10	X	X
11	±	±
12	+	±
13	+	+
14	X	X
15	+	+
16	+	+
17	±	X
18	X	X
19	±	X
20	+	+
21	X	X
22	+	+
23	±	X
24	+	X
25	±	NA
26	+	X

Cine-Loop Total:

+ = Good quality (13)

± = Partial quality (8)

X = Poor quality (5)

NA = Not activated/Not launched

3D-MPR Total:

+ = Good quality (7)

± = Partial quality (4)

X = Poor quality (12)

NA = Not activated/Not launched (3)

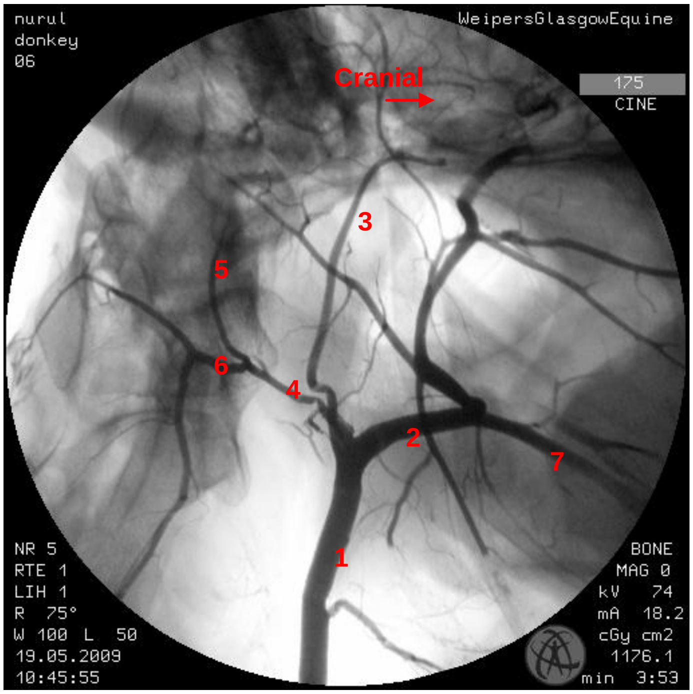

Figure 3-1: Lateral angiogram (left) of the common pattern of the carotid trifurcation and the internal carotid artery of a donkey.
1 common carotid artery; 2 external carotid artery; 3 internal carotid artery; 4 occipital artery; 5 cranial branch of occipital artery; 6 caudal branch of occipital artery; 7 linguofacial trunk (x 1/3).

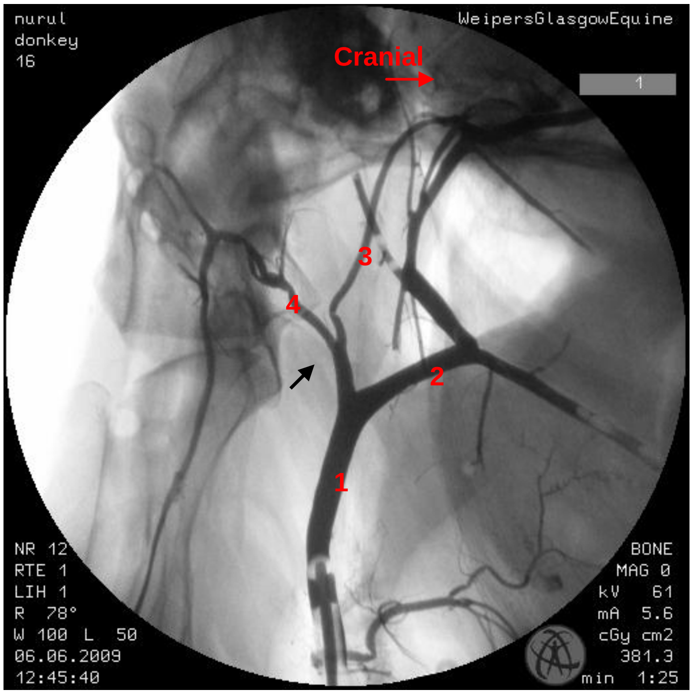

Figure 3-2: Lateral angiogram of the left carotid arterial tree of a donkey shows variation from the common pattern of this structure where the occipital and the internal carotid arteries share a common trunk (black arrow).
1 common carotid artery; 2 external carotid artery; 3 internal carotid artery; 4 occipital artery (x 1/3).

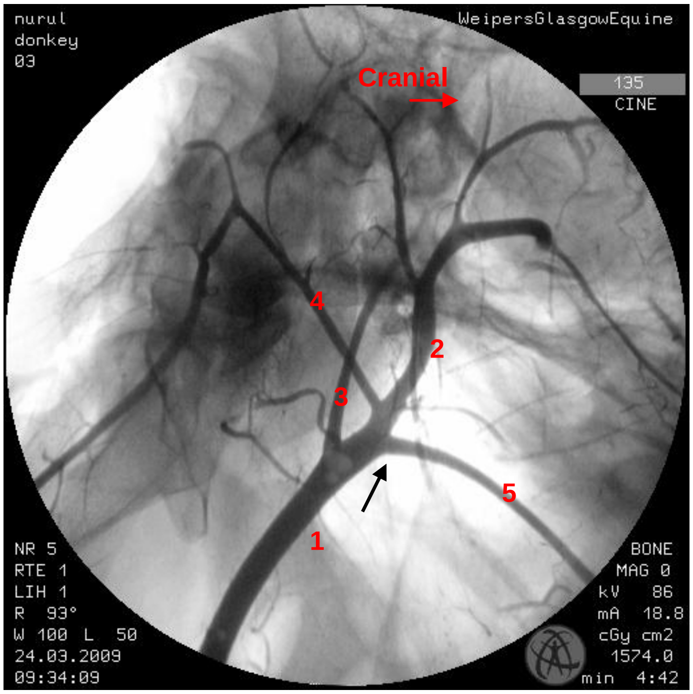

Figure 3-3: Lateral angiogram of the left carotid arterial tree of a donkey shows variation from the common pattern of this structure. The origin of the linguofacial trunk (black arrow) is directly from the common carotid artery.
1 common carotid artery; 2 external carotid artery; 3 internal carotid artery; 4 occipital artery; 5 linguofacial trunk (x 1/3).

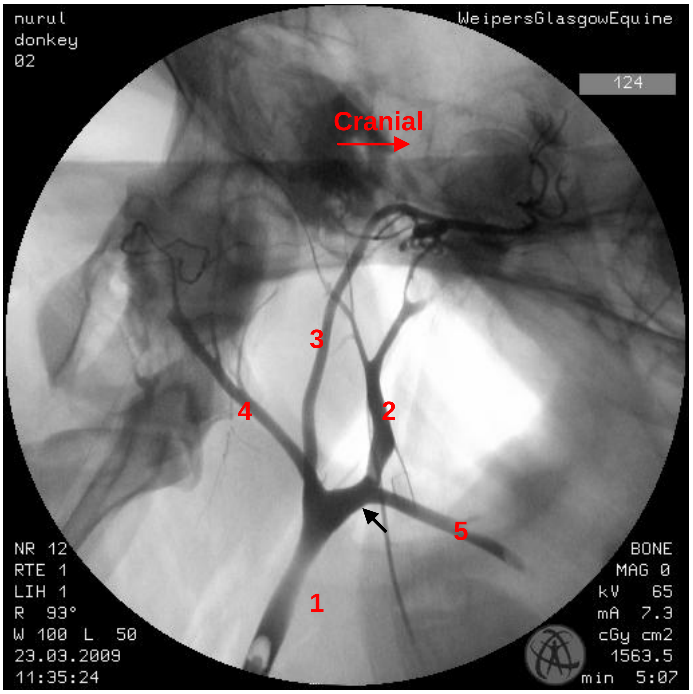

Figure 3-4: Lateral angiogram of the left carotid arterial tree of a donkey shows variation from the common pattern of this structure. The linguofacial trunk shares the same origin with the external carotid artery (black arrow).
1 common carotid artery; 2 external carotid artery; 3 internal carotid artery; 4 occipital artery; 5 linguofacial trunk (x 1/3).

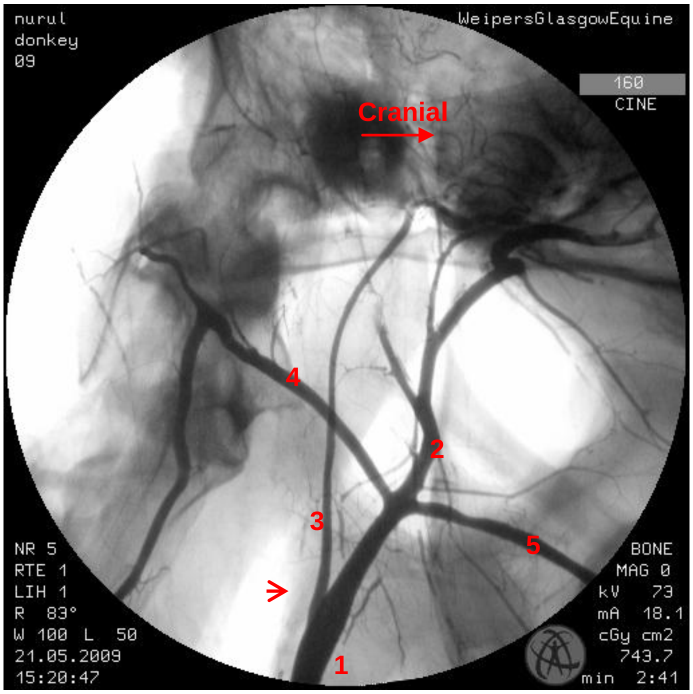

Figure 3-5: Lateral angiogram of the left carotid arterial tree of a donkey shows variation from the common pattern of this structure. The left internal carotid artery (red open arrow) originates very caudal to the common carotid artery termination.
1 common carotid artery; 2 external carotid artery; 3 internal carotid artery; 4 occipital artery; 5 linguofacial trunk (x 1/3).

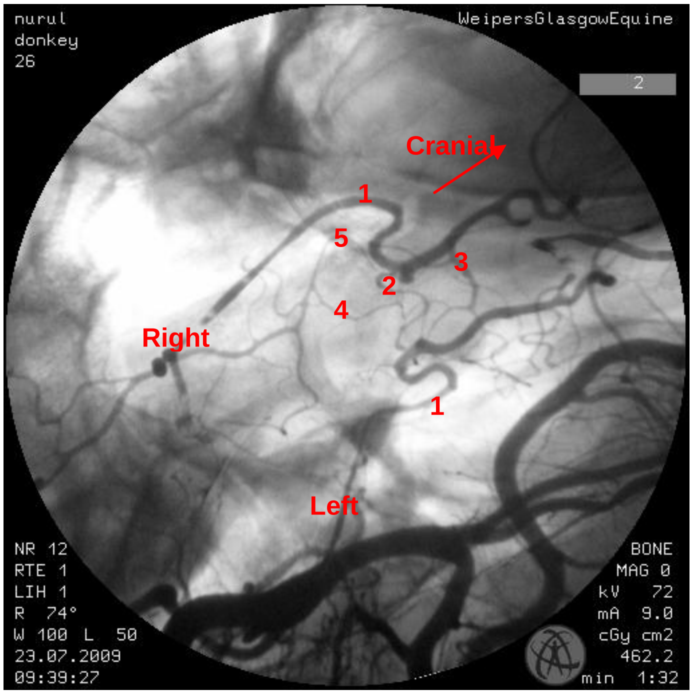

Figure 3-6: Dorsoventral angiogram of the cerebral arterial circle of a donkey. The basilar artery was not straight and leaning more to the right side. Note the presence of the right caroticobasilar artery (arising from the second curve of the internal carotid artery).
1 internal carotid artery; 2 intercarotid artery; 3 caudal communicating artery; 4 basilar artery; 5 caroticobasilar artery (x 1/3).

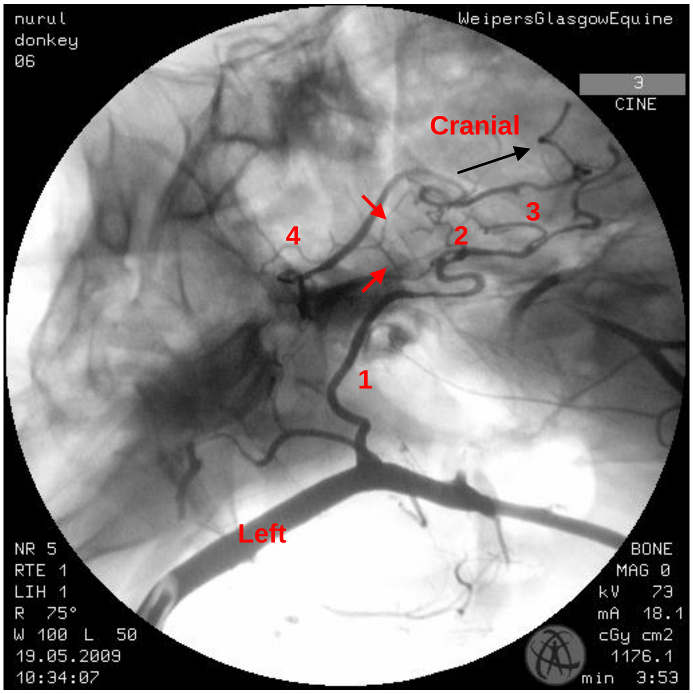

Figure 3-7: Dorsoventral angiogram of the common pattern of the internal carotid arteries and formation of the cerebral arterial circle of a donkey. Note the bilateral presence of caroticobasilar arteries (red arrows).
1 internal carotid artery; 2 intercarotid artery; 3 caudal communicating artery; 4 basilar artery (x 1/3).

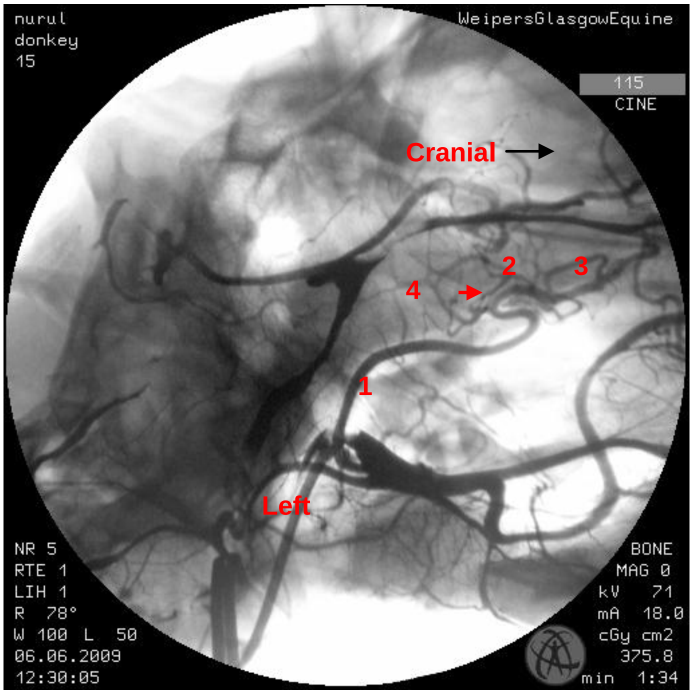

Figure 3-8: Dorsoventral angiogram of the cerebral arterial circle of a donkey. A peculiar connection is seen (red arrow) from the second curve of sigmoid flexure of the internal carotid artery to the caudal intercarotid artery. This connection may be due to superimposition artefact.
1 internal carotid artery; 2 intercarotid artery; 3 caudal communicating artery; 4 basilar artery (x 1/3).

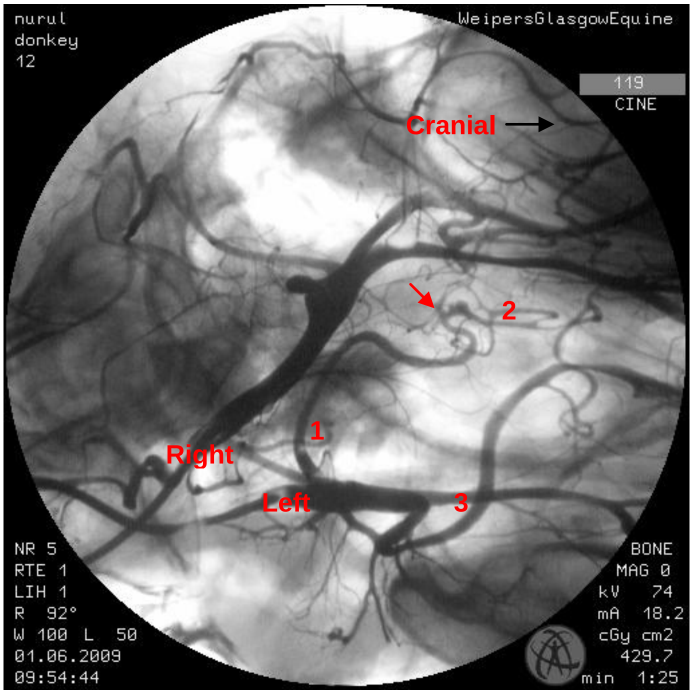

Figure 3-9: Dorsoventral angiogram of the cerebral arterial circle of a donkey. A connection is seen from the second curve of the right internal carotid artery to the caudal communicating artery (red arrow). This connection may be due to superimposition artefact.
1 internal carotid artery; 2 caudal communicating artery; 3 external carotid artery (x 1/3).

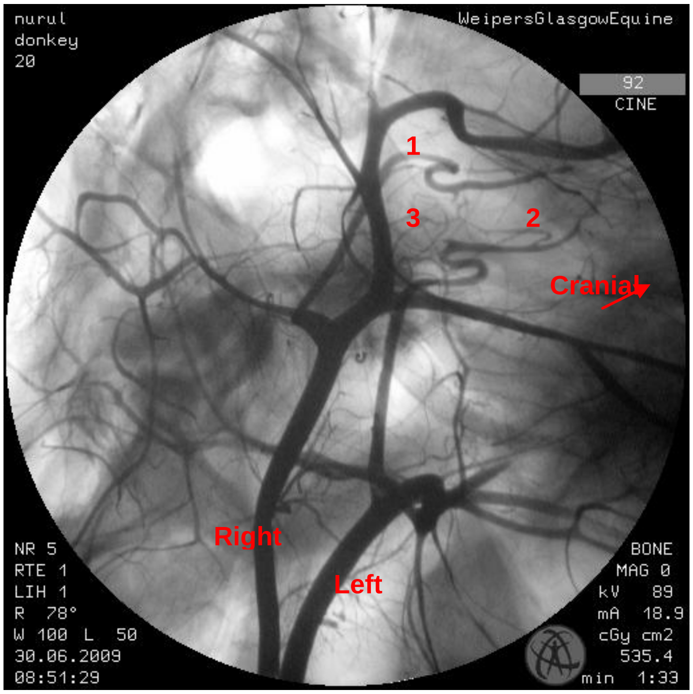

Figure 3-10: Oblique angiogram of the carotid and cerebral vessels of a donkey where the caudal intercarotid artery was very small and tortuous, making identification more difficult.
1 internal carotid artery; 2 caudal communicating artery; 3 basilar artery (x 1/3).

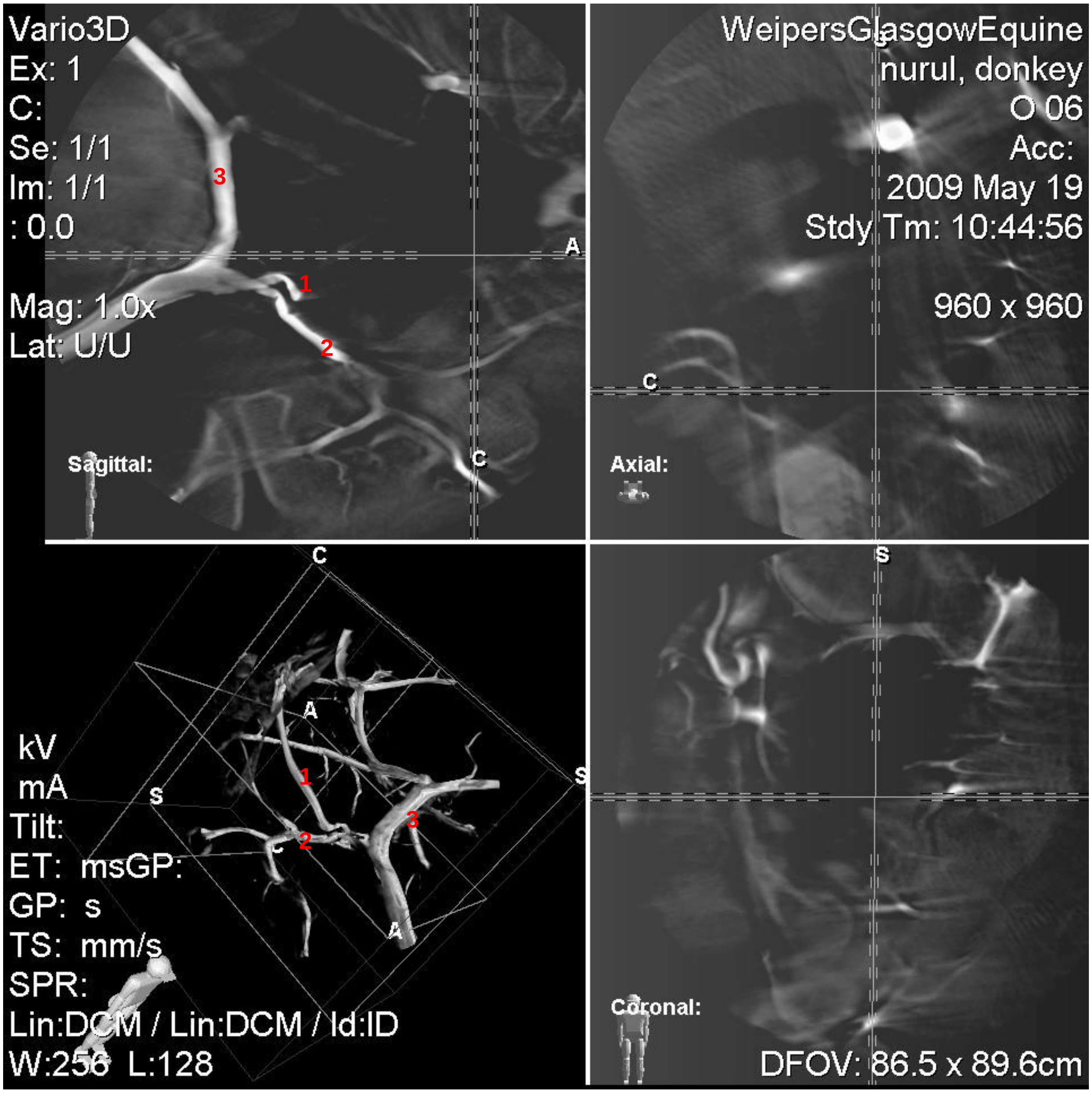

Figure 3-11: A 3D screenshot image of a donkey to highlight the common pattern of carotid trifurcation of the donkey (left). Part of the left internal carotid artery was lost during rendering in the sagittal view (top left quadrant). The 3D volume view (left bottom quadrant) provides a better reconstruction on the subject.
The orientation on each quadrant is determined by the position of a cartoon man at the left side of the quadrants. The 3D volume view presentation is best viewed on software that supports this program. 1 internal carotid artery; 2 occipital artery; 3 external carotid artery.

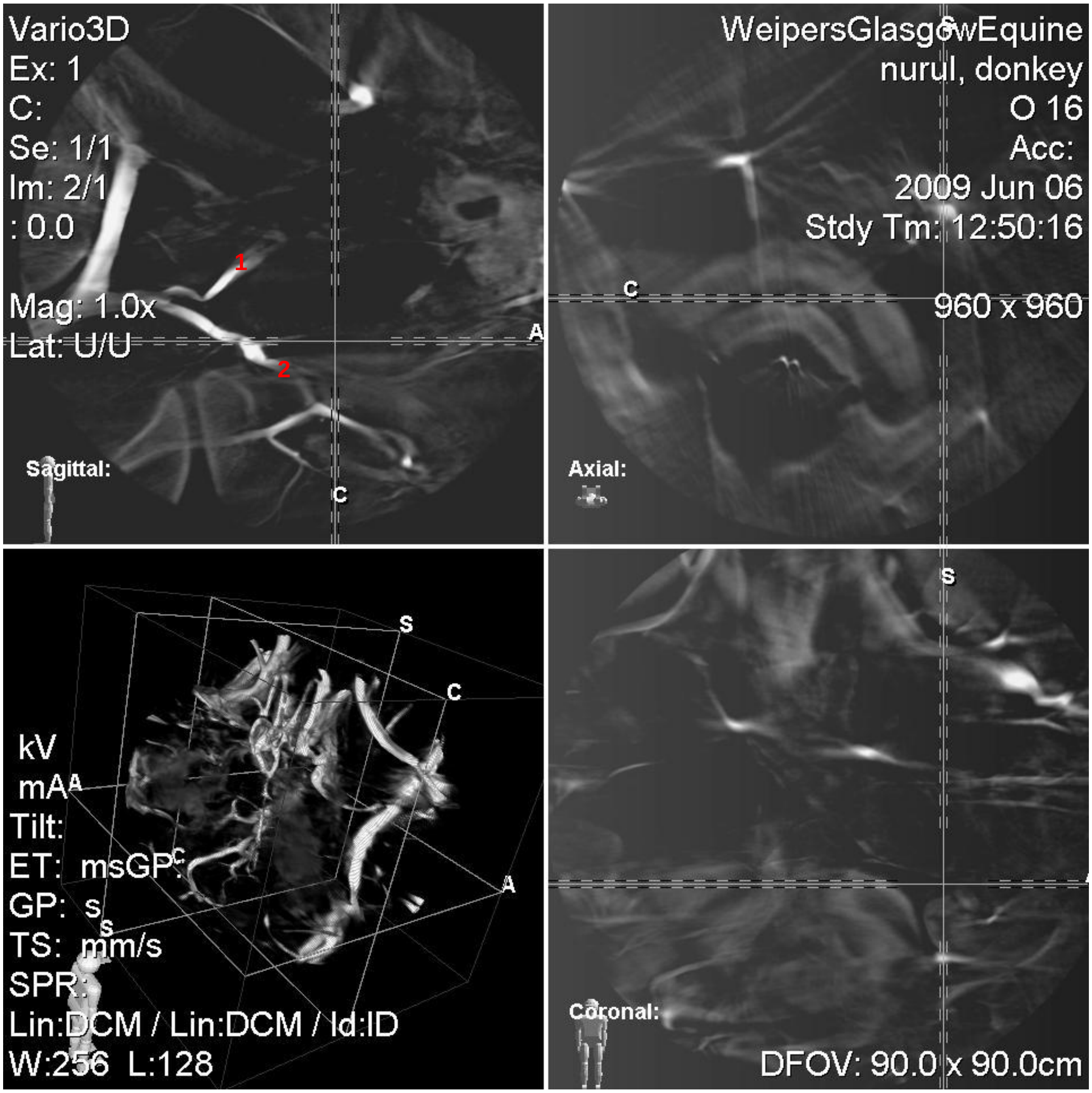

Figure 3-12: A 3D screenshot image of the carotid arterial tree of a donkey shows variation from the common pattern of this structure. On sagittal view, the left internal carotid artery shares a common trunk with the occipital artery.
Position of the subject on the 3D volume view (left bottom quadrant) on this screenshot image impaired the ability to observe this variation. 1 internal carotid artery; 2 occipital artery.

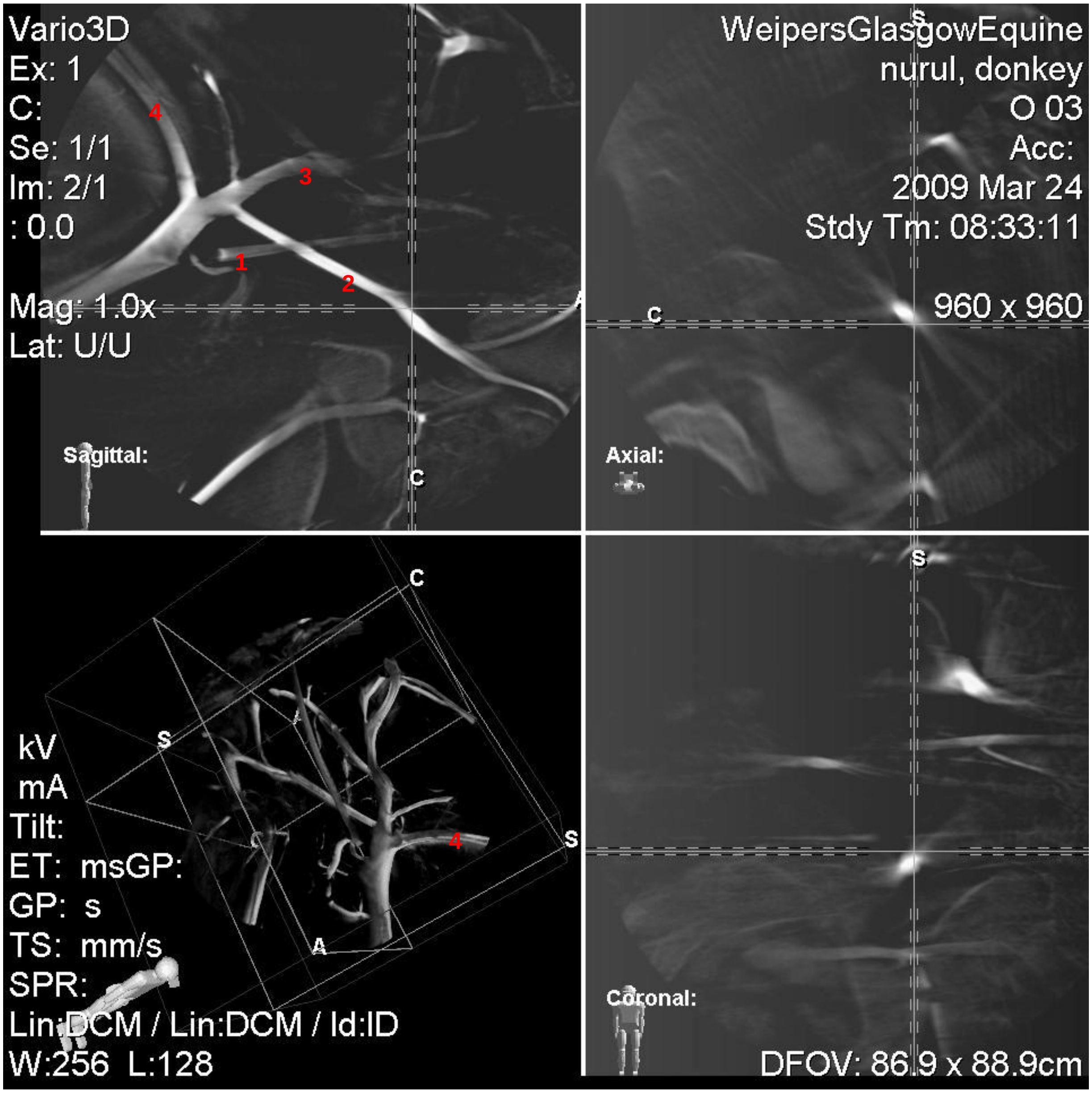

Figure 3-13: A 3D screenshot image of the left carotid arterial tree of a donkey shows variation from the common pattern of this structure. Note that the linguofacial trunk originates from the common carotid artery.
However on the sagittal view, there is a gap at the origin of the internal carotid artery due to a gas bubble which is not seen on the 3D volume view due to positioning. 1 internal carotid artery, 2 occipital artery, 3 external carotid artery, 4 linguofacial trunk.

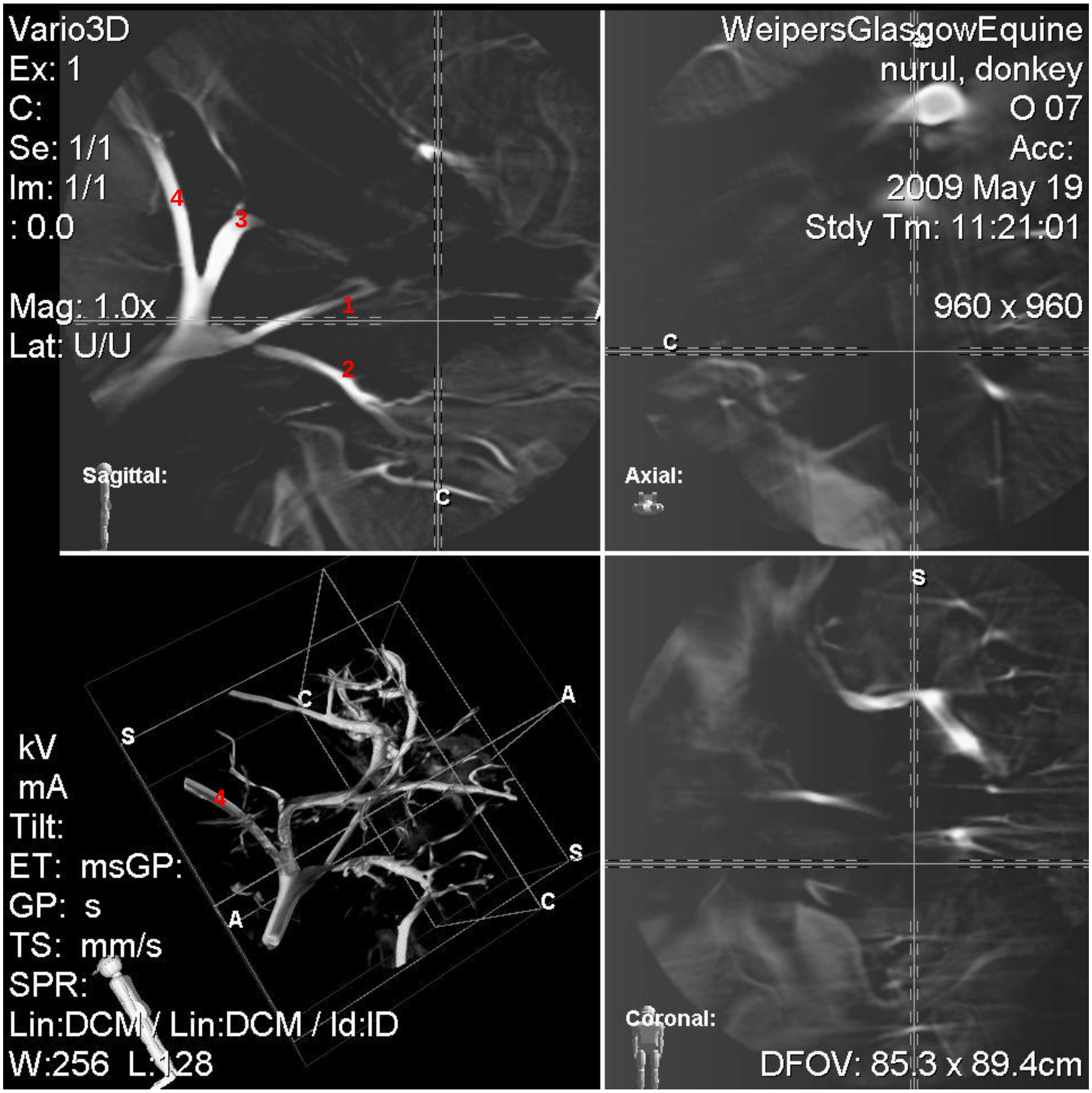

Figure 3-14: A 3D screenshot image of the left carotid arterial tree that highlights the linguofacial trunk sharing a common origin with the external carotid artery.
Sagittal section and the 3D volume view provide the best plane to observe this anatomical variation. 1 internal carotid artery, 2 occipital artery, 3 external carotid artery, 4 linguofacial trunk.

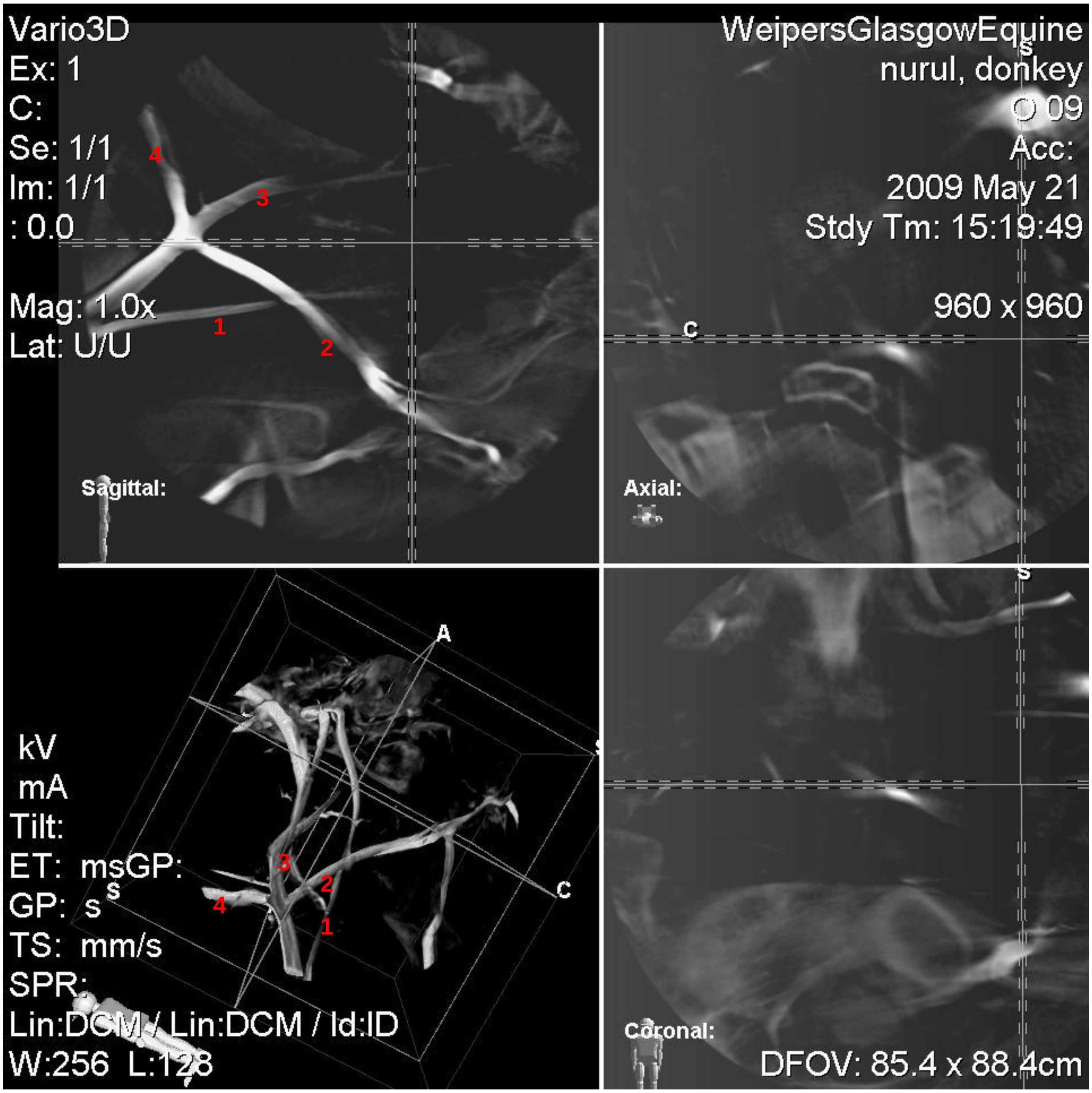

Figure 3-15: A 3D screenshot image of the left carotid arterial tree of a donkey that shows variation from the common pattern of this structure. The internal carotid artery originates very caudal to the carotid termination, and the linguofacial trunk originating from the common carotid artery.
Sagittal section and the 3D volume view provide the best plane to observe these anatomical variations. 1 internal carotid artery, 2 occipital artery, 3 external carotid artery, 4 linguofacial trunk.

4 Angiographic Study of the Carotid Trifurcation and the Internal Carotid Artery in a Zebra

4.1 Introduction

Zebras belong to another member of the family Equidae and are of course well known for their distinctive black and white stripe patterned hair coat. This pattern is unique to each individual zebra. Unlike their closest equine relatives, zebras were never truly domesticated like the horse or the donkey. There are three species of zebra that are included in the genus *Equus*; the plains zebra (*Equus quagga,* formerly known as *E. burchelli),* Grevy's zebra (*E. grevyi*) and the mountain zebra (*E. zebra*). The plains zebras are also known as the common zebra or Burchell's zebra.

There has been sparse research interest in this species with regard to cerebral vascular anatomy, which has been focused on thermoregulatory adaptation in their natural hot habitat. Zebra like any other equidae, do not posses a carotid rete mirabile and it has been alleged that selective brain cooling does not occur in the zebra (Fuller et al., 2000, Mitchell et al., 2002).

There is a paucity of literature concerning the angiographic anatomy of the blood supply to the zebra's brain. Nevertheless, it was found that the similarities between the horse and zebra were obvious, with only one notable exception (Du Boulay and Verity, 1973). In the horse, after the internal carotid artery passes through the foramen lacerum (fibrocartilaginous skull base) it forms a communication with contralateral side via the intercarotid artery. However, in the zebra the internal carotid artery after it passes through the foramen lacerum forms an anastomotic network of vessels to provide supply to the ventral surface of the brain stem. It was also reported that the basilar artery of a zebra deviated from the midline and interconnected by small indirect channels with interconnecting branches (Du Boulay and Verity, 1973).

An opportunity to study this species arose when a zebra was sent to the post mortem unit, Pathology department of the School of Veterinary Medicine, University of Glasgow from a local safari park. The cause of death of the specimen was determined to be due to impaction colic. Signalment data were not recorded during collection of the specimen. Since there was very limited information regarding zebra and its cerebral vascular anatomy in the literature, it appeared that there was academic value in studying the angiographic anatomy of this animal.

This investigation was carried out with the objective to define and record the anatomy of the carotid trifurcation and the internal carotid artery up to the level of cerebral arterial circle in the zebra using 3D rotational angiographic imaging.

4.2 Material and Methods

The same preparation method and rotational angiographic technique applied in Chapters 2 and 3 were used to study the zebra (Figure 4-1). Approximately, 15-20ml of contrast material (Barium sulphate) was injected into the left common carotid artery to fill the carotid arterial tree to the level of internal carotid artery in the cranium. A further 15-20ml of contrast material was injected to allow filling of the cerebral vessels and the contralateral carotid arterial tree. After injection of contrast, the Foley catheters on both sides were clamped to prevent leakage of the contrast agent during image acquisition. Then, three ball bearing markers were placed in a triangular configuration at the right lateral side of the carotid trifurcation to mark or identify the right carotid arterial tree from the left side during rotational angiographic analysis.

For carotid and cerebral vascular angiography in this zebra, a single radiograph was taken prior to rotational scanning to ensure the scan centre was positioned at the centre of the internal carotid artery, between the carotid trifurcation and the caudal rostral quadrant of the cerebral arterial circle.

Then, automatic rotational scanning was initiated by activating the Iso-Cine and 3D operating modes. Due to the smaller size of the zebra head compared to the horse, a single cycle of automatic scanning was enough to visualise both the carotid trifurcations and the internal carotid arteries in a single screen. A sequence of radiographic images was presented in the Cine-Loop function. After acquisition of rotational angiographic images, the multi-planar reconstruction (MPR) was launched by pressing the 3D-MPR button after the completion of an automatic scan to produce a 3D representation of the vessels. Step by step protocols on 3D-MPR mode on the Ziehm Vario 3D fluoroscopic unit were followed (Ziehm, 2007). Arterial latex casting was not pursued in this specimen at this stage as it had become apparent that poor specimen quality obviated good casts.

4.3 Results

Rotational angiography findings in this common zebra revealed that the anatomy and pathway of the carotid trifurcation and the internal carotid artery were the same as those considered common anatomical pattern of these structures in horses (Figure 4-2 and Figure 4-3). Bilateral presence of caroticobasilar arteries can be appreciated clearly in Figure 4-4. From Figure 4-4, one could also observe that the angiographic anatomy of the cerebral arterial circle of this zebra was also similar to the horse. The intracranial pathway of the internal carotid artery was seen to have a branch that communicated with the contralateral side via the intercarotid artery. Then the internal carotid artery gives rise to the caudal communicating artery that turned caudal and had small and narrow connections to the basilar artery.

4.3.1 Cine-Loop Function

Dynamic movements of the carotid arterial tree up to the level of the cerebral arterial circle in this zebra were observed in a 2D angiographic series using the Cine-Loop function in the Iso-Cine mode (video 4-1). Cine-Loop images were graded as good quality because of complete delineation of all important vessels within the scan centre with minimum artefact.

4.3.2 Three Dimensional with Multi-Planar Reconstruction (3D-MPR)

The zebra specimen underwent bilateral rotational angiography with 3D reconstruction imaging of the carotid trifurcation, the internal carotid artery and the cerebral arterial circle. Issues regarding 3D-MPR quality were observed to be similar to those described in the horse in the previous chapter (2), where the 3D-MPR images depend on the quality of the angiographic series on the Cine-Loop function. Following 3D reconstruction of an image, a screenshot of the 3D-MPR images was generated (Figure 4-5).

4.4 Discussion

It must be appreciated from the outset that this was a single opportunity to study the carotid artery of a zebra and as a result, limited cautious conclusions can be drawn. The images produced in Cine-Loop function and 3D-MPR matched the good quality images as seen in horses and donkeys. Furthermore, the angiographic images produced in this study were of an excellent quality compared to any other angiographic study reported so far in the zebra. Contrary to the observation of the cerebral arterial circle pattern in one zebra by Du Boulay (1973), the zebra investigated in this study showed that the basilar artery was not deviated and was near the midline from both of the internal carotid arteries. Some indirect channels, originating from the caudal communicating artery and uniting with the basilar arteries, were seen. The anastomotic variation of the internal carotid or deviation of the basilar arteries that was observed by Du Boulay in one zebra was also observed in several angiograms of horses and donkeys.

Until now, cerebral vascular angiography in equine species is only clinically important in cases of guttural pouch mycosis. Even though there are no reports to substantiate the occurrence of guttural pouch mycosis in the zebra, it is important to appreciate that the zebra also possesses the same anatomical pattern of the carotid arterial tree as in the horse. Given that angiograms in two zebras gave different patterns of the carotid and cerebral vessels (e.g. the presence of caroticobasilar arteries), one might speculate that the “normal” angiographic appearance has not been established and perhaps, if angiograms were performed on a larger number of zebra specimens, a range of anatomical variations of this region would be revealed as appears to be the case in the horse and in the donkey.

Figure 4-1: The zebra cadaver prepared for rotational angiographic technique.

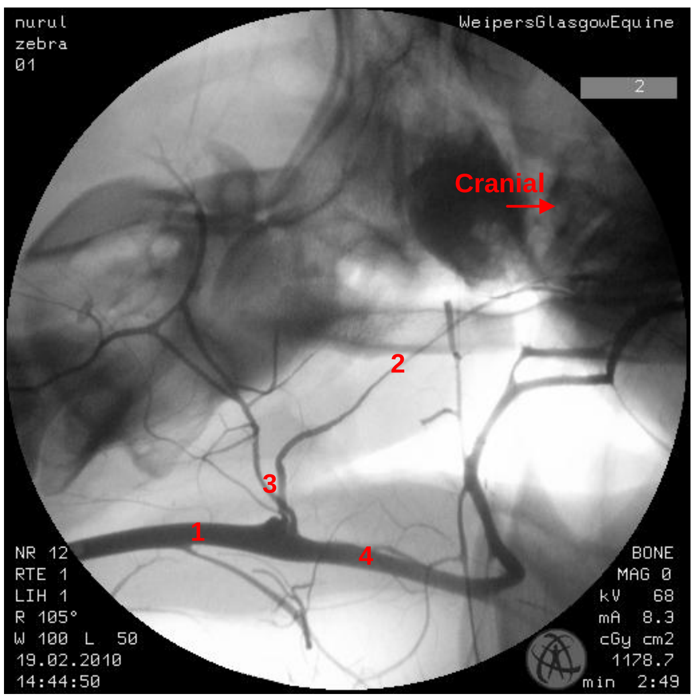

Figure 4-2: Left lateral angiogram of the carotid trifurcation and internal carotid artery of a zebra.
1 common carotid artery; 2 internal carotid artery; 3 occipital artery; 4 external carotid artery (x 1/3).

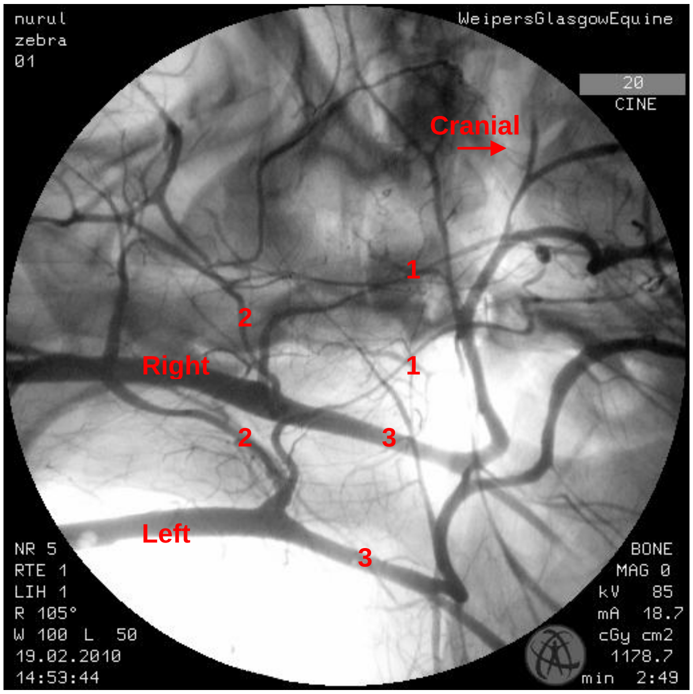

Figure 4-3: Oblique angiogram of the bilateral carotid trifurcation to appreciate the anatomy of the internal carotid arteries of a zebra.
1 internal carotid artery; occipital artery; 3 external carotid artery (x 1/3).

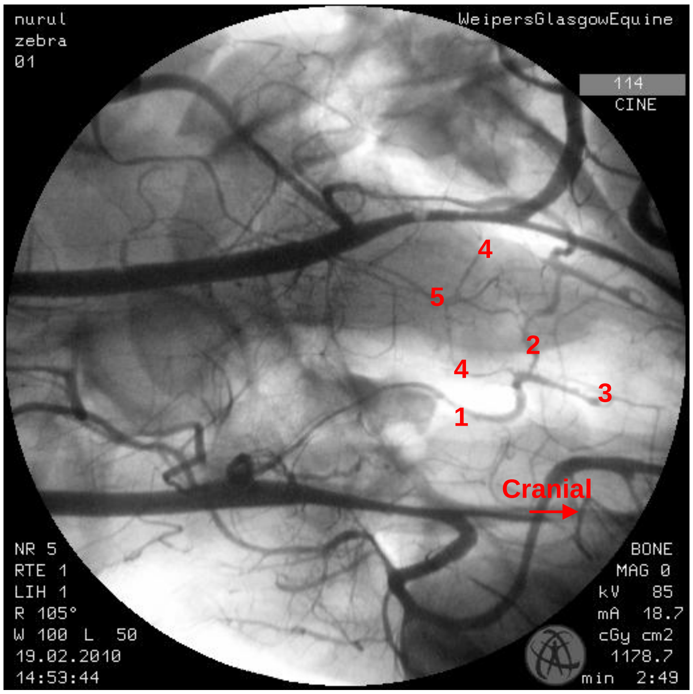

Figure 4-4: Dorsoventral angiogram of the carotid trifurcation and the cerebral arterial circle of a zebra. Note the presence of bilateral caroticobasilar arteries.
1 internal carotid artery; 2 intercarotid artery; 3 caudal communicating artery; 4 caroticobasilar artery; 5 basilar artery (x 1/3).

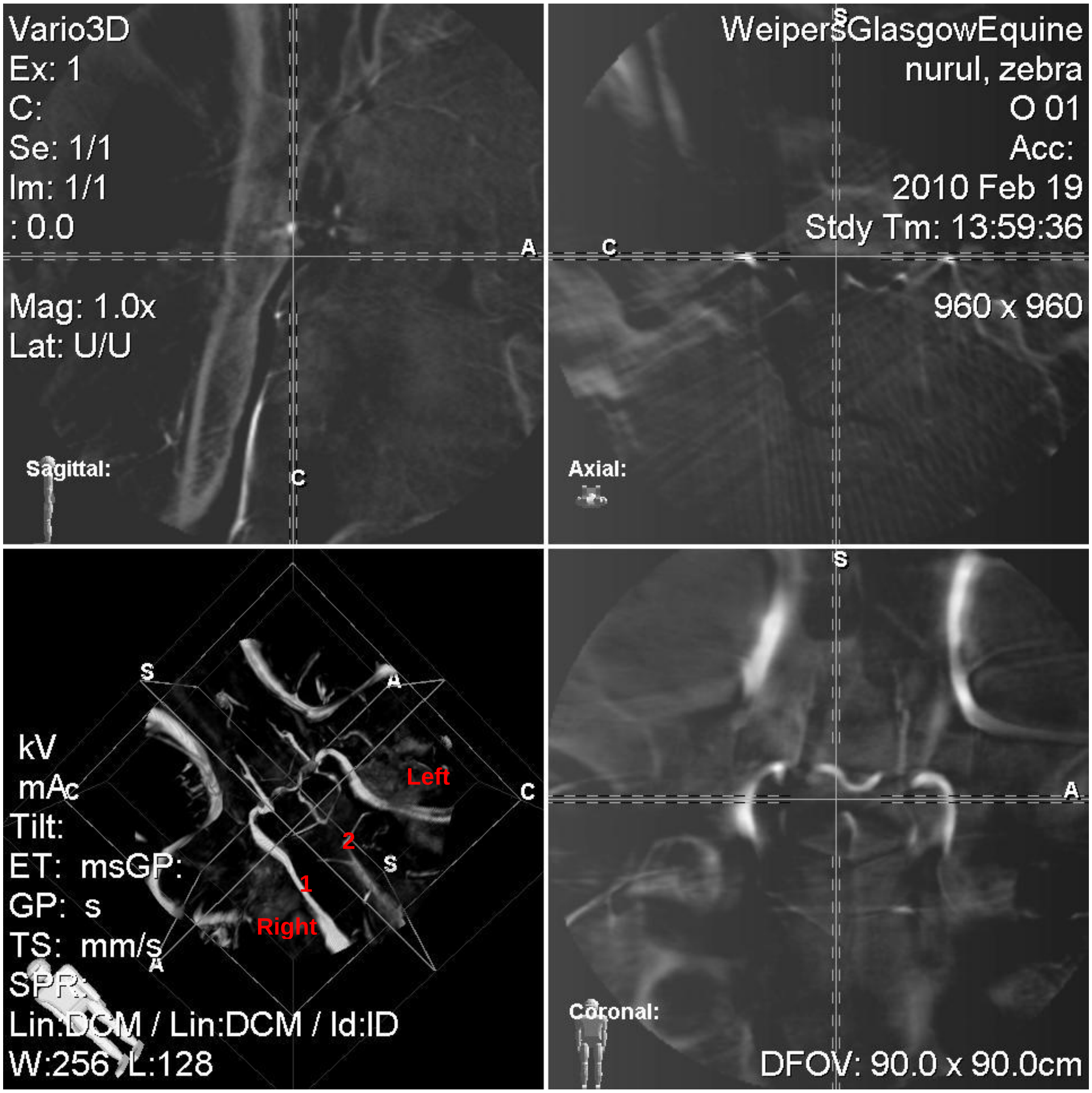

Figure 4-5: A 3D screenshot image that highlights a common pattern of the internal carotid artery and the formation of the cerebral arterial circle on the 3D volume view (left bottom quadrant) and the coronal slice view (right bottom quadrant) of a zebra.
The orientation on each quadrant is determined by the position of a cartoon man at the left side of the quadrants. The 3D volume view presentation is best viewed on software that supports this program. A axial; C coronal; S sagittal; 1 internal carotid artery; 2 basilar artery.

5 ARTERIAL LATEX CASTING OF THE CAROTID TRIFURCATION IN HORSES AND DONKEYS

5.1 Introduction

Arterial casting involves the injection of a suitable material into a major artery where the material will cure with time to produce a three dimensional vascular cast. Historically the use of casting materials started at the beginning of the 16th century and various materials have been tested since. The earliest casting materials used were different metals with low melting temperatures, such as lead and its mixtures, bismuth or cadmium (Tompsett, 1970). Celluloid and celloidin were employed in the 19th and early part of the 20th century. Subsequently, synthetic resin and natural rubber and its derivative solutions were employed and became very popular among biologists and morphologists. Other types of casting materials available include nylon, neoprene latex, polyester resin and vinyl (Grabherr et al., 2007).

5.1.1 Fixation Material

Prior to injecting casting material into a vascular system, the cadaver needs to be preserved or fixed first. The purpose of fixation is to make the tissues firmer and resistant to decomposition so that it will last for a long time. A variety of fixatives are available and the selection of fixatives depends on what kind of preservation effect is needed. Usually, biological morphologists use either formaldehyde or ethyl alcohol. Isopropyl alcohol or saturated brine of rock salt can also be used to fix tissues, but the latter are not suitable for histological preparation.

Formaldehyde, which is also known as formalin, was first discovered by Butlerov in 1859 as cited by Fox *et. al* (1985). After its discovery, there was considerable interest in developing uses for formaldehyde. Even to the present day, an issue of naming commercial preparations of formaldehyde still exists. The name formalin was given by the American producers of formaldehyde for their commercial aqueous solution. In this thesis, the term formaldehyde will be used.

Commercial formaldehyde is supplied by the manufacturer in a 40% saturated aqueous solution. It is cheap, readily available and stable under a broad variety of conditions. Penetration of formaldehyde is about 6mm per 12 hours, and a period of 24 hours is recommended to fix almost any tissue (Hildebrand, 1968). Furthermore, tissues that are fixed in formaldehyde do not become hardened unpredictably as in "over fixation" because formaldehyde is not a coagulating fixative. Compared to alcohol fixed tissues, minimal shrinkage and distortion of formaldehyde fixated tissue occurs. In general, formaldehyde is considered an effective fixative material, but it is a slow fixative and a slow agent for killing bacteria (Fox et al., 1985). Since formaldehyde is known to fix slowly, some investigators reasoned that unfixed tissues may undergo autolysis before tissues reach a preserved or fixed state. So it was suggested one way to retard the process of autolysis was by chilling the tissues whilst fixation takes place (Tompsett, 1970, Fox et al., 1985). Other workers have recommended fixing the tissues at room temperature as formaldehyde fixation process is not a chemical reaction in the usual sense (Hildebrand, 1968).

5.1.2 Method of Preservation

There are several methods to preserve a specimen with chosen fixatives. The easiest method is by direct immersion of the tissue in the fixative solution and storage in containers for at least 24 hours. Another method of preservation is by direct injection of the fixation material into the tissues. Usually this method is only suitable for an animal that is smaller than a cat. For a larger animal, an embalming method is more appropriate where the fixative can be distributed uniformly to the whole body through the circulatory system (Hildebrand, 1968).

The embalming fluid recipes vary between each centre/laboratory and are influenced by the local climate. In general, an embalming fluid may contain: about 2% full strength formaldehyde; about 2% liquid phenol; about 6% glycerine; about 20% alcohol; and about 70% water. Preservation of a specimen results in a bleached appearance to the tissue. By adding phenol, which is also a fixative, the bleaching tendency of the other reagents is reduced. It also renders the tissue sterile and affords protection from fungal growth. Phenol produces white patches when it reaches the skin and this gives a good indication of the adequacy embalming fluid circulation. Glycerine acts by softening so the tissues are more pliable and also retards drying of the tissues.

Injection of the embalming fluid can be done via major veins or arteries. If the vein or the arteries are to be injected with different coloured material, a good result could be achieved if the animal was bled properly after death. There are a few techniques available to administer the embalming fluid into the circulatory system, either by using a disposable syringe with hand pressure or the gravity feed technique from a container filled with embalming fluid held 1-2 metres above the specimen. A more modern technique of administration embalming fluid is by using a proper embalming pressure pump in a special embalming suite.

The objectives of this study were: (i) to produce latex casts of the carotid arterial tree of horses and donkeys in order to display the anatomy of the carotid trifurcation and the internal carotid artery, (ii) to appreciate and identify the carotid trifurcation and the internal carotid artery through dissection, (iii) to verify and confirm the anatomical observation of the carotid trifurcation and internal carotid artery as seen in angiograms of the specimens through dissection.

5.2 Materials and Methods

Dissections were performed on 50 horse and 26 donkey cadavers that had undergone a prior angiographic study. Before dissection, the cadavers were embalmed using the arterial injection method via the left and right common carotid artery. The Cambridge formulation of embalming fluid was used[2].

[2] Vickers Laboratories, Pudsey, West Yorkshire, LS28 6QW

One litre of embalming fluid contained:

Industrial Methylated Spirits	625ml
Phenol	125ml
Formaldehyde	75ml
Glycerol	175ml

For this study, an arterial latex casting technique using Trylon latex[3] was used to produce a cast of the carotid arterial tree. Prior to the casting technique, the common carotid arteries had been catheterised to allow injection of embalming material into the arterial system. Then the cadaver was dissected to observe the carotid arterial tree anatomy and collect the hardened cast.

5.2.1 Catheterisation of the Common Carotid Artery

The head and neck of the cadavers used in this study were disarticulated at the level of the third and the fourth cervical vertebrae. Thus, identification and catheterisation of the common carotid arteries were much easier and straight forward.

The common carotid arteries were identified from the disarticulation region of the neck. They were located medial to the jugular vein and accompanied by the vagosympathetic nerve fibres and lay close to the trachea. The left common carotid artery may differ from the right because it usually separates from the trachea as part of its course. However, at the level of the third and the fourth cervical vertebrae, the left common carotid artery is still in contact with the trachea for a distance of 6-8cm.

A 16Fr Foley catheter was advanced into each common carotid artery for about 5-10 cm. The balloon on the tip of the catheter was inflated with 1-2 ml of water and a constriction ligature was placed caudal to the balloon to prevent the catheter from slipping out of the artery. This was left in place for both embalming and latex injection.

[3] Trylon Ltd, Bury Close, Higham Ferrers Northants, NN10 8HQ

5.2.2 Arterial Latex Casting

There were two protocols involved in casting the carotid arteries; the embalming protocol, followed by arterial latex injection protocol.

5.2.2.1 Embalming protocol

Embalming fluid was injected into the common carotid artery via the Foley catheter. During injection, the common carotid artery of the contralateral side was clamped to retain the fluid in the tissue. Any other leakages from other severed arteries or veins were also clamped. A volume of 8-10 litres of embalming fluid injected into the arterial system was sufficient to preserve a horse head. For a donkey head, a volume of 3-5 litres of embalming fluid was sufficient. Once the arterial injection was completed, the cadaver was left at ambient temperature for two days to allow the fixative to take effect.

5.2.2.2 Arterial latex injection

Once the initial arterial injection (embalming) was completed, 1 litre of 20% ammonia in warm water was injected through the carotid artery to flush out the remaining embalming fluid and debris from the arterial system and also to prevent premature setting of latex. With one common carotid artery clamped, about 300-350ml of latex solution was injected using a 50ml disposable syringe into the other common carotid artery. The latex solution consisted of 250-300ml of white latex, 50ml of cold water and blue Trylon latex dye. For a donkey head, only half of that volume of latex solution was required. Extreme care was taken during latex injection to avoid air accumulating along the vessel, as well as maintaining a constant pressure to prevent the vessel from bursting. After the arterial latex injection, the cadaver was carefully placed in a large heavy duty container inside a store. The temperature of the store usually depended on the surrounding environmental temperature as the store was not equipped with heating or cooling equipment. Improved air movement in the store was achieved with a fan. Air changes were not monitored. The cadaver was left to allow the latex to cure for 10-

14 days. Assessments of embalmed tissue were done by digital pressure and observation of the bleached look of tissue to indicate if it was well embalmed. Typically after 10 days (depending on the size of head), the cadaver was ready for dissection.

5.2.3 Dissection Technique

Dissection of the cadaver was done to study the carotid trifurcation and the pathway of the internal carotid artery *in situ*. Paragon size 10 scalpel blades on a number 3 handle was used along with a rat tooth forceps for the dissection. The dissection protocols were adapted from dissections described in *Clinical Dissection Guide for Large Animal* (Constantinescu and Constantinescu, 2004). The extracranial portions of the internal carotid arteries were exposed up to the level of the foramen lacerum. However, the gross anatomy of the intracranial segment of the internal carotid artery was not studied at dissection, as at the planning stage it was not considered important to pursue observation at the intracranial level.

Photographs of the carotid trifurcation and the extracranial internal carotid artery were taken initially using a Kodak 8.2 megapixel digital camera then a Nikon D60 D-SLR camera, as the latter was found to produce much better quality images.

5.2.3.1 Dissection protocols

- Attention was devoted to the parotid region. The skin incision was started from the cutaneous colli muscle that covered the parotid gland and transversely crossing the parotidoauricularis muscle

- The incision was continued along the sternomandibularis muscle, parallel to the external jugular vein and the common carotid artery, which lie deep to the muscle

- The common carotid artery was exteriorised from its attachment to the fascia and the muscle to expose it more clearly

- The skin over the parotid gland was reflected laterally to expose the gland. The gland was removed rostroventrally, with care, from the facial nerve to allow better visualisation of the pathway of the common carotid artery

- Between the tendons of the sternomandibularis and cleidomastoideus muscles, the subparotid aponeurosis was dissected. This aponeurosis lies deep to the maxillary vein and separates the parotid gland from the mandibular salivary gland

- Deep to the maxillary vein, the occipitomandibular part of the digastricus muscle was found

- The maxillary vein was retracted rostrally and the occipitomandibular part of the digastricus muscle was transacted to expose the caudal belly of the digastricus, occipitohyoideus and stylohyoideus muscles, the stylohyoid bone, the glossopharngeal and hypoglossal nerves and the external carotid artery

- The digastricus muscle was reflected caudally to expose the deepest structures of the area covering the guttural pouch

- To appreciate the trifurcation of the carotid artery, the course of the common carotid artery was followed to the level of the atlas and its contact with the guttural pouch

- The anatomy of the carotid cranial tree and the carotid trifurcation which consist of internal carotid artery, occipital artery and external carotid artery were observed and recorded

- In order to observe the internal carotid artery pathway from the carotid trifurcation to the foramen lacerum, the medial compartment of the guttural pouch was breached

- The course of the internal carotid artery could be tracked towards the carotid foramen, parallel to the cranial cervical ganglion, into the foramen lacerum. This was covered with periosteum that serves as a barrier to the brain cavity

- To harvest the arterial latex cast, the common carotid artery and its branches were carefully extracted, dissecting the very small vessels that attached the common carotid artery tree to the muscles and body structures

- At the level of the carotid trifurcation, the occipital artery was cut at the termination of its caudal and cranial branch. As for the external carotid artery, the cut was made at the most rostral part of the artery before it was obscured by the ramus of mandible. The linguofacial trunk, a large branch coming from the external carotid artery, was also cut at the same level as the external carotid artery

- Finally, the internal carotid artery was severed very close to the foramen lacerum, at the base of the skull, to fully detach the carotid arterial tree containing latex cast from the rest of the cadaver

- Once the arterial tree was successfully extracted, it was placed on cardboard and the vessel wall that lined the cast was removed using scissors, leaving only the latex cast

- The latex cast was then attached to a piece cardboard and placed in an airtight container for storage

5.3 Results

5.3.1 Observations on Dissections

Dissections were carried out on 50 horse and 26 donkey specimens that were prepared by latex casting of the carotid arterial tree. The dissection findings in all the specimens showed no discrepancy with the angiographic findings, except in one horse. Here on the left angiogram it was first thought that the internal carotid artery and occipital artery shared a common trunk before separating as individual vessels. However, on dissection it was actually found to be that the internal carotid artery had an aberrant branch. In this specimen, the left occipital artery completely failed to fill with contrast material and the aberrant branch of the internal carotid artery was wrongly thought to be the occipital artery. The presence of the left occipital artery in this horse was confirmed on dissection.

The success of an embalmed specimen was reflected in the quality of the latex cast (Table 5-1 and Table 5-2). Where specimens were well embalmed, dissections were straight forward, important structures were easily identified and casts of both carotid arterial trees could be harvested successfully (six horses). Cadavers, which were not fresh or had already undergone post-mortem changes prior to embalming, suffered from failure to be preserved with the embalming fluid producing less than ideal specimens. The impact of this resulted in failure of the latex solution to harden and was categorised as partial filling or failure to fill with latex (Table 5-1 and Table 5-2). Yet, it was also noted that in five horse specimens and two donkeys, only one side was well embalmed and the other side was partially embalmed. As a result, only one satisfactory (good) cast was able to be harvested from these specimens.

Properly embalmed tissues became firm, discoloured and appeared whitish. A common anatomical pattern of the carotid trifurcation and the internal carotid artery on dissection of a well embalmed horse and donkey are shown respectively in Figure 5-1 and Figure 5-2. Blue coloured latex filled the whole carotid arterial tree including small arterial branches. An example of a less than ideal specimen is shown in Figure 5-3 where it was almost impossible to recognise the structures surrounding the carotid arterial tree. As for partially embalmed tissue, it sometimes caused part of the tissues to be infected by fungus permitting mould growth (Figure 5-4).

There was no difference in structures of the guttural pouch in the donkey compared to the horse. Dissection wise, it was easier and less time consuming to dissect a donkey specimen as they were much smaller and had less muscle mass compared to a horse specimen. Interestingly in donkeys, layers of fat were observed covering the whole length of the internal carotid artery and sometimes the whole carotid trifurcation too (Figure 5-5). These layers of fat were easily peeled off to reveal the arterial blood vessels beneath. Layers of fat were not found surrounding these structures in any of the horse specimens.

The presence of the aberrant branch of the internal carotid artery in some horses was appreciated easily on dissections, especially when the artery was well filled with latex (Figure 5-6). Even small branches of satellite vessels coming from an aberrant branch of the internal carotid artery were filled with latex and made visualisation and identification much better as seen in Figure 5-7. Sharing of a common trunk of the occipital artery and internal carotid artery on dissections of a horse and a donkey can be appreciated in Figure 5-8 and Figure 5-9 respectively.

Occasionally, during dissection of horse specimens, evidence of a dilated carotid sinus within the carotid trifurcation (as described by Furuhata, 1964) was observed. However, as this study focused on the internal carotid artery, this incidental observation was not recorded thus the exact numbers found cannot be offered.

One interesting finding seen on the unilateral angiograms in two donkeys as reported in the previous chapter was the origin of the internal carotid artery being more caudal to the termination of the common carotid artery. Upon dissection of these donkeys, the fat formation surrounding the carotid trifurcation and internal carotid artery seemed to be thicker and the areas covered by layers of fat were more extensive, extending to the caudal part of the common carotid artery as well.

Figure 5-10 shows a carotid tree where the internal carotid artery originates very caudal to the common carotid artery termination after the layers of fat had been removed. The distance of the origin of internal carotid artery to the common carotid artery termination was measured during dissection to be 4cm in the first donkey and 2cm in the second donkey. The linguofacial artery in these donkeys also originated from the common carotid artery. The measurement of the origin of the internal carotid artery to the carotid termination in one donkey is shown in Figure 5-11. In the donkeys, other variations of arterial arrangement from the common carotid artery termination included; the linguofacial trunks originated from the common carotid artery, or shared the common origin with external carotid artery. These are shown in Figure 5-12 and Figure 5-13.

5.3.2 Latex Cast

Out of 50 horses that were prepared for bilateral carotid arterial latex casting, 18 well formed latex casts of the carotid arterial tree were obtained out of 100 casts (Table 5-1). Figure 5-14, 5-15 and 5-16 show the best three latex casts of the normal anatomy of the carotid arterial tree of the horse. Initially, casts from partially embalmed cadavers with partial filling (nine) or empty of latex (nine) were collected, but the vessel wall around the casts was not removed and left intact in order to preserve the anatomical shape of the arterial tree. Issues with latex filling occurred because the specimens were not adequately embalmed, and when the carotid arterial tree was harvested from the cadaveric head and neck, the latex flowed out leaving the arterial lumen partially filled or empty. However when harvested, these samples shrunk within three days.

Therefore, in other specimens that were not well embalmed and the latex partially filled up or even failed to fill the arterial lumen, these casts were not harvested (64 samples). In spite of this, the arterial tree was examined and assessed in all 64 samples.

The presence of an aberrant branch of the internal carotid artery could be identified by latex cast, where Figure 5-17 and Figure 5-18 show such examples of well done good quality casts. Figure 5-19 illustrates the internal carotid artery and occipital artery sharing a trunk from the common carotid artery before they separate into individual arteries. Due to the clinical importance of an aberrant branch of the internal carotid artery as an anatomical variation, other photographs of specimens with the aberrant branch of the internal carotid artery were included in this chapter even if the arterial lumen were not filled up with latex and are shown in Figure 5-20 to Figure 5-24. Though the vessel diameter could not be measured for comparative purposes, it was still possible to identify anatomic variation.

In the 26 donkeys where bilateral carotid arterial tree latex casting was attempted, two satisfactory casts of the carotid arterial tree were obtained (Figure 5-25 and Figure 5-26) out of 52 casts. For unsuccessful casts where the tissues embalming and latex failed to fill up the arterial lumen satisfactorily, the vessel walls of the arteries were not removed and eventually the samples shrunk with time (25 casts). However, carotid arterial trees that were partially filled with latex were harvested because they still can retain their shape (3 casts). For these reasons, 22 latex casts from any non-embalmed specimens were not harvested. An immediate anatomical observation on these specimens was made and recorded during dissections. For reference, a table showing all the latex cast quality and availability in the donkey specimens are shown in Table 5-2.

Different arrangements of the origin of the linguofacial trunk structure are shown in Figure 5-25 and Figure 5-26 where the linguofacial trunk shared the same origin with the external carotid artery, or originated directly from the common carotid artery respectively. Important anatomical variations of the carotid arterial tree arrangement in donkeys in latex cast preparations are shown in Figure 5-27 and Figure 5-28 where the internal carotid artery originates very caudal to the common carotid artery termination, and the linguofacial trunk originated directly from the common carotid artery.

Overall, several issues were faced during collection of the latex cast. Some latex casts were presented with interruptions along the cast causing it to be fragile or having a lack of strength and flexibility. This was due to the presence of air in the embalmed vessel despite efforts to prevent such air accumulation. Glue was used on these latex casts to bridge the interruptions along the vessel. In some specimens of both horses and donkeys, the latex casts did not depict the actual diameter of the arterial lumen and appeared narrow or even misshapen. Supposedly the arterial latex cast should be rounded, but this was not the case in some arterial casts as they appeared flattened upon collection. Dissecting out the vessel wall from the cast was a particular challenge in specimens that were very fragile, involving fine vessels or partially cured latex. Extreme care was taken to avoid incidents of iatrogenic damage to the cast while dissecting the vessel wall of the arteries. If not, the cast could be broken or worst; branches of fine arterial vessels could be lost.

5.4 Discussion

One of the objectives in this study was to attempt the production of latex casts of the carotid trifurcation and the internal carotid artery in horses and donkeys. The anatomical structures of the carotid trifurcation and the internal carotid artery in both horses and donkeys corresponded to the common/standard description of these structures in the literature (Nanda, 1975, Abdel-Rahman et al., 1995, Constantinescu and Constantinescu, 2004, Alsafy et al., 2008). Arterial latex casting technique is the technique of choice if the specimen is to be dissected after the cast has set. The latex cast possess, theoretically, a greater elasticity and pliability so that during dissection the danger of breaking or severing small vessels or twigs should be reduced. Other purported advantages of the arterial latex technique described in this study are that latex is a readily available solution that does not require mixing of various components, and is able to cure at the ambient temperature (Hildebrand, 1968).

The entire specimen studied here underwent angiography prior to casting of the carotid arterial tree. The arterial latex casting technique served as a verification method to confirm the findings on angiography. It should be mentioned here that dissection was carried out only to the level of the foramen lacerum that exposed the extracranial internal carotid artery and arterial casts that were collected only represent the carotid trifurcation and extracranial part of internal carotid artery. Intracranial dissection was not carried out at that time because during the course of this study, it was felt that intracranial observation of equine cerebral vessels was not considered valuable or relevant from a clinical perspective related to diagnostic investigation of guttural pouch mycosis in the horse. Thus, any intracranial angiographic observations in this study were not confirmed at dissection.

5.4.1 Factors Influencing the Success of Arterial Latex Cast

The most significant factor in achieving good arterial casts is the quality of the specimen used. The best results should be achieved if the specimen is embalmed within one hour of death. However, in this study, getting a fresh cadaver was not always possible as the anatomy department that supplied cadaver materials was engaged with a high number of post mortems, preparing materials for student classes and meeting demands from pathologists and other researchers. The time taken to perform angiography prior to latex casting also contributed to loss of freshness and quality of the specimen. Usually, for horse specimens, latex casting was performed at the earliest opportunity the next day, or the subsequent day, depending on when the specimen was transported and availability of the fluoroscopy unit to be used for angiography. Most frequently, the horse specimens needed to be kept frozen to prevent autolysis before any procedure could be carried out. As for the entire donkey sample, they were transported frozen from Devon, United Kingdom. However, the time of death to the time a head was put in the freezer was not known. Retrospectively, this may explain why in this study the arterial latex casting outcome for the horse specimens was much better than the donkey specimens.

Another factor that influenced the outcome of the cast was the quality of the embalmed tissue. Based on the results, most of the specimens that were not well embalmed resulted in the failure of the cast to cure properly. Overall, 82 latex casts of the horse and 50 of the donkeys were considered unsuccessful. One of the contributing factors that led to difficulty in obtaining satisfactory embalming was the size of the specimen used for this study. The very thick muscle of the equine neck and the vast size of its head made penetration of the fixatives much slower and less efficient. The ability of the embalming fluid to remain within the muscular tissue for preservation to take effect was also reduced due to leakage of the fixatives through transected muscle and bone. Even though donkey heads and necks were smaller with less muscle mass compared to a horse head and neck, the quality of the donkey specimens upon collection was already deteriorating. Consequently, more embalming fluid was administered than what was recommended by the literature (Hildebrand, 1968, Tompsett, 1970). In specimens that were found to be embalmed unilaterally (5 horses, 2 donkeys) it could be possibly due to the lateral positioning of the specimens during the whole process such that most of the embalming fluid pooled on the dependent side.

To achieve the best result when using latex as a casting material, latex should not be stored longer than two months (Hildebrand, 1968). Perhaps this is another reason that influenced the outcome of the quality of cast in this study where latex was purchased in bulk. Paradoxically, in small vessels, old latex may set too quickly before the injection is complete, thus causing overflow of latex from vessels. But here, large vessels were being studied. Another drawback of using latex is that, according to Tompsett (1970), it may take up to a month for latex to set right through in large vessels like the vena cava or aorta of a human. However, 10-14 days was used in this study as it is the standard used in the human laboratory where the technique was first learned, and where the advice given was that 10 days was adequate. Given that the size of the common carotid artery and carotid trifurcation of the horse are considered large vessels, a period of two weeks before dissection was carried out in this study may have been inadequate when the quality of embalming an 'old' specimen was taken into account. It has been noted that latex setting can be hastened if injected specimens are cooled to -20ºC for 48 hours (Tompsett, 1970).

5.4.2 Interesting Findings

One of the interesting observations on donkey specimens during dissection was that the internal carotid artery and sometimes the carotid trifurcation were covered with layers of fat. The presence of fat may be due to the donkeys being obese. However, the fat layers were observed to surround only the carotid trifurcation and the internal carotid artery and were not generalised in distribution as is supposed to be the case in an obese animal. Perhaps the layers of fat surrounding the internal carotid artery or the carotid trifurcation act as a physical barrier or buffer between these major arteries and other adjacent structures.

However, the presence of fat observed here, did not extend to the level of the sigmoid flexure of the internal carotid artery, where mycotic plaques tend to affect the region of the internal carotid artery caudal to this flexure. Thus, it is highly controversial to speculate that mycotic plaque would be unable to cause major damage or erosion to this artery. This is because the common location of fungal infection tends to occur much higher, where the layers of fat were not observed to be surrounding this specific location of the artery.

Perhaps, if the whole length of extracranial internal carotid artery in the donkey is covered with layers of fat, one could speculate that maybe cases of guttural pouch mycosis are rare in donkeys because of the presence of fat layers protecting this artery and the other important nerves adjacent to the pouch from fungal invasion. Thus typical clinical signs of epistaxis and neurological disorders in guttural pouch mycosis are not seen. Nevertheless, it is interesting to note that these layers of fat around the carotid trifurcation and the internal carotid artery were not observed in a single horse in this study. Perhaps this feature warrants further investigation.

5.4.3 Other Casting Techniques

There are other methods of producing a cast of arterial or venous vessels in cadaveric specimens, and these techniques are well described in the human anatomy literature. An injection-corrosive technique involves the injection of hard setting casting material into the vessels. When the solid cast has formed, the tissues or muscular substance surrounding the cast are macerated by immersion of the organ in concentrated corrosive acid. The best material to use for this technique is polyester resin as the quality of cast produced is excellent with minimum shrinkage (Hildebrand, 1968, Tompsett, 1970). Even though the technique is considered simple, it has to be done diligently and with practice to prevent failure. According to Tompsett (1970), great difficulty is experienced in getting a satisfactory material for corrosion casting relative to the instability and inflammability of resin, which consequently makes the resin difficult to transport.

An injection-corrosive technique on the horse head had been described (Macdonald et al., 1999), where the common carotid arteries were infused with Batson's No. 17 monomer base solution and left to cure at room temperature for 48 hours. Maceration of the tissue surrounding the arterial cast was then done by placing the head in anhydrous sodium hydroxide. However, any cast produced with an injection-corrosive technique would not allow the observation of the anatomy of the internal carotid artery in relation to the wall of the guttural pouches of the horse. Thus, these techniques were not considered.

Combining casting material, with a radio-opaque compound for post-mortem angiography is another technique that can be used. Using this technique, formation of artefacts is rare. However, the disadvantages of this technique are; it is only suitable for single organ studies, the material injected cannot be flushed out after angiography and the cast may shrink after hardening (Grabherr et al., 2007). With shrinkage of the arterial cast, it would obviate an appreciation of true vessel size.

In other studies (Smith et al., 1990, Baptiste et al., 1996), silicone casting material was used to produce casts of the canine and feline lung and guttural pouch of the horse. In comparison with the use of acrylic or polyester resin, silicone casting material does not require mixing with hardeners, and there is no concern regarding tissue damage or distortion because silicone does not require an exothermic reaction such as the process of hardening of plastic when using resin. Silicone material able to cure at room temperature for 24 hours and then silicone cast can be removed by dissection. This technique using a silicone cast was also found to be simple, inexpensive and the outcome of the cast is flexible and durable compared to acrylic or polyester cast. Perhaps, the use of silicone material in this study could have averted the problems of brittle and fragile casts, and slow setting of latex material. However, cast distortion is still a problem if air or gas is trapped in the vessel during injection of the casting material.

Plastination is another technique of tissue preservation that can be used to produce dry, odourless and durable biological specimens. Before fixation of a specimen, the blood vessels can be filled with a coloured epoxy resin that is specially formulated for plastination purposes. The epoxy resin used in plastination (Biodur ™ E20) is not inhibited by wet surfaces, cures well with less than 2% shrinkage and does not break down in acetone (von Hagens et al., 1987). There are four principles in the plastination procedure, which are; (i) Fixation, (ii) Dehydration, (iii) Forced impregnation and (iv) Curing (hardening). However, a standard silicone plastination technique could take up to 12 weeks to produce a successfully plasticated specimen (von Hagens et al., 1987). Set up of equipment for dehydration by freeze-substitution and vacuum-impregnation is required for these procedures. Due to limited resources at the institute where this research study was carried out, this technique of producing cast of the arterial tree was not pursued.

Table 5-1: Arterial latex casts in horse specimens

	Left			Right		
Horse number	Good	Partial fill	Fail to fill	Good	Partial fill	Fail to fill
1						
2						
3	×					
4						
5						
6	N			Δ		
7	N				×	
8						
9				N		
10	N			N		
11						
12						
13	×					
14		×				
15	N			N		
16				N		
17				N		
18					×	
19						Δ
20						
21						
22						
23						
24						
25	N			N		
26		N			N	
27		N			N	
28	N			N		
29						×
30						
31						
32			N			N
33						
34						×
35			N			N

Continued on next page

	Left			Right		
Horse number	Good	Partial fill	Fail to fill	Good	Partial fill	Fail to fill
36						
37						
38			×			Δ
39						
40	N			N		
41		N			N	
42						
43						
44						
45						
46						
47						
48						
49						
50						
SAMPLE COLLECTED	9	4	3	9	5	6
NOT COLLECTED	34			30		

N = Common/standard anatomical pattern of the carotid trifurcation and internal carotid artery

× = Presence of aberrant branch of the internal carotid artery

Δ = Internal carotid artery and occipital artery share a common trunk

Table 5-2: Arterial latex casts in donkey specimens

	Left			Right		
Donkey number	Good	Partial fill	Fail to fill	Good	Partial fill	Fail to fill
1						
2	N				N	
3						
4						
5						
6			N			N
7			Ø			N
8			N			O
9			Y			
10			N			N
11			N			N
12			N			N
13			N			N
14			N			N
15			N			N
16			∆			N
17			N			N
18			N			Y
19						
20	Ø					
21						
22		Ø			N	
23						
24						
25						
26						
SAMPLE COLLECTED	2	1	13	0	2	12
NOT COLLECTED	10			12		

N = Common/standard anatomical pattern of the carotid trifurcation and internal carotid artery

Ø = Linguofacial trunk share its origin with the common carotid artery

O = Linguofacial trunk share its origin with the external carotid artery

∆ = Internal carotid artery and occipital artery share a common trunk

Y = Internal carotid artery originated very caudal to the termination of common carotid artery

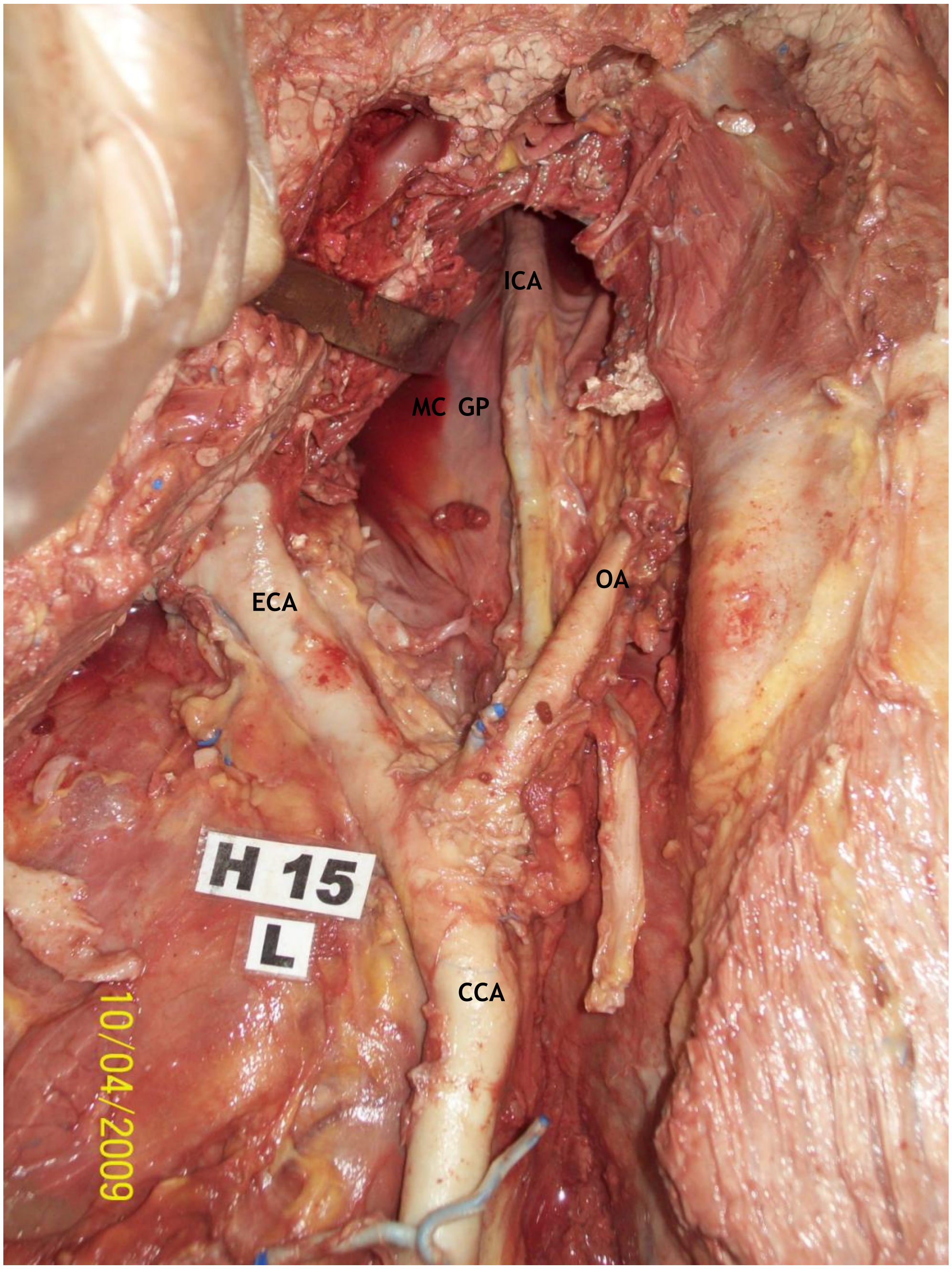

Figure 5-1: Common anatomical pattern of the carotid trifurcation and the internal carotid artery of a well embalmed horse specimen (left side).
Note that the wall of the medial compartment of the guttural pouch is still intact and the internal carotid artery lies very close to it. ICA= internal carotid artery; CCA= common carotid artery; ECA= external carotid artery; OA= occipital artery; MC= medial compartment; GP= guttural pouch.

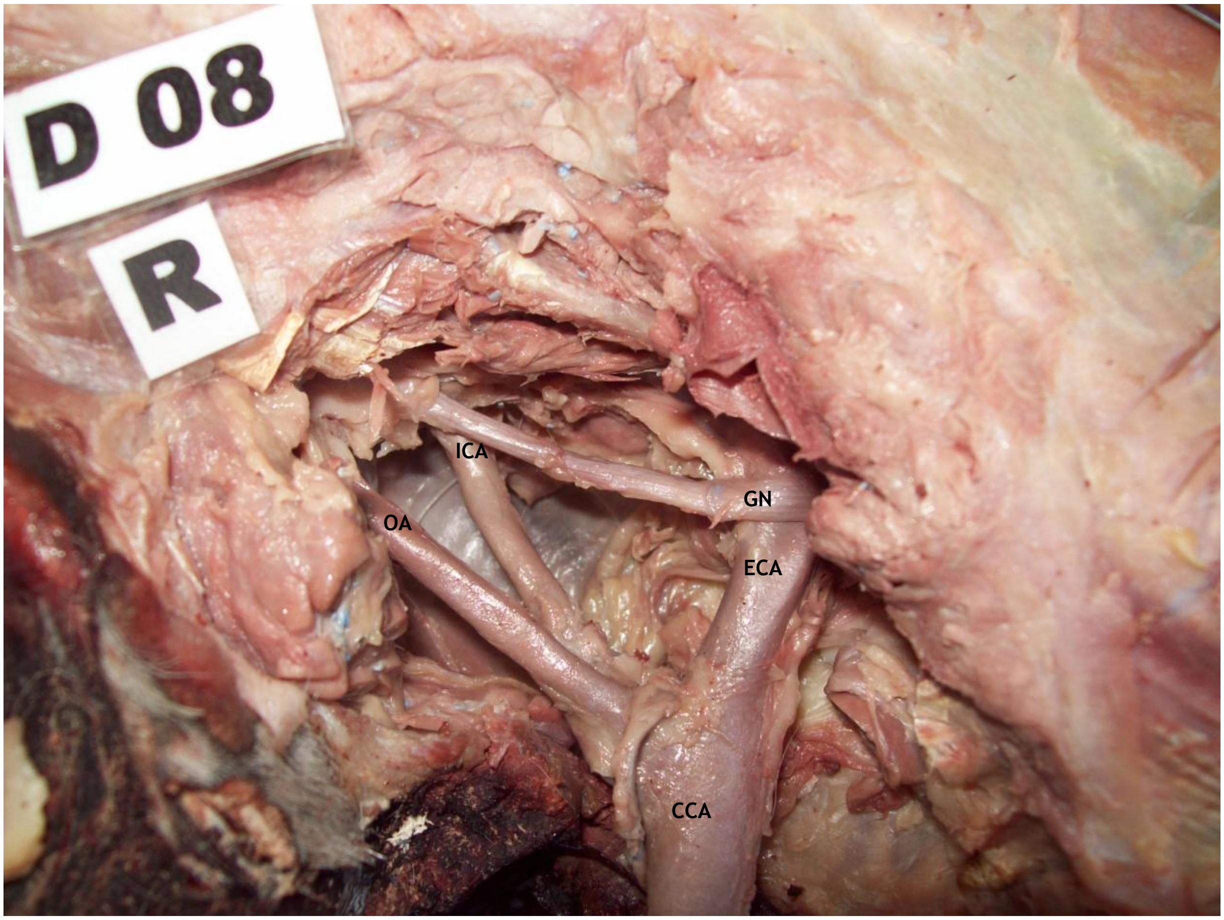

Figure 5-2: Common anatomical pattern of the carotid trifurcation and the internal carotid artery of a well embalmed donkey specimen (right side).
ICA= internal carotid artery; CCA= common carotid artery; ECA= external carotid artery; OA= occipital artery; GN= glossopharyngeal nerve.

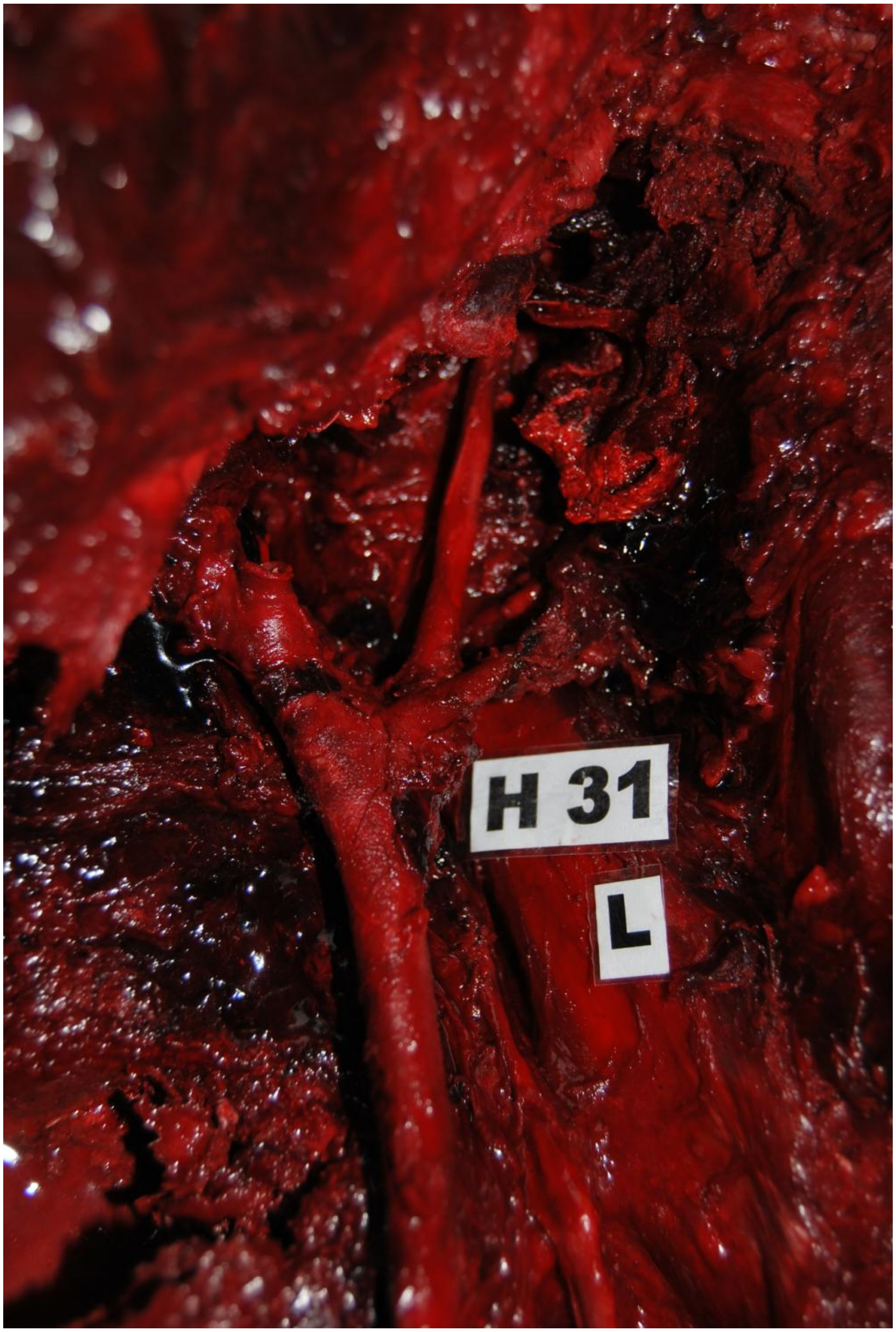

Figure 5-3: Non embalmed horse specimen due to poor penetration of the embalming solution into the tissue.

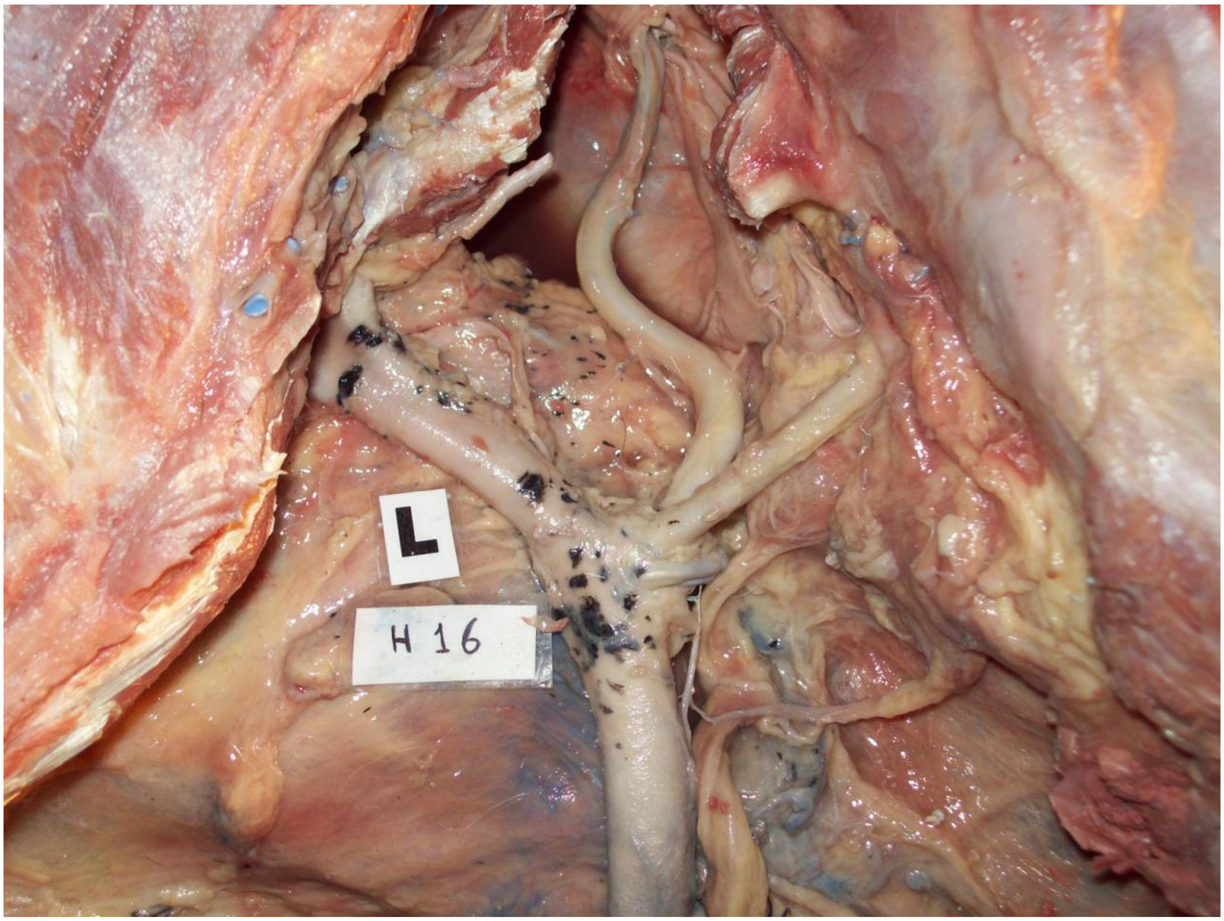

Figure 5-4: Fungus formation on the left carotid trifurcation of an embalmed horse specimen due to poor embalming.

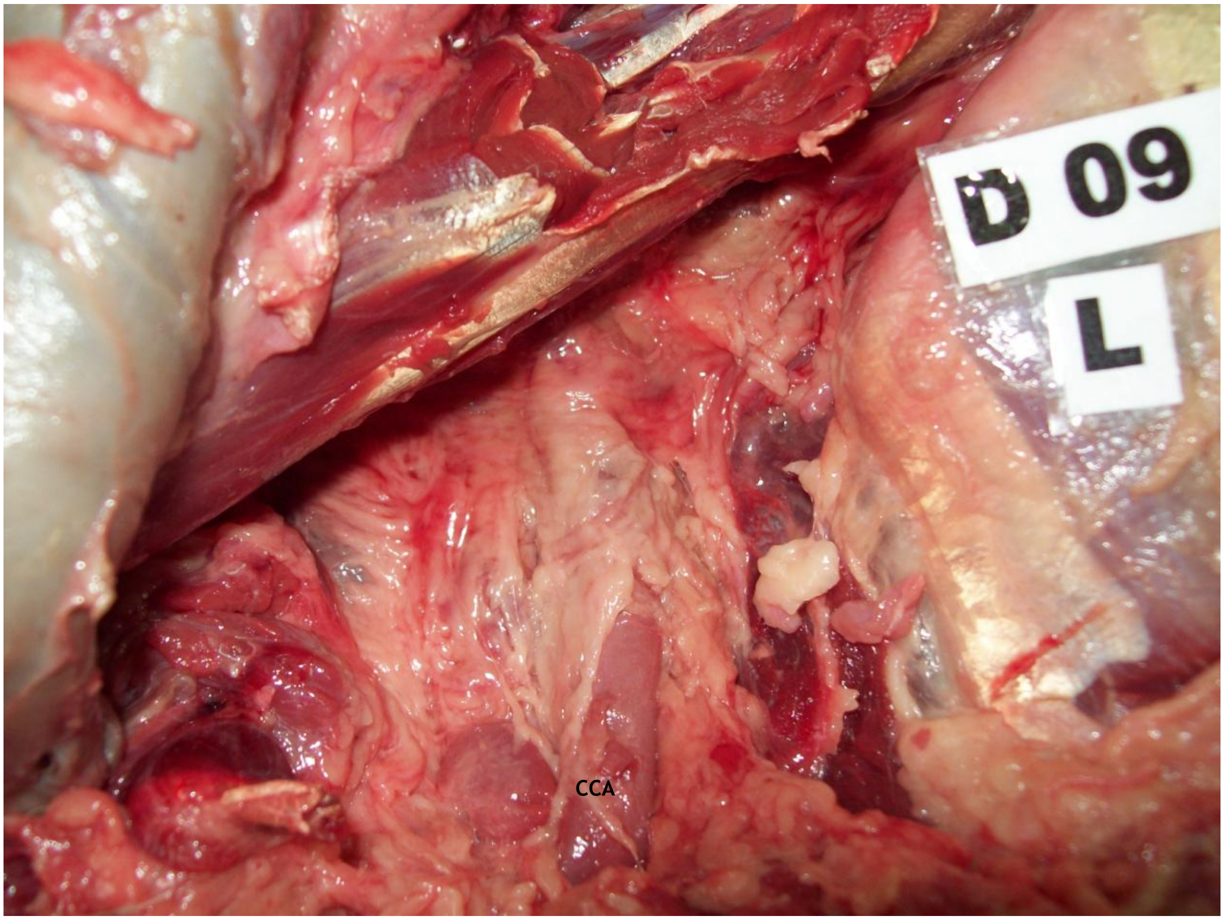

Figure 5-5: The carotid trifurcation is entirely covered with fat in this donkey (left side). CCA= common carotid artery

Figure 5-6: Anatomy of the right internal carotid artery in this horse shows variation from the common pattern of this structure in which the artery gives rise to an aberrant branch. The carotid trifurcation and the internal carotid artery were filled with latex.
Note that the wall of the medial compartment of the guttural pouch was still intact. ICA 1=the original internal carotid artery; ICA 2= the aberrant branch of internal carotid artery; MC= medial compartment; GP= guttural pouch.

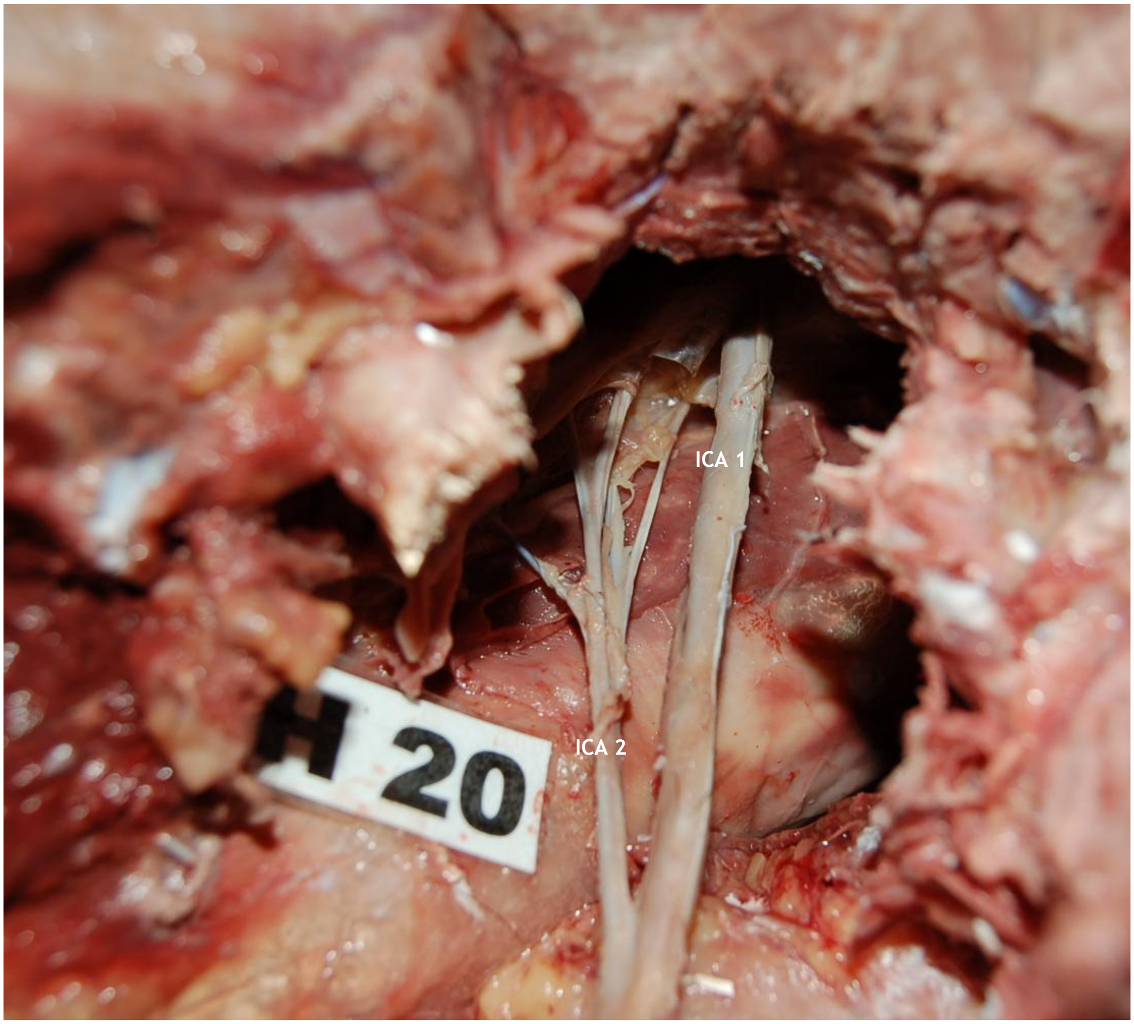

Figure 5-7: Anatomy of the right internal carotid artery in this horse shows variation from the common pattern of this structure in which the aberrant branch of the right internal carotid artery gives rise to several satellite vessels.
ICA 1=the original internal carotid artery; ICA 2= the aberrant branch of internal carotid artery.

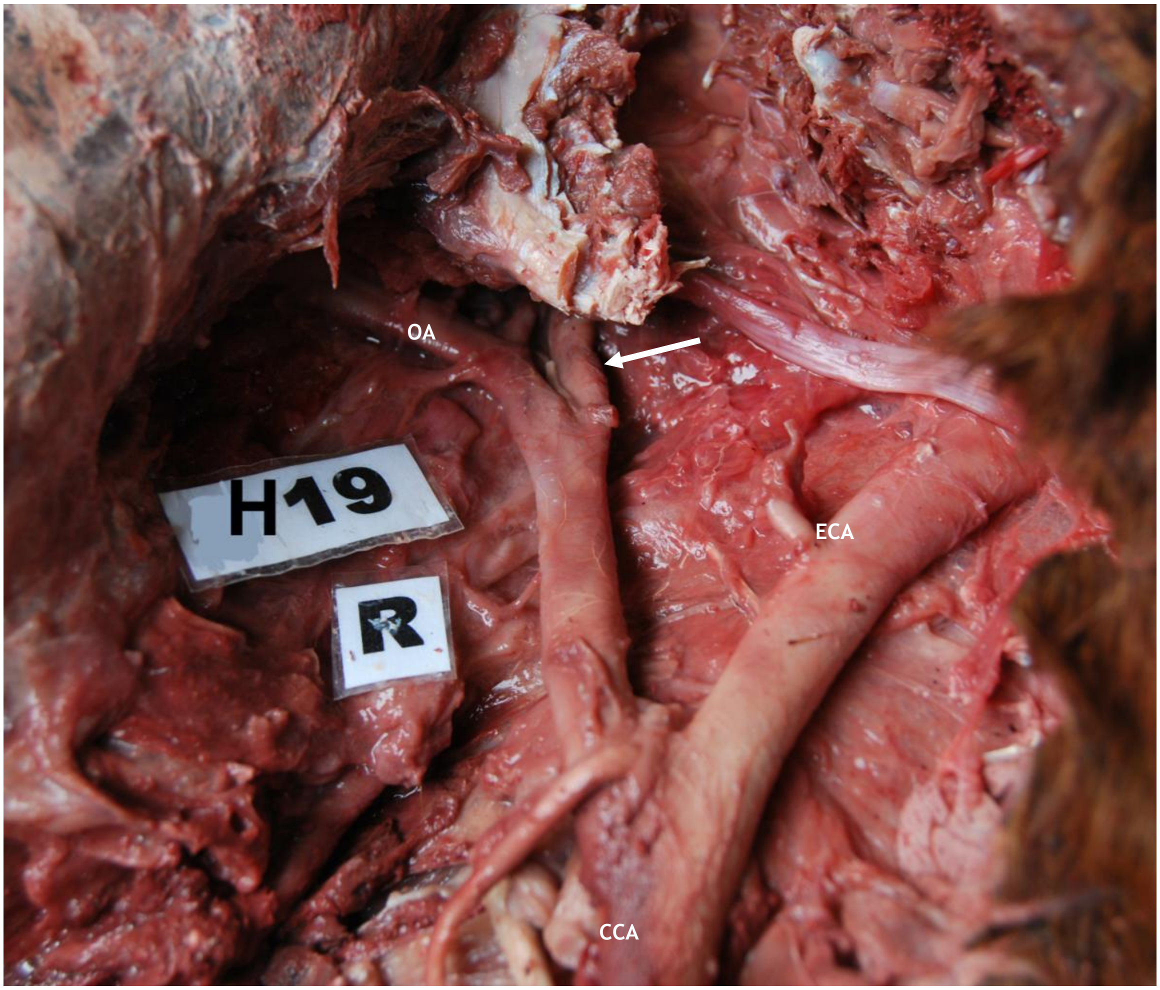

Figure 5-8: Anatomy of the right internal carotid artery in this horse shows variation from the common pattern of this structure in which the internal carotid artery (white arrow) and the occipital artery share a common trunk from the common carotid artery.
CCA= common carotid artery; ECA= external carotid artery; OA= occipital artery.

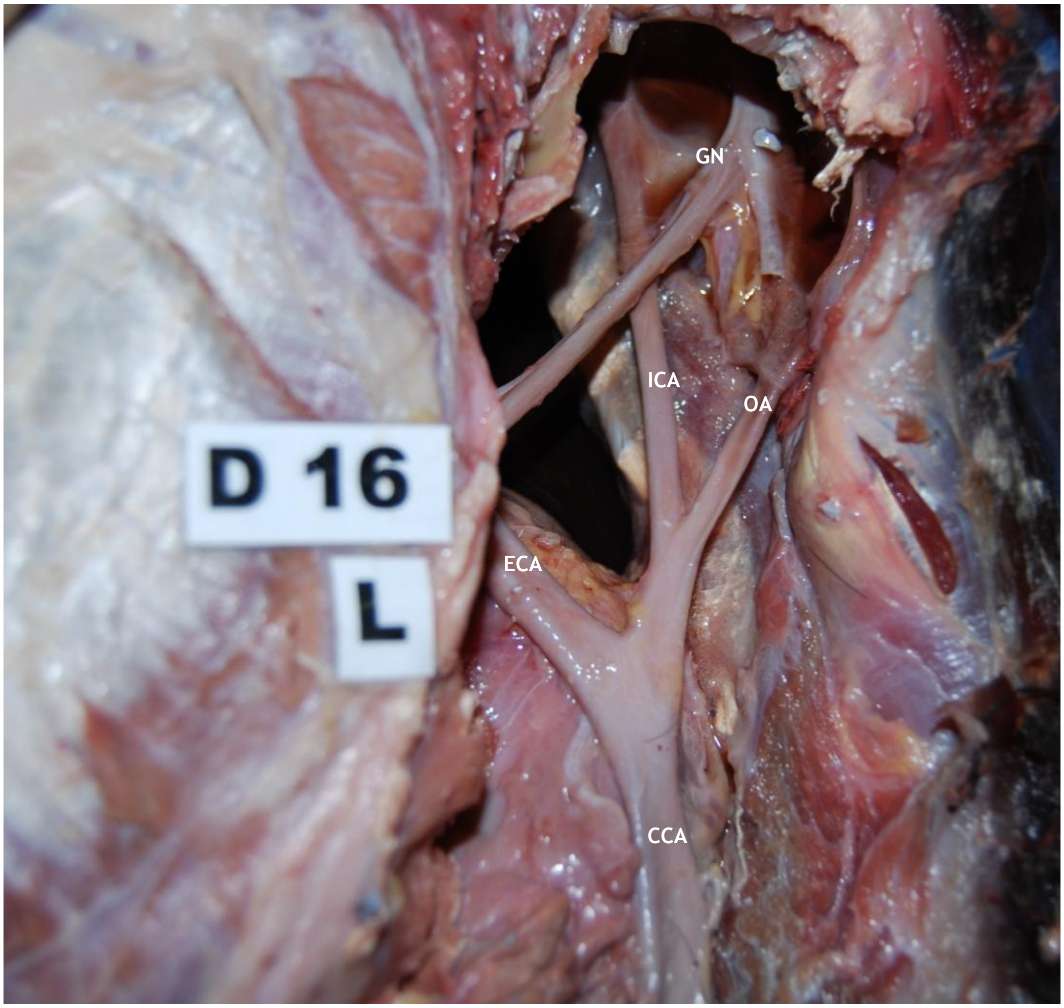

Figure 5-9: Anatomy of the left internal carotid artery in this donkey shows variation from the common pattern of this structure, where the internal carotid artery and the occipital artery share a common trunk from the common carotid artery.
ICA= internal carotid artery; CCA= common carotid artery; ECA= external carotid artery; OA= occipital artery; GN= glossopharyngeal nerve.

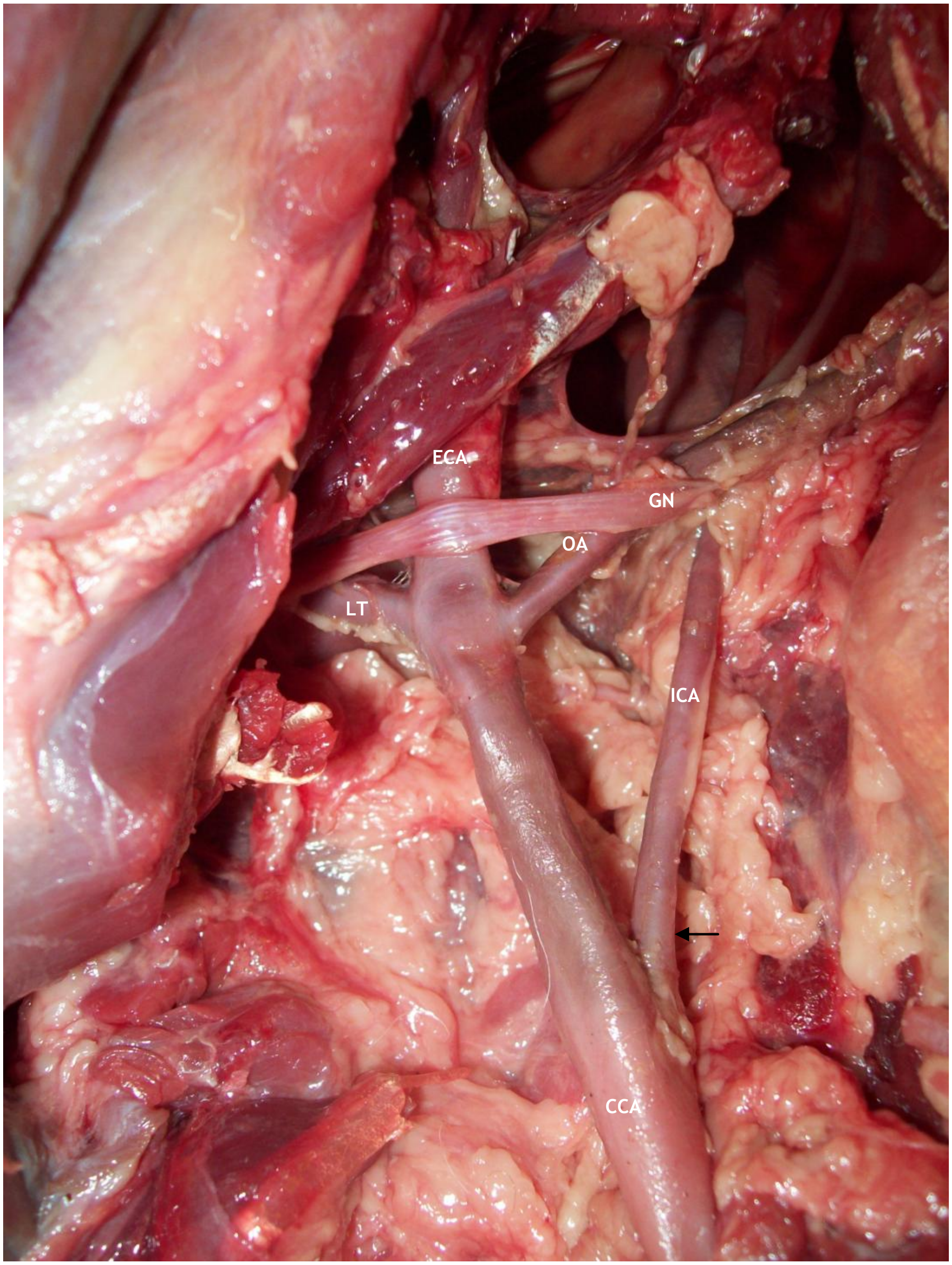

Figure 5-10: Anatomy of the left internal carotid artery in this donkey shows variation from the common pattern of this structure, where the internal carotid artery (arrow) originates very caudal to the termination of the common carotid artery.
ICA= internal carotid artery; CCA= common carotid artery; ECA= external carotid artery; OA= occipital artery; LT= linguofacial trunk; GN= glossopharyngeal nerve.

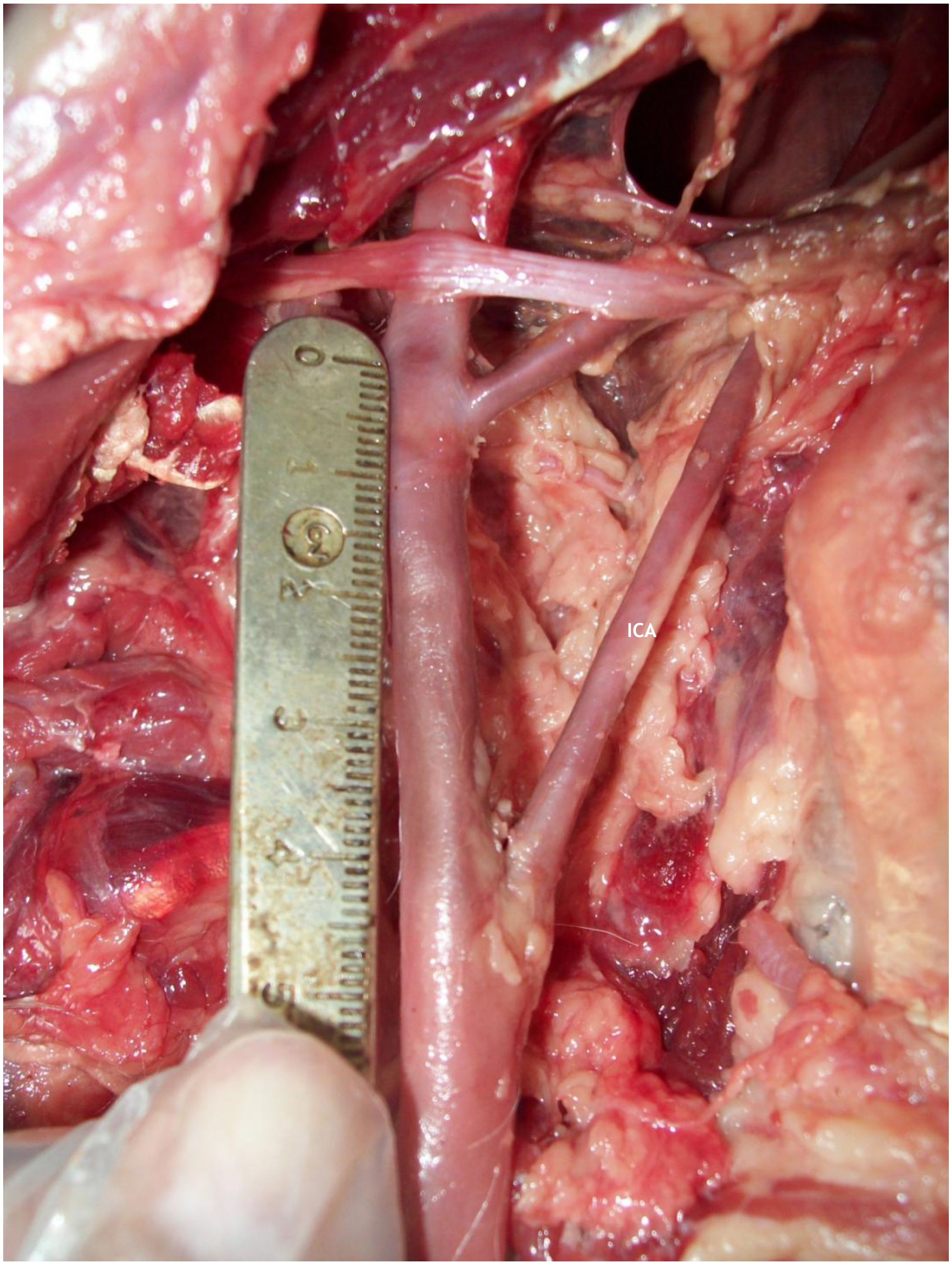

Figure 5-11: Anatomy of the left internal carotid artery in this donkey shows variation from the common pattern of this structure, where the internal carotid artery (arrow) originates very caudal to the termination of the common carotid artery. The distance of the origin of the internal carotid artery to the termination of the common carotid artery measured 4cm.
ICA= internal carotid artery

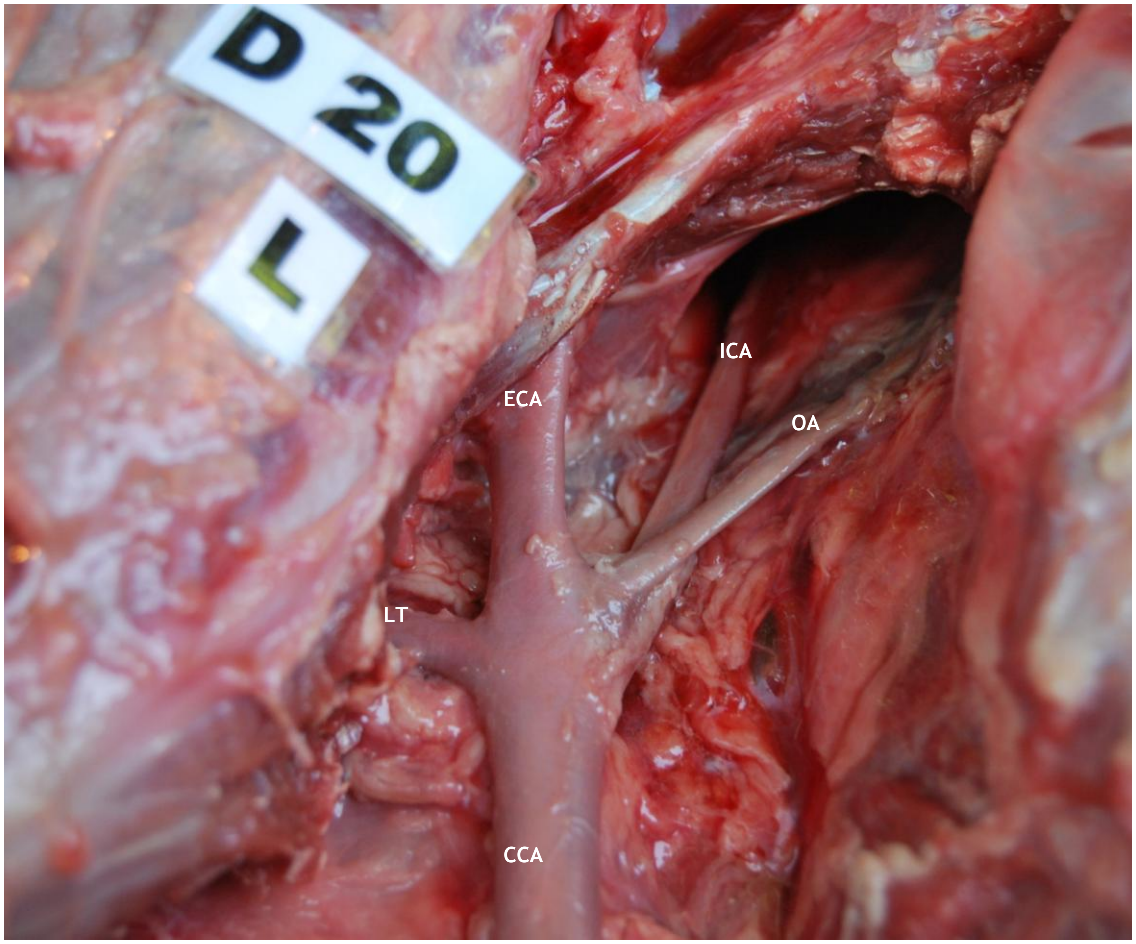

Figure 5-12: Anatomy of the left carotid termination in this donkey shows variation from the common pattern of this structure, where the linguofacial trunk originates from the common carotid artery.
ICA= internal carotid artery; CCA= common carotid artery; ECA= external carotid artery; OA= occipital artery; LT= linguofacial trunk.

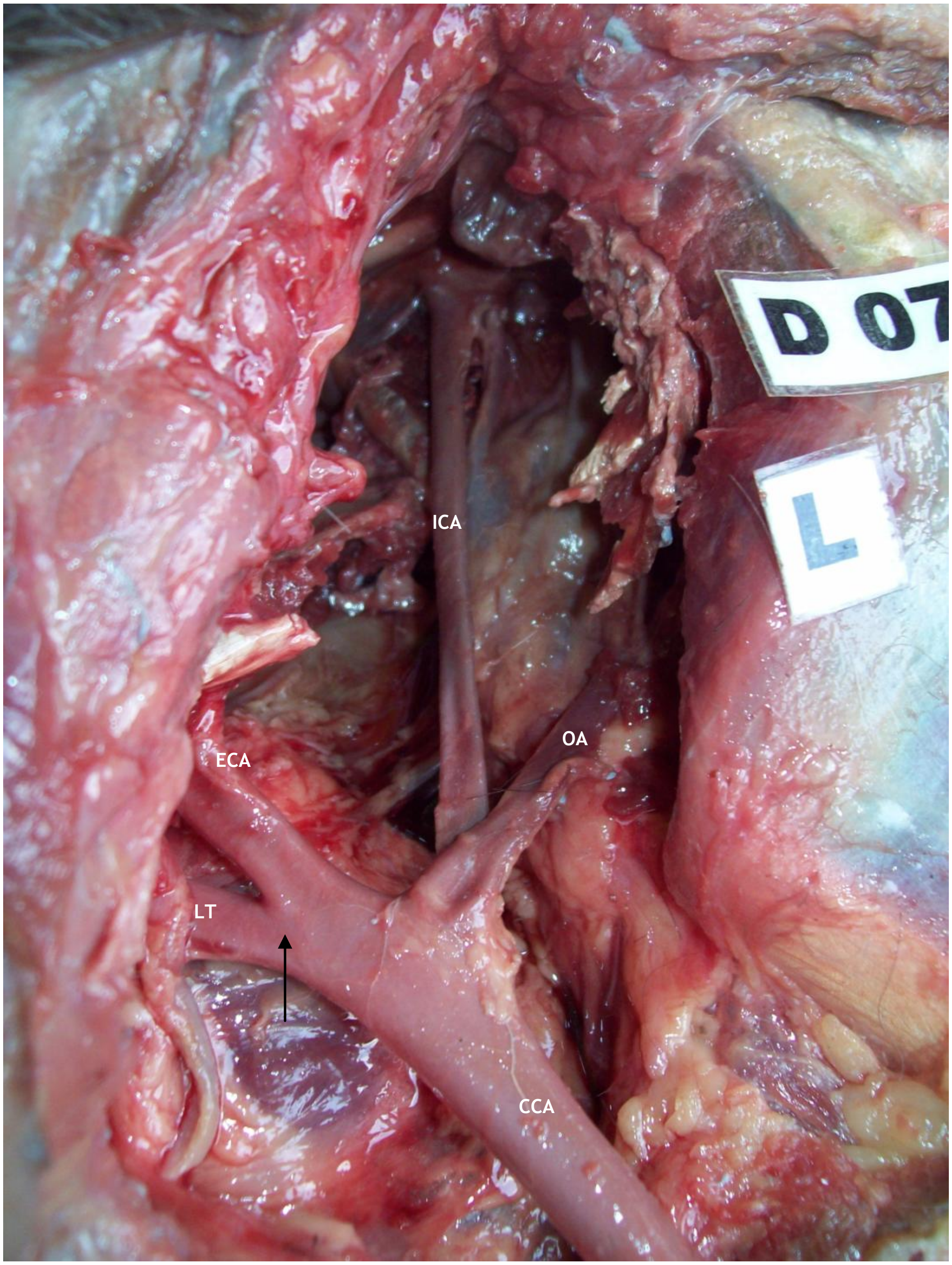

Figure 5-13: Anatomy of the carotid termination in this donkey shows variation from the common pattern of this structure, where the linguofacial trunk (arrow) shares the same origin with the external carotid artery.
ICA= internal carotid artery; CCA= common carotid artery; ECA= external carotid artery; OA= occipital artery; LT= linguofacial trunk.

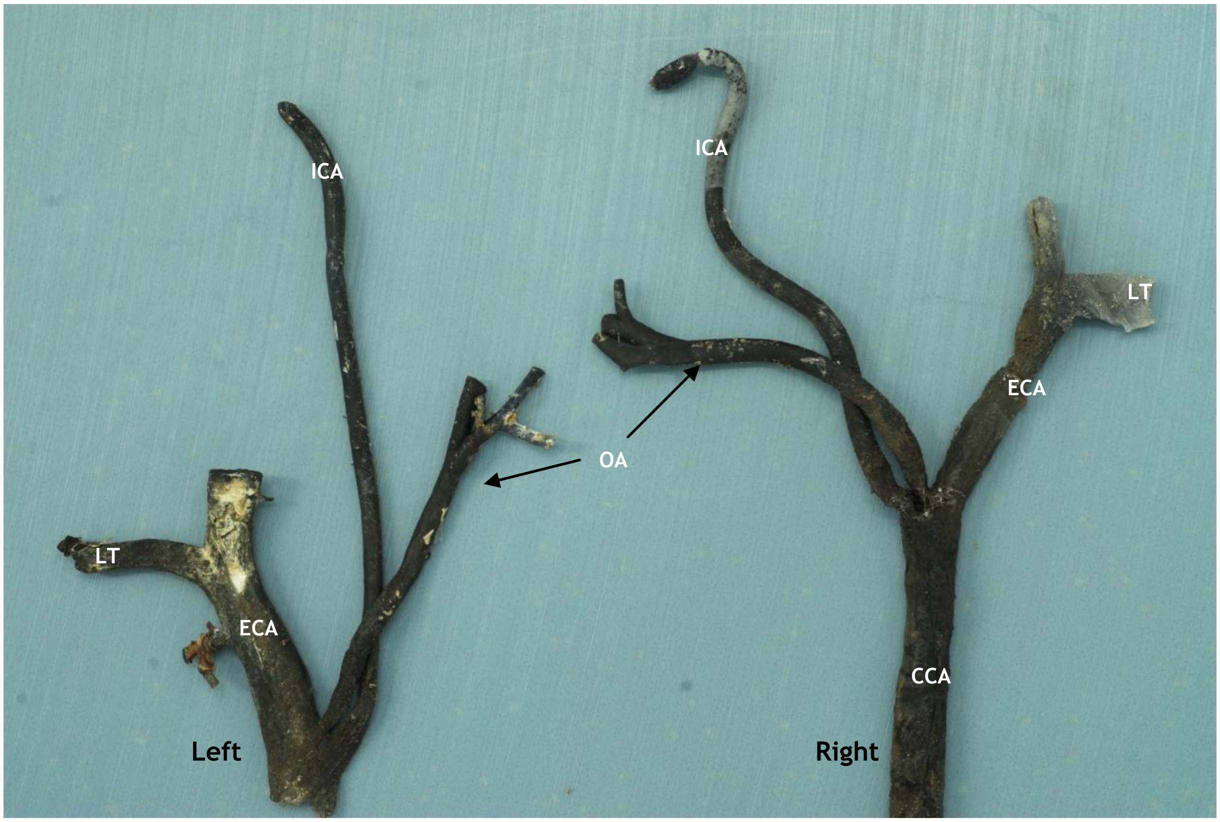

Figure 5-14: Horse (10)-Arterial latex cast of common anatomical pattern of the left and right carotid trifurcation and internal carotid artery.
ICA= internal carotid artery; CCA= common carotid artery; ECA= external carotid artery; OA= occipital artery; LT= linguofacial trunk.

5-15: Horse (15)-Latex cast of common pattern of the left carotid arterial tree.

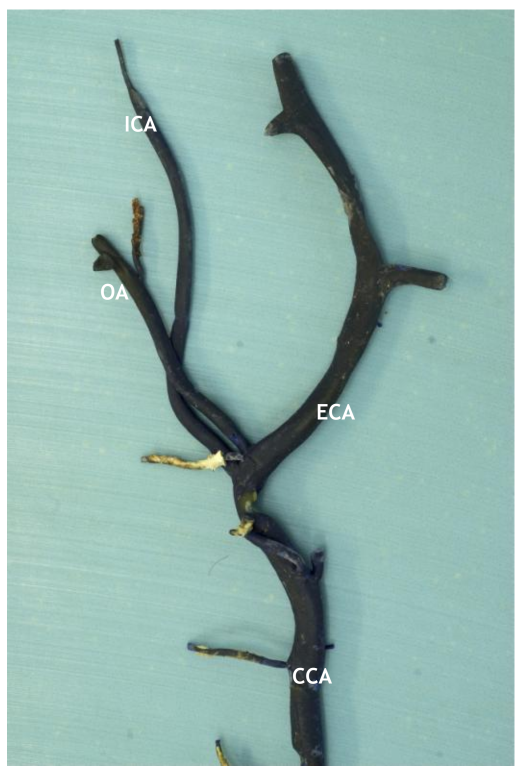

5-16: Horse (15)-Latex cast of a common pattern of the right carotid arterial tree.

Figure 5-17: Horse (3)-Latex cast to show the presence of an aberrant branch of the left internal carotid artery.
ICA 1= original internal carotid artery; ICA 2= aberrant branch; CCA= common carotid artery; ECA= external carotid artery; OA= occipital artery; LT= linguofacial trunk.

Figure 5-18: Horse (13)-Latex cast to show presence of aberrant branch of the left internal carotid artery. ICA 1= original internal carotid artery; ICA 2= aberrant branch.

Figure 5-19: Horse (6)-Latex cast to show the right internal carotid artery and occipital artery share a common trunk from the common carotid artery before diverging (arrow).

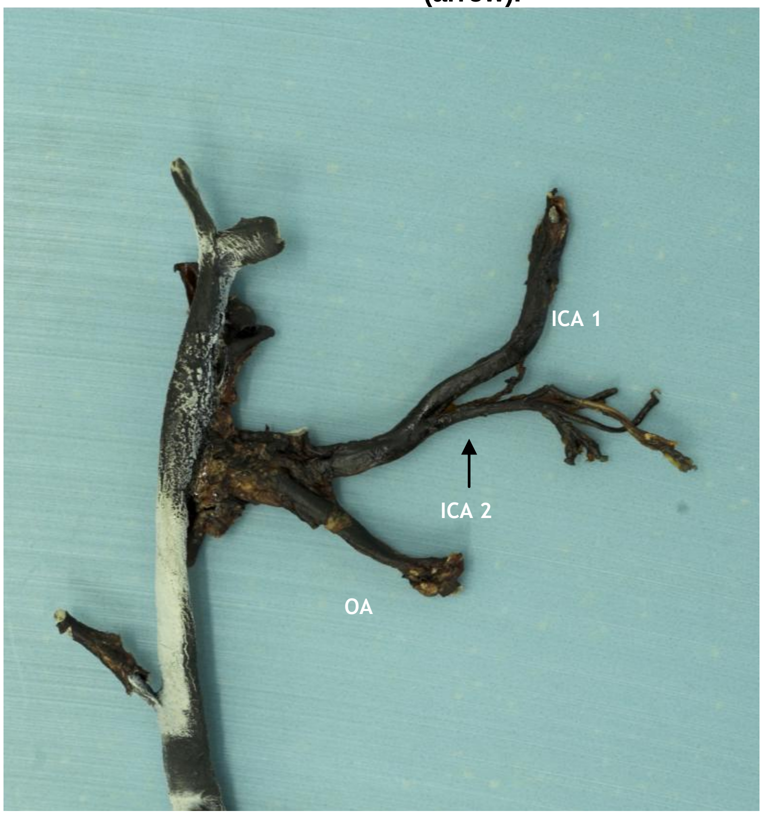

Figure 5-20: Horse (14)-Latex cast of the left aberrant internal carotid artery with satellite vessels.

Figure 5-22: Horse (29)-Latex cast showing the aberrant branch of the right internal carotid artery (arrow).

Figure 5-21: Horse (18)-Latex cast showing the aberrant branch of internal carotid artery (right) with satellite branches.

Figure 5-23: Horse (7)-Latex cast showing that the aberrant branch of the right internal carotid artery gives rise to another branch (arrow).

Figure 5-24: Horse (34)-Latex cast showing that the aberrant branch of left internal carotid artery gives rise to several satellite branches (arrow).

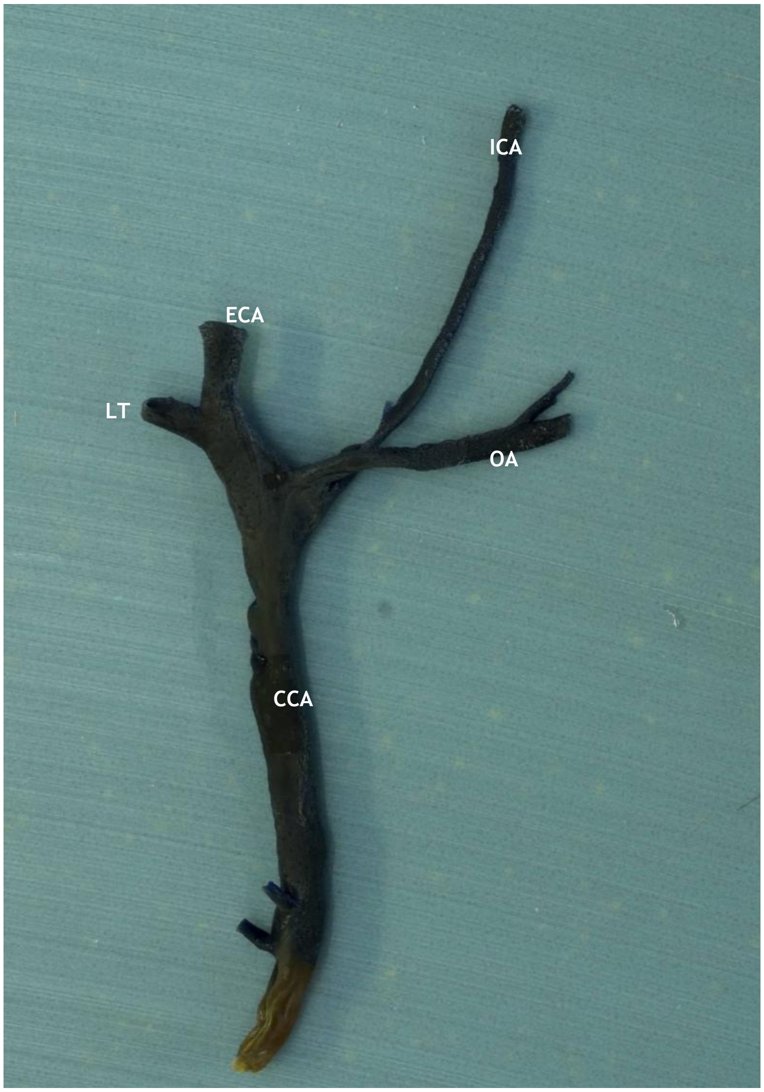

Figure 5-25: Donkey (2)-Latex cast showing the left linguofacial trunk sharing the same origin with the external carotid artery from the common carotid artery.
ICA= internal carotid artery; CCA= common carotid artery; ECA= external carotid artery; OA= occipital artery; LT= linguofacial trunk.

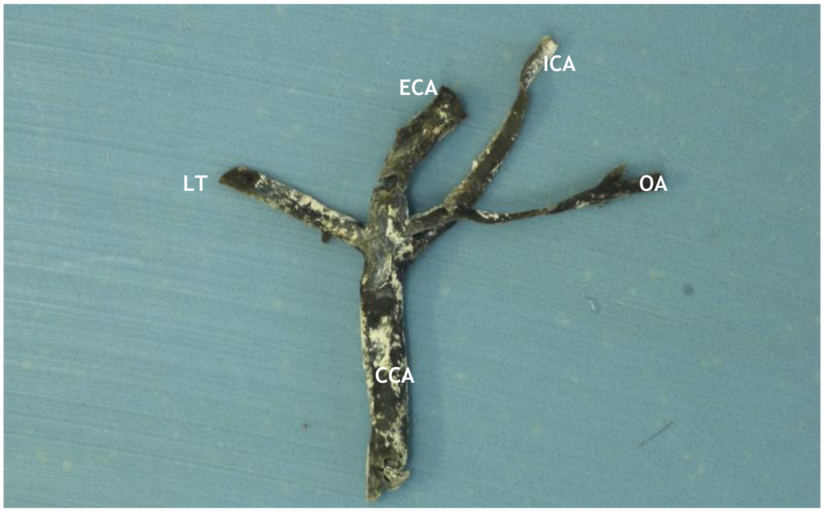

Figure 5-26: Donkey (20)-Latex cast showing the origin of the left linguofacial trunk coming directly from the common carotid artery.
ICA= internal carotid artery; CCA= common carotid artery; ECA= external carotid artery; OA= occipital artery; LT= linguofacial trunk

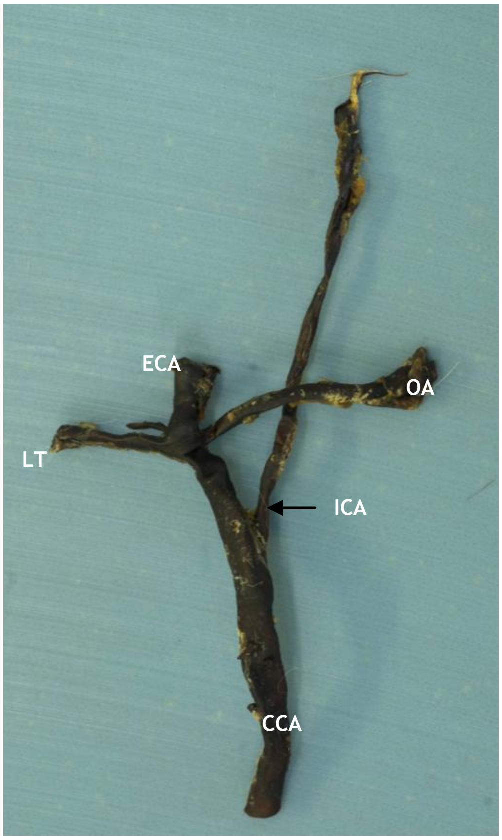

Figure 5-27: Donkey (9)-Latex cast showing the origin of the left internal carotid artery was very caudal to the common carotid artery termination, and its linguofacial trunk arose directly from the common carotid artery.
ICA= internal carotid artery; CCA= common carotid artery; ECA= external carotid artery; OA= occipital artery; LT= linguofacial trunk

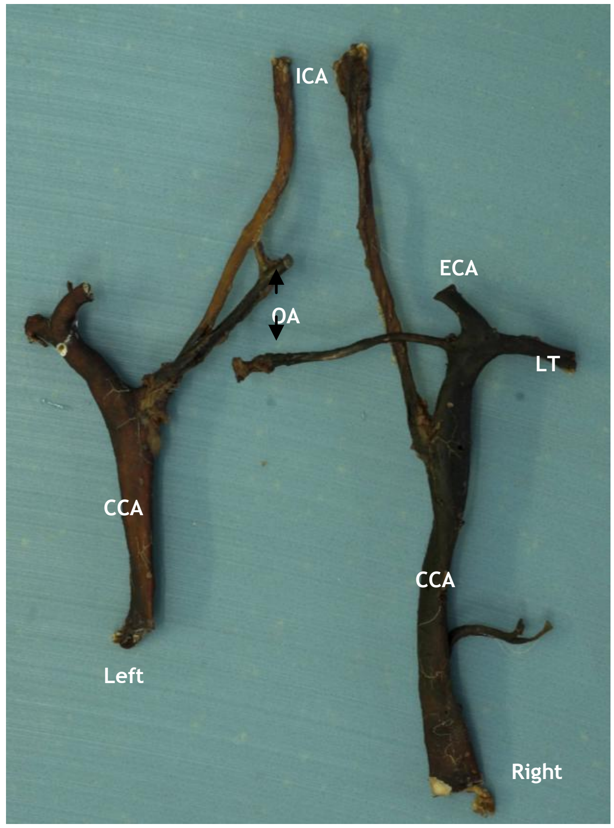

Figure 5-28: Donkey (18)-Latex cast of the right side of carotid arterial tree of a donkey showing that the origin of the internal carotid artery was very caudal to the common carotid artery termination and its linguofacial trunk arose directly from the common carotid artery. The left carotid trifurcation shows a common anatomical pattern of this structure.
ICA= internal carotid artery; CCA= common carotid artery; ECA= external carotid artery; OA= occipital artery; LT= linguofacial trunk.

6 GENERAL DISCUSSION

The aim of the work was threefold. First, was to record the anatomy of the carotid trifurcation and the internal carotid artery in horses and donkeys. Second, was to determine the variation of the carotid trifurcation and internal carotid artery within, and between, species of the genus *Equus*. To achieve this, two investigative techniques were employed namely; rotational angiography and arterial latex casting/dissection, the latter as corroboration for the angiographic findings. Third, was to use these findings and consider their clinical relevance with regard to guttural pouch disease.

Until recently, carotid and cerebral vascular imaging of horses were performed commonly using conventional angiography where the horse was positioned in lateral recumbency with the head on a radiographic cassette, plate changer, or alternatively using a fluoroscope. Several radiographic views were taken by changing the position of the tube head manually. Usually, only lateral and dorsoventral views of the carotid arterial tree or the cerebral vessels were obtained (Colles and Cook, 1983). The dorsoventral view for carotid angiography was thought to be of limited diagnostic value because the carotid tree was obscured by the rami of the mandibles. However, for cerebral angiography in horses, both lateral and dorsoventral views were used frequently (Cook, 1973, Colles and Cook, 1983).

Conventional angiography of the vascular network is limited always by its 2-dimensional representation of the 3-dimensional structure and course of the blood vessels. Among the problems faced are vessel overlap, and difficulties in determining the course of eccentric or tortuous vessels (Green et al., 2004). In the horse, this could be a problem when a surgeon needs to determine the point of take off where the internal carotid artery and occipital artery share a common trunk. Optimal visualisation of an aberrant branch of the internal carotid artery is also limited during two dimensional studies and could lead to the misrepresentation of such a branch as a dilatation or aneurysm of the vessel.

Furthermore, the techniques used in conventional angiography are not standardised and chosen subjectively by the operators depending on their personal preference for visualising a 3D structure of the region of interest from 2D images. Imaging techniques intended to address the weaknesses of conventional angiography have been developed in the form of rotational angiography (Green et al., 2004).

Major advantages of using rotational angiography are that it is a very rapid technique and fully automated, thus it maintains consistency during imaging and requires fewer personnel to acquire such a large number of angiographic images in a series. Another advantage is that it requires less contrast material and radiation compared to conventional angiography (Tommasini et al., 1998).

Based on the works performed here, it would not be unreasonable to claim that 2D and 3D rotational angiography definitely complement/superior to conventional 2D angiography, in which the rotational modality improves imaging and analysis of cerebral vessels which also in agreement with rotational angiographic work performed in human (Bosanac et al., 1998, Heautot et al., 1998, Grass et al., 1999, Elgersma et al., 1999, Anxionnat et al., 2001, Hochmuth et al., 2002, Hirai et al., 2003, Hyde et al., 2004, Pedicelli et al., 2007, McKinney et al., 2008, Van Rooij et al., 2008).

It should be mentioned here that all the 3D images, using the Ziehm Vario 3D mobile fluoroscopic machine, have been reconstructed from non-subtracted rotational images. The 3D rotational angiographic (non-subtracted input data) has several theoretic advantages over 3D digital subtraction angiography. 3D digital subtraction angiography requires a contrast material opacified image and a mask image to obtain a subtraction image dataset, whereas 3D rotational angiography does not need a mask image. The post processing capabilities of the 3D rotational angiography dataset allow viewing in any desired projection with high resolution without interference by superimposed bony structures (Van Rooij et al., 2008). With this in mind, the theoretical advantages of 3D rotational angiography technique over digital subtraction angiography include misregistration artefact associated with this subtraction technique could be avoided, reduction in occurrence of motion artefacts by single image acquisition and lower the radiation dose to patients (as radiation dose for mask image is not necessary) (Hirai et al., 2003). Support for the avoidance of subtraction is evidenced by the data that shows that when motion artefacts occurred during image acquisition of subtracted images, the non-subtracted image was found to be diagnostic and reliable (Bosanac et al., 1998). Thus, the clinical usefulness of unsubtracted rotational angiography or with combination of its 3D modelling cannot be disregarded.

As far as alternatives methods are concerned, carotid and cerebral vascular imaging can also be obtained by using computed tomography angiography (CTA) and magnetic resonance angiography (MRA). Whilst superficially attractive, there are a number of logistical problems of getting horses onto the operating tables designed for the average human. The sheer volume of the bone of the equine skull and neck will lead to a degree of beam hardening (Joseph and Spital, 1978, Mostrum and Ytterbergh, 1986). This hardening contributes to a hypoattenuating artefact, called the *Hounsfield bar*, which makes identification and interpretation of the course of smaller vessels difficult in the equine caudal fossa and upper neck region (Barbee et al., 1987, Hathcock and Stickle, 1993). The use of thinly collimated slices for reformatting of thick section images has been shown to reduce skull base (bone) artefacts in man and the horse (Alberico et al., 2000, Porat-Mosenco et al., 2004). The drawbacks of using helical computed tomography angiography in man have been described (Young et al., 1999, Korogi et al., 1999). This technique has reduced sensitivity in the detection of small intracranial aneurysms (less than 3mm in size) which lead to false negatives diagnosis. Problems can also arise if the time of scanning does not match the time of peak intra-arterial contrast-medium concentration (Young et al., 1999). Nevertheless, intra-arterial CT angiography for distal limb vascular anatomy has been described (Collins et al., 2004).

The attraction of standing magnetic resonance imaging in the horse is obvious. However, as the horse is conscious, even if sedated, movement will be a major cause of artefact. Although motion correction is possible in the standing horse for the distal limb, but here at least the foot is on a stable surface, compared to the head which is capable of movement as is the trunk of the horse (McKnight et al., 2004). Furthermore, compared to computed tomography, magnetic resonance studies require prolong acquisition times for each of the sequences, thus prolonged the time of general anaesthesia or sedation.

However, even in man when compared to intra-arterial digital subtraction angiography in identifying an aneurysm on cerebral vessels, magnetic resonance imaging angiography has proven to have its own limitations due to low spatial resolution. In addition, the matter of slow or turbulent flow that leads to loss of signal within the vessel, which results in missing information on the image (Schuierer et al., 1992, Anzalone et al., 1995). Thus, even though the magnetic resonance angiography has evolved over the past decade, but it cannot replace catheter based angiography as the initial tool for identification and localisation of aneurysms (Bederson et al., 2009).

In comparison to selective intra arterial angiography, both magnetic resonance angiography and computed tomography angiography do not provide imaging of the entire cerebral vasculature and lack of precise information regarding intracranial hemodynamics (Anxionnat et al., 2001). Thus, selective intra arterial digital subtraction angiography remains the technique of choice for cerebral vascular imaging and identification of intracranial aneurysms and to assist in an endovascular procedure (Anxionnat et al., 2001). Less invasive methods of carotid and cerebral vascular imaging such as the computed tomography and magnetic resonance may act as a screening examination or to complement catheter angiography technique, if the significant technical and safety issues could be overcome.

Rotational angiography is a superior image acquisition technique that allows imaging of vascular structures in a three dimensional format and provides more visual information than conventional angiography, particularly lesions involving the internal carotid artery. This technique allows vascular structures to be viewed from multiple projection angles and produce a series of 2D angiographic images which can be viewed using a Cine-Loop function. Algebraic reconstruction algorithms of the 2D angiographic series generate true 3D images where these images can be manipulated using a 3D multi-planar reconstruction (3D-MPR) modality. The combination of the rotational angiography and 3D modelling algorithms ideally results in more accurate and dynamic angiographic images that may be used to identify, diagnose and treat any vascular abnormalities or diseases.

The key point in achieving accuracy in rotational angiography depends on the isocentring of the subject or positioning of the subject in the centre of the detector. Improper positioning of the isocentring beam will result in the subject of interest being unable to be seen in full in a single 3D frame when the C-arm changes position. The technique of isocentring the subject was an easy task to learn but it required some understanding of the basic anatomy and 3D output of the area of interest. Once the technique was mastered, isocentring required less than 10 seconds, and could be performed even in an emergency situation.

It would be interesting, as a follow up to the work presented here, to conduct a study among surgeons and imaging experts to rate the angiographic images and obtain data on intra-observer and inter-observer agreements when comparing images from conventional 2D, rotational angiography (presented in Cine-Loop function) and 3D-MPR modelling of the carotid arterial tree and the internal carotid artery. This would perhaps provide for a better understanding of the clinical value of different imaging techniques and the confidence that can be attached to imaging findings. This is another substantial study where organisation and management would be not inconsiderable.

The carotid and cerebral anatomy of the horse has been used as the reference against which the anatomy of other species in the genus *Equus* is compared (Nanda, 1975, Colles and Cook, 1983). In this study, anatomical variation and vessel eccentricity of the carotid arterial tree in Equidae (horses, donkeys and one zebra) were determined and classified into groups. Based on carotid angiography and dissection findings, five variations of the internal carotid artery in the horses were identified:

1. **The internal carotid artery and occipital artery arose as a common trunk**

2. **Aberrant branch of the internal carotid artery that united with the basilar artery**
3. **Aberrant branch of the internal carotid artery that did not unite with the basilar artery**
4. **Aberrant branch of the internal carotid artery that gave rise to several satellite branches**
5. **Aberrant branch of the internal carotid artery that had a satellite branch that was connected to the caudal branch of the ipsilateral occipital artery**

On the other hand, in the donkeys, the anatomical variations were seen at the termination of the common carotid artery, rather than on the internal carotid artery itself. The variations of the carotid arterial tree in donkeys were identified as follows:

1. **The internal carotid and occipital arteries sharing a common trunk**
2. **The linguofacial trunk originating from the common carotid artery causing the common carotid artery to terminate as four branches**
3. **A short external carotid artery before it gave rise to the linguofacial trunk, giving the appearance of the common carotid artery terminating into four branches**
4. **The internal carotid artery originating caudal to the common carotid artery termination**

In one zebra studied, the anatomy of the carotid arterial tree and the internal carotid artery followed the common or standard anatomic description of these structures in the horse. Whilst this was an interesting opportunity to study a zebra and the images showed an anatomy analogous to the horse, the results of the work in the horse and the donkey demonstrate that the results from a single study cannot be considered a reference specimen.

Some of the anatomical variation findings of the carotid arterial tree, and especially the internal carotid artery, have been reported previously in relation to diseased and non-diseased horses, and one donkey with guttural pouch mycosis

(Table 6-1). The importance of investigating arterial variations involving the internal carotid lies in the fact that this artery is a surgical target in cases of guttural pouch mycosis. The typical location of invasion of mycotic plaque on the internal carotid artery is at the dorsal aspect of internal carotid artery just caudal to its sigmoid flexure. The purpose of surgical occlusion of the internal carotid artery in cases of guttural pouch mycosis is to prevent fatal haemorrhage due to erosion of the artery caused by invasion of mycotic plaque across the wall of the medial compartment of the guttural pouch, clinically manifested by epistaxis. The haemorrhage from the blood vessels runs into the guttural pouch, from where it flows to the pharynx and out through one or both nostrils. Occlusion of affected arteries has been stated to cause regression of the fungal plaque (Freeman and Donawick, 1980a, Church et al., 1986, Caron et al., 1987, Greet, 1987, Freeman et al., 1989, Speirs et al., 1995, Lévéille et al., 2000, Lepage, 2005). However, occlusion of the affected artery could be hampered when there is anatomical variation of the arteries, most importantly the internal carotid artery as most cases of guttural pouch mycosis involve this artery (Colles and Cook, 1983).

The internal carotid artery is not an end artery, thus to prevent haemorrhage from the internal carotid artery, normograde and retrograde blood flow should be prevented. Occlusion of the affected internal carotid artery at its origin does not reduce the risk of fatal haemorrhage because retrograde blood flow from the cerebral arterial circle maintains the arterial pressure distal to the occlusion site. Successful occlusion of the internal carotid artery to overcome this problem was achieved by occluding the vessel rostral to the mycotic lesion (preventing retrograde flow) and also on the cardiac site of the lesion (preventing normograde flow) (Freeman and Donawick, 1980a).

In the past, balloon tipped catheter technique was the recommended technique for occlusion of affected blood vessels (Freeman and Donawick, 1980a, Freeman et al., 1989). For the internal carotid artery, the balloon catheter was inserted into a vessel and inflated rostral to the mycotic lesion and the internal carotid artery was then ligated at the cardiac side of the lesion or at its origin (due to easier access at surgery) (Freeman and Donawick, 1980a). A recent advance in vascular occlusion is transarterial coil embolisation technique introduced by Matsuda et. al (1999) and Leveille et. al (2000). With this technique, angiography is essential before embolisation for correct identification of vessels and to appreciate any vascular anomalies and anatomical variations, particularly aberrant vessels. A multipurpose angiographic catheter is advanced within the vessel (internal carotid artery/external carotid artery/maxillary artery) and the first coil/s is delivered rostral to the lesion. Then the angiographic catheter is withdrawn and the second coil/s is delivered on the cardiac side of the lesion (Lepage, 2011) (personal communication). Coils were inserted until the artery was completely occluded and vessel leakage had ceased as judged by intra-operative contrast angiography. Following placement of coils, angiography is performed again to confirm cessation of blood flow to the embolisation site. Accurate placement of coil is possible with this technique, and ligation at the origin of the internal carotid artery is not required.

In relation to the finding of an aberrant branch of the internal carotid artery connected to the basilar artery, retrograde blood flow from the cerebral arterial circle into the internal carotid artery would be maintained by this connection in the live horse. However, the aberrant branch of the internal carotid artery found here usually arises caudal to the typical location of mycotic plaque. If transarterial coil embolisation technique is used for occlusion of this vessel, the presence of an aberrant branch caudal to the mycotic lesion is not an issue because a coil can be place very accurately caudal to the lesion. Thus, any aberrant branch (caudal to the lesion) would not need to be occluded so that it could provide a channel for the retrograde blood flow to the distal part of the internal carotid artery.

On the other hand, if a balloon tipped catheter technique is used, ligation of the internal carotid artery close to the mycotic lesion at a more dorsal part of this artery is not possible due to limited surgical access to expose the internal carotid artery closer to the mycotic site. Thus normograde blood flow is prevented by ligation at the origin of internal carotid artery. For this reason, any aberrant branch that arose at any point along the internal carotid artery (caudal to the mycotic lesion), needs to be occluded too in order to prevent retrograde blood flow from the cerebral arterial circle that will maintain blood flow into the affected site and contribute to continued haemorrhage. If this aberrant branch of internal carotid artery is not connected to the basilar artery, retrograde blood flow is no longer an issue for such a horse (depending on the size and the diameter of this aberrant vessel). Consequently, a surgeon would have the option of not ligating this vessel, provided one is sure it does not unite with the basilar artery. A satellite vessel originating from an aberrant branch of the internal carotid artery was observed to be connected to the ipsilateral occipital artery. Perhaps, if such variation is found and occlusion of the internal carotid artery using balloon tipped catheter technique is to be attempted, occlusion at the origin of this satellite vessel should also be carried out to prevent normograde blood flow contributed by the occipital artery to the bleeding site.

The factors that may dictate the choice of surgical management in cases of guttural pouch mycosis involving important blood vessels are cost, access to fluoroscopic unit, surgical and imaging expertise (Freeman and Donawick, 1980a, Lévéille et al., 2000, Lepage, 2005). Thus, if an equine hospital is equipped with the facilities and expertise to conduct a transarterial coil embolisation technique and cost is not an issue for the owner, definitely this technique is currently the gold standard for the surgical treatment of guttural pouch mycosis. However, in other equine practises where this advance in technology is not feasible, occlusion of affected vessel can still be carried out using balloon tipped catheter technique, which is much cheaper and does not require diagnostic imaging support.

Retrospectively, the findings reported here might explain a number of incidents of post operative haemorrhage due to variation of the internal carotid artery. Greet (1987) reported the presence of satellite vessels on the internal carotid artery and these satellites were also ligated at their origin (one horse). However, this horse died of exsanguination four weeks post-operatively. Perhaps, this post operative exsanguination was due to retrograde blood flow, which was contributed to by these satellite vessels of the internal carotid artery. It was of note that we found such satellite vessels from aberrant branches of the internal carotid artery, which were seen to connect to the basilar artery (two horses). In one specimen, one of the satellite vessels was connected to the ipsilateral occipital artery.

On the other hand, Church et. al (1986) described a variation where the common carotid artery bifurcated, presumably the internal carotid and occipital arteries arose from a common trunk, but this vessel did not appear to separate despite extensive dissection. This was ligated without certainty of which vessel it could be, whether it was internal carotid, occipital or a common trunk. This horse died of severe haemorrhage six weeks post operatively. In the light of our findings, possibly the separation of internal carotid and occipital arteries from the common trunk occurred much higher and the branching point was obscured by the presence of the wing of atlas, and which would also be difficult to observe during surgery (as seen in two horses in this study-Fig. 5-8). In addition to that, as a single ligation technique was used to occlude this vessel at its origin, it had failed to prevent retrograde blood flow coming from the cerebral arterial circle, resulting in post operative haemorrhage.

Another post operative haemorrhage has been reported in a horse where the presence of an aberrant branch of the internal carotid artery resulted in failure to prevent retrograde blood flow from the cerebral arterial circle (Freeman et al., 1993). This aberrant branch of the internal carotid artery was found to be connected to the basilar artery. These authors believed that this aberrant branch was an unusual form of the caroticobasilar artery because the typical caroticobasilar artery could not be found at the affected site. However, our acknowledged limited finding in one horse might not support this suggestion as in one specimen with an aberrant branch of the left internal carotid artery, a left caroticobasilar artery was also present (H43, Table 2-2).

Caroticobasilar arteries were found in the three species studied here and were considered a common variation in accordance with Nanda (1975), Nanda and Getty (1975), Frackowiak (1997) & Ozgel and Dursun (2007). One variation noted with regard to the caroticobasilar artery was that an anastomosing vessel was seen connecting this vessel to the caudal intercarotid artery (one horse) and regarded as another common variation.

Only in the horse, and regarded as a variation of the caudolateral quadrants of the cerebral arterial circle, was the finding of rete/plexuses at the union of the caudal communicating and the basilar arteries. The rete was seen as various anastomotic fine vessels interconnecting the basilar artery to the caudal communicating and caudal intercarotid arteries. It should also be mentioned here that this observation was based on images from 2D rotational sequence. Issue of superimposition from other vessels were taken into consideration and verified at each different angle of rotational view. The question arises as to whether this anatomical variation would affect any surgical option in the treatment of guttural pouch mycosis. In our opinion, the importance of this variation would arise if bilateral ligation of the common carotid artery was to be performed.

An emergency surgical treatment for guttural pouch mycosis has been described (Woodie et al., 2002, Hardy and Léveilé, 2003) where temporary ligation of the common carotid artery on the side of epistaxis can be performed to prevent further haemorrhage while the horse is transported to a hospital. In a personal communication (Lepage, 2011), suggested that permanent ligation of both carotid arteries was possible and had been performed in a number of cases without any major side effects. In his opinion, even though blood supply to the brain would be impaired with this technique, the basilar artery would still be able to supply the brain of the horse and perhaps with time, more new blood vessels from the basilar will generate to meet the blood demand of the brain. This view is supported by a research study in the dog that found simultaneous bilateral single ligation of both common carotids and vertebral arteries was compatible with life (Bunce, 1960).

However, if the intercarotid or basilar arteries are small or form a rete/plexus (as seen in the angiograms of the cerebral arterial circle in four horses studied here), perhaps the circulation within the cerebral arterial circle will be impaired acutely to the extent that the chances of survival are less promising for that horse. Thus, bilateral ligation of common carotid arteries would be contraindicated in horses presented with this type of variation at the level of the cerebral arterial circle.

Even though there has only been one report of guttural pouch mycosis in a donkey (Laus et al., 2011), the importance of studying the carotid and cerebral vessel anatomy is paramount. Based on the findings here, veterinary surgeons need to be aware that the variations of this structure in the donkey were different from those observed in horses.

Table 6-1: Review of publications that report carotid arterial variation (1928- 2011)

Reference	No. of animals studied	No. with GPM	No. with vessel variation	Description of arterial variations found
Winogradow (1928)	1 horse	-	1	Internal carotid artery and occipital artery arose from a common trunk
Meijling (1938)	Not given	-	(?)	Internal carotid artery and occipital artery arose from a common trunk (no. not given)
Furuhata (1964)	43 horses	-	3	Internal carotid artery and occipital artery arose from a common trunk (2 unilateral side, 1 bilateral side)
Orr et. al (1983)	12 horses	-	(?)	Internal carotid artery and occipital artery arose from a common trunk (no. not given)
Colles and Cook (1983)	37 horses	25	9	Aberrant branch of internal carotid artery based on angiography (5) and endoscopy (4)
Church et. al (1986)	17 horses	17	1	Only one branch of common carotid artery that did not separate as internal carotid and occipital arteries
Greet (1987)	35 horses	35	1	Left internal carotid and occipital arteries arose from a common trunk
Caron et. al (1987)	13 horses	13	?	Internal carotid artery and occipital artery arose from a common trunk (number not given)
Hardy et. al (1990)	2 horses	2	1	Left internal carotid artery and occipital artery arose from a common trunk
Freeman et. al (1993)	1 horse	1	1	Aberrant branch of left internal carotid artery with presence of fine branches of unknown course
Miller et. al (1998)	1 horse	1	1	Absence of sigmoid flexure of the left internal carotid artery. Left occipital artery was also absent
Leveille et. al (2000)	16 horses	4	1 (?)	1 case: aberrant branch of external carotid artery Internal carotid and occipital arteries arose from common trunk (no. not given)

GPM= Guttural Pouch Mycosis

Continue on the next page

Reference	No. of animals studied	No. with GPM	No. with vessel variation	Description of arterial variations found
Marcus (2002)	14 horses	-	2	Aberrant branches of the internal carotid artery; 1 found endoscopically and the other at post-mortem
Lepage et. al (2005)	31 horses	31	2	2 had aberrant branches of the internal carotid artery
Laus et. al (2010)	1 donkey	1	1	Dilatation of the maxillary artery following fungal plaque invasion on that site

GPM= Guttural Pouch Mycosis

In this study, high contrast delineation of the carotid trifurcation and the internal carotid artery during rotational angiography provided excellent Cine loop and 3D-MPR images, but there was a recognised problem with 3D-MPR in demonstrating small arteries. However, it is probably not important for the equine surgeon to appreciate very fine vessels (in 3D representation) as compared to situation in man.

It should be mentioned here that observation of intracranial arterial peculiarities was based on 2D rotational imaging. Issues of superimposition from other vessels were taken into consideration and verified at each different angle of rotational view. Ideally, the 3D modelling of the cerebral vessels and dissectional confirmation of this region are needed to verify any peculiarity at the intracranial level. Unfortunately, the 3D-MPR representation for specimens with peculiarities at this level failed to highlight these due to limited reconstruction of small vessels. Furthermore, confirmation based on dissection was not carried out intracranially because during the course of the study, it was felt that such dissection could not be valuable from a clinical perspective. With completion of this thesis, it is apparent that it would have been beneficial to have carried out such dissection despite the fact that intracranial variation at that moment is not thought to be relevant to guttural pouch mycosis in terms of diagnostic investigation. Thus, any peculiar angiographic observation at intracranial level in this study were not confirmed.

Several surgical techniques have been described to treat cases of guttural pouch mycosis, however, the Transarterial Coil Embolisation technique (TCE) is considered to be the treatment of choice where this technique combines angiographic studies with coil embolisation of the affected vessel (Lévéille et al., 2000, Lepage, 2005). The use of 3D rotational angiography of the carotid arterial tree during TCE technique would definitely maximise the ability of a surgeon to identify the affected vessel and any aberrant vessels. In addition, it aids selection of the most appropriate C-arm angulation for guiding and controlling the embolisation procedure. Furthermore, this modality improves the diagnostic accuracy of angiography by providing a series of angiographic views that would not have been achieved routinely with the conventional method of angiography. Thus, more anatomical variations or abnormalities of the cerebral vessels may well be identified in the horse, particularly important lesions such aneurysms and stenosis.

In man, accurate diameter and length measurement of a vessel or a lesion is significantly important to aid the decision on coil or stent placement in a vessel (Elgersma et al., 1999, Berg van den et al., 2001). In order to achieve measurement accuracy, calibration and quality assessment must be done during routine maintenance using a known test phantom with a measured size deviation of less than 2% from the actual size (Berg van den et al., 2001). In the horse, accurate measurement of vessels particularly the internal carotid artery will allow accurate sizing and perhaps reduce the number of the coils required to occlude any affected vessel, thus provide effective cost management in the long run. Perhaps in the future, 3D rotational angiography would also allow a true aneurysm in the horse to be defined in detail where quantitative determination of the size of the aneurysmal sac, neck or parent vessels could be identified.

On review of the literatures from the year 1966 to 2011, few important papers in the field of guttural pouch mycosis have described the finding of aneurysms (Table 6-2). It would appear that the reported angiographic identification of aneurysms has declined over the years. A re-evaluation of Colles and Cook (1983) figures raises questions as to whether the aneurysms illustrated are actually artefacts such as superimposition, or in fact branches coming off the affected artery. This poses several questions if the aneurysms reported are genuine. Are they in fact secondary or a consequence of invasion of the guttural pouch with fungal plaque, or are aneurysms exceedingly rare, yet a precipitating factor in the development of guttural pouch mycosis. It may be that advances in imaging modalities and technologies have improved the ability to distinguish the presence of artefact from true aneurysms. Thus, in two more recent angiographic studies combined (Lévéille et al., 2000, Lepage, 2005), the use of a fluoroscopic unit perhaps has resulted in the finding of a low number of aneurysms.

Possibly in the past, the misrepresentation of an aberrant vessel as an aneurysm occurred due to the limitation of the conventional angiographic technique. It is proposed that with increased angiographic views at different angles of the internal carotid artery, one could confirm whether “aneurysm” formation was actually an aberrant branch of the internal carotid. As described in chapter 2, conventional 2D angiographic technique performed here identified the limitations of relying on two views as they can create a recognisable “pseudoaneurysm” due to vessel superimposition. With 3D-rotational angiography, this error would be significantly reduced.

Table 6-2: Review of literatures regarding aneurysm in cases of guttural pouch mycosis.

Reference	No. of horses with guttural pouch mycosis	Aneurysm reported
Colles and Cook (1983)	25	18/25
Greet (1987)	35	8/10 (that underwent angiography)
Speirs (1995)	6	2/6
Leveille et.al (2000)	4	2/4
Lepage et. al (2005)	31	2/31

Aneurysm formation was also reported to be found endoscopically in a donkey affected with guttural pouch mycosis (Laus et al., 2011), and also in two horses (Pollock, 2011) (personal communication). However, questions arise as to whether the observation of an aneurysm of a vessel underneath the mucosa of the guttural pouch via an endoscope really depicts a true representation of this pathological lesion of an arterial wall, because the vessel wall itself was not directly observed. In the light of the finding of fat layers surrounding the whole carotid trifurcation and the vessels that branch from the carotid termination during the dissection of donkeys, perhaps, the dilatation of the vessel seen endoscopically underneath the mucosa of the guttural pouch in the donkey could possibly be due to presence of uneven fat layers that surround the maxillary artery giving the impression of a vessel dilatation, rather than a true aneurysm. The presence of aberrant branches of the internal carotid artery have also been appreciated endoscopically (Colles and Cook, 1983, Marcus, 2002). However, the pathway of an aberrant branch would be difficult to determine endoscopically and other small satellite branches might not be visible, thus angiography would still be the best tool to verify its termination or continuation. As for diagnostic imaging to detect an aneurysm, intra-arterial digital subtraction angiography is the current gold standard used in human (Bederson et al., 2009).

In human, aneurysms are classified based on several features including aetiology (congenital, acquired, dissecting, infectious, tumorous), size, shape (fusiform, saccular) or based on its association with a specific intracranial vessel (Pritz, 2011). In relation to aneurysm formation, the predisposing factors and intracranial aneurysm development related to the arterial wall properties were described based on work done in human (Crawford, 1959, Crompton, 1966, Tognetti et al., 1983, Steiger et al., 1987). The microscopic anatomy of the cerebral arteries revealed the medial layers of the cerebral arteries (which provide the main strength to an artery) are much thinner compared to other vessels. Although the internal elastic lamina was well developed, the external elastic lamina are poorly developed and maybe even absent (Crawford, 1959). In addition to that, the developmental faults in the media, leave gaps of varying size, commonly at the points of arterial junction (Crawford, 1959, Crompton, 1966). Thus, the internal elastic lamina takes most of the responsibilities to maintain strength of the arterial wall in the cerebral arteries. Other considerations in the production of aneurysms are blood pressure and atherosclerotic lesions in a vessel. Hypertension is clinically and experimentally established as an aneurysm promoting factor (Steiger et al., 1987). Haemodynamic stress was postulated as another factor favouring aneurysm formation (Crompton, 1966, Tognetti et al., 1983, Steiger et al., 1987).

Although there were morphological and histological studies of the carotid trifurcation in horses (Furuhata, 1964, Nakamura et al., 1992), to date, a search of the literature has failed to reveal a single publication that describes the gross anatomy and histopathology of an aneurysm of the carotid and cerebral arterial in the horse in order to confirm the true presence of an aneurysm in this species and to corroborate the few angiographic studies that have reported the presence of this arterial lesion in relation to guttural pouch mycosis (Colles and Cook, 1983, Greet, 1987, Lévéille et al., 2000, Lepage, 2005).

Cerebral mycotic aneurysm were demonstrated in a study where the lumen of the internal carotid artery of 16 healthy dogs that were exposed with *Staphylococcus aureus* (Molinari et al., 1973). At post mortem, the infection had produced aneurysms that were tough, fibrotic and adhered to the adjacent dura. None of the aneurysms had ruptured. Macroscopically, aneurysmal lesions showed wall opacification. Microscopically, an intense acute inflammatory response was observed in the adventitial layer penetrating the muscularis layer with irregular borders and sequestration of polymorphonuclear leukocytes into the subarachnoid space. Direct infiltration of the media and outer layer of muscularis of the vessel wall were also observed and were correlated with an increase in the vessel lumenal diameter. While it would be satisfying to extrapolate these experimental findings to the clinical situation in the horse affected with guttural pouch mycosis, it would have to be done so with caution for the following reasons. First, this experiment was conducted on healthy dogs. Perhaps, mycotic lesion on the arterial wall of the horse would not react the same way as it does in the dog. Second, the insult was caused by bacterial rather than fungal as in guttural pouch mycosis. Thus, this aspect really does warrant a histopathology investigation of the diseased artery of the horse affected with guttural pouch mycosis.

Following discussion during the planning stage of this study, the signalment data (age, gender, breed, purpose) as well as the source of the cadaver/specimen materials were not considered relevant. Consequently, as the heads were acquired, such data were not captured. In retrospect, as this was a study of ‘apparently’ healthy as far as the guttural pouch was concerned, it would in fact have been interesting to have recorded where possible the age, gender, breed and working purposes of all the specimens to appreciate if any trends emerged. However, the literature related to guttural pouch mycosis and where anatomical variations of the arteries have been identified, did not report any predilections as far as age, gender, breed or working purposes of horses to the development of guttural pouch mycosis (Cook, 1966, Greet, 1987). In addition to that, even though the horse specimens are a sample of a horse population, but it is arguably if they are representative of United Kingdom population because they were all harvested from the west of Scotland. There would have to be other question marks raised on the validity of any extrapolation of the relatively small number of animals surveyed in this study. First, the last census of horses in Britain occurred in 1934 (Urquhart, 1983). Second, another official assessment of the horse population relates only to the number of horses and the number of holdings (MAFF, 1968). A survey of the demographic characteristics of the equine population in northern Britain (Mellor, et. al 1999) was based on surveys of horse information gleaned from sentinel veterinary practices, i.e, horse owners registered with specific veterinary practitioners. Thus this survey was a sampling rather than a census. Thus it is not possible to ascertain that the horse specimens gathered for this study are truly representative of the Scottish or even the United Kingdom horse population. As for donkey specimens, they were a sample from a population of donkeys owned by the Donkey Sanctuary, United Kingdom, where it was reported that in 2007, 40% of donkey population in the UK was owned by this association (Cox et al., 2010). However, as the name of the organisation suggests their function is to rescue and home unwanted donkeys often from unknown sources.

An interesting suggestion related to the nomenclature of the internal carotid artery in the order Perissodactyla has been proposed (Du Boulay et al., 1975). They proposed that the 'internal carotids' in the whole order of Perissodactyla should be called the 'ascending pharyngeal artery' due to the fact that the artery in question does not pass through a carotid canal in the temporal bone, instead it enters the cranium (from a position that is closely associated with the guttural pouch) directly by piercing the foramen lacerum. An addition to that, there is neither an *arteria anastomotica* nor a *ramus anastomocus* associated with the internal carotid artery in the equine family, as commonly found in other mammals (Du Boulay et al., 1975). A study of the cranial artery ontogeny in mammals also shown that the internal carotid artery in four orders of mammals (Monotremata, Marsupialia, Perissodactyla and Hyracoidea) are presented in the extrabullar state (medial to the auditory bulla and middle ear cavity) (Wible, 1986). Ontogenetically, in the extrabullar state, the internal carotid artery is described to be shifted medially and then lies medial to the middle ear cavity and the auditory bulla, and retains this position in adulthood (Wible, 1986). The phylogenetic importance of this extracranial course of this artery is related to the presence of the guttural pouches that block the course of this artery to the tympanic bulla, and perhaps may explain the reduction of *sulcus caroticus* in these orders of mammals (Fischer, 1989). However, the comparative anatomist and embryologists' understanding of this artery in the Perissodactyla (e.g. horses) (Du Boulay and Verity, 1973, Du Boulay et al., 1975, Wible, 1986, Du Boulay et al., 1998), is that it served the brain via different routes, and does not always correspond to the understanding of today's veterinarian. While arguments on the nomenclature of this artery is of academic value, more important is the physiological consequences of calling it the 'ascending pharyngeal artery'. One might speculate that the blockage of this artery (by the presence of the guttural pouch (during its development) (Fischer, 1989), maybe a factor of predisposing in the development of guttural pouch mycosis, apart from other proposed factors such as aneurysms and anomalous vessels (Colles and Cook, 1983, Greet, 1987). Perhaps in the future, more focus should be devoted to the embryologic development of this artery in the horse. Such work needs to be better disseminated to the veterinary community rather than restricted to specialist anatomical journals. This would allow further research study to be directed to the relationship between internal carotid artery development, its anatomical variations and possible association with the development of guttural pouch mycosis.

6.1 Conclusion

Finally, this study, using rotational angiography and dissection, has demonstrated that there are more variations of the carotid arterial tree, in particular the internal carotid artery, than reported previously in the Equidae, and that the use of 3D rotational angiography is superior to conventional angiography in the imaging of the whole carotid arterial tree. These findings have implications for surgeons seeking to identify abnormalities when performing occlusion of the internal carotid artery in cases of guttural pouch mycosis.

GLOSSARY

BA = Basilar artery

CAC = Cerebral arterial circle

CCA = Common carotid artery

CT = Carotid trifurcation

ECA = External carotid artery

ICA = Internal carotid artery

GP = Guttural pouches

GPM = Guttural pouch mycosis

LT = Linguofacial trunk

MPR = Multi-planar reconstruction

OA = Occipital artery

RA = Rotational angiography

TCE = Transarterial coil embolization

3D = Three dimensional

REFERENCES

ABDEL-RAHMAN, YOUSRIA, A., ABOU-ELMAGD, A. & SALEM, A. O. 1995. Morphological studies on the guttural pouch of donkey. II-The subepithelial glands. *Assiut Veterinary Medical Journal,* 32, 39-51.

AIELLO, S. E. & MAYS, A. (eds.) 1998. *The Merck Veterinary Manual*: Merck & Co. Inc.

ALBERICO, R. A., LOUD, P. & POLLINA, J. 2000. Thick section reformatting of thinly collimated helical CT for reduction of skull-base-related artifacts. *American Journal of Roentgenology,* 175, 1361-1366.

ALSAFY, M. A. M., EL-KAMMAR, M. H. & EL-GENDY, S. A. A. 2008. Topographical anatomy, computed tomography, and surgical approach of the guttural pouches of the donkey. *Journal of Equine Veterinary Science,* 28, 215-222.

ALTMAN, F. 1947. Anomalies of the internal carotid artery and its branches; their embryologic and comparative significance: report of a new case of persistent stapedial artery in man. *Laryngoscope,* 57, 313-319.

ANTUNES, J. L. 1974. Egas Moniz and cerebral angiography. *Journal of Neurosurgery,* 40, 427-432.

ANXIONNAT, R., BRACARD, S., DUCROCQ, X., TROUSSET, Y., LAUNAY, L., KERRIEN, E., BRAUN, M., VAILLANT, R., SCOMAZZONI, F., LEBEDINSKY, A. & PICARD, L. 2001. Intracranial aneurysms: clinical value of 3D digital subtraction angiography in the therapeutic decision and endovascular treatment. *Radiology,* 218, 799-808.

ANZALONE, N., TRIULZI, F. & SCOTTI, G. 1995. Acute subarachnoid haemorrhage: 3D time of flight MR angiography versus intra-arterial digital angiography. *Neuroradiology,* 37, 257-261.

ARMSTRONG, P., WASTIE, M. & ROCKALL, A. 2009. *Diagnostic Imaging. Sixth edition.* Blackwell publishing.

BAPTISTE, K. E. 1998. A preliminary study on the role of the equine guttural pouches in selective brain cooling. *Veterinary Journal,* 155, 139-148.

BAPTISTE, K. E. 2004. The mystery of guttural pouch mycosis: the paradox of advancing knowledge of a rare disease. *Veterinary Journal,* 168, 1-2.

BAPTISTE, K. E., HOLLADAY, S. D. & FREEMAN, L. E. 1996. Alterations in equine guttural pouch morphology with head position: Observations using a new technique for producing accurate casts. *Anatomical Record,* 246, 579-584.

BAPTISTE, K. E., NAYLOR, J. M., BAILEY, J., BARBER, E. M., POST, K. & THORNHILL, J. 2000. A function for guttural pouches in the horse. *Nature,* 403, 382-383.

BARBEE, D. D., ALEEN, J. R. & GAVIN, P. R. 1987. Computed tomography in horses-technique. *Veterinary Radiology,* 28, 144-151.

BARRY, A. 1951. The aortic arch derivatives in the human adult. *The Anatomical Record,* 111, 221-238.

BEDERSON, J. B., CONNOLY, E. S., BATJER, H. H., DACEY, R. G., DION, J. E., DIRINGER, M. N., DULDNER, J. E., HARBAUGH, R. E., PATEL, A. B. & ROSENWASSER, R. H. 2009. Guidelines for the management of aneurysmal subarachnoid haemorrhage. *Stroke,* 40, 994-1025.

BERG VAN DEN, J. C., OVERTOOM, T. T. C., VALOIS, J. C. & MOLL, F. L. 2001. Using three dimensional rotational angiography for sizing of covered stents. *American Journal of Roentgenology,* 178, 149-152.

BLOOD, D. C. & STUDDERT, V. P. 1999. *Saunders Comprehensive Veterinary Dictionary. Second edition*. W.B. Saunders.

BOSANAC, Z., MILLER, R. J. & JAIN, M. 1998. Rotational digital subtraction carotid angiography: technique and comparison with static digital subtraction angiography. *Clinical Radiology,* 53, 682-687.

BUNCE, D. F. M. 1960. Survival of dogs following section of carotid and vertebral arteries. *Proceedings of the Society for Experimental Biology and Medicine,* 103, 581-585.

CARMALT, J. L. & BAPTISTE, K. E. 2004. Atypical guttural pouch mycosis in three horses. *Pferdeheilkunde,* 20, 1-5.

CARON, J. P., FRETZ, P. B., BAILEY, J. V., BARBER, S. M. & HURTIG, M. B. 1987. Balloon-tipped catheter arterial occlusion for prevention of haemorrhage caused by guttural pouch mycosis: 13 cases (1982-1985). *Journal of American Veterinary Medicine Association,* 191, 345-349.

CHERAMIE, H. S., PLEASANT, R. S., ROBERTSON, J. L., MOLL, H. D., CARRIG, C. B., FREEMAN, D. E. & JENSEN, M. E. 1999. Evaluation of a technique to occlude the internal carotid artery of horses. *Veterinary Surgery,* 28, 83-90.

CHURCH, S., WYN-JONES, G., PARKS, A. H. & RITCHIE, H. E. 1986. Treatment of guttural pouch mycosis. *Equine Veterinary Journal,* 18, 362-365.

CLEMMONS, R. M. 1976. Subtraction radiography. *Journal of the American Veterinary Radiology Society,* 17, 67-76.

COLLES, C. M. & COOK, W. R. 1983. Carotid and cerebral angiography in the horse. *Veterinary Record,* 113, 483-489.

COLLINS, J. N., GALUPPO, L. D. & THOMAS, H. L. 2004. Use of computed tomography angiography to evaluate the vascular anatomy of the distal portion of the forelimb of horses. *American Journal of Veterinary Research,* 65, 1409-1420.

CONGDON, E. D. 1922. Transformation of the aortic-arch system during the development of the human embryo. *Contributions to Embryology,* 14, 47-110.

CONSTANTINESCU, G. M. & CONSTANTINESCU, I. A. 2004. *Clinical Dissection Guide for Large Animal. Second edition.* Blackwell Publishing Co.

COOK, W. R. 1966. Observations on the aetiology of epistaxis and cranial nerve paralysis in the horse. *Veterinary Record,* 78, 396-405.

COOK, W. R. 1968a. The clinical features of guttural pouch mycosis in the horse. *Veterinary Record,* 83, 336-345.

COOK, W. R. 1968b. The pathology and aetiology of guttural pouch mycosis in the horse. *Veterinary Record,* 83, 422-428.

COOK, W. R. 1973. The auditory tube diverticulum (guttural pouch) in the horse: its radiographic examination. *Journal of the American Veterinary Radiology Society,* 14, 51-71.

COX, R., BURDEN, F., PROUDMAN, C. J., TRAWFORD, A. F. & PINCHBECK, G. L. 2010. Dermographics, managment and health of donkeys in the UK. *Veterinary Record,* 166, 552-556.

CRAWFORD, T. 1959. Some observations on the pathogenesis and natural history of intracranial aneurysms. *Journal Neurology and Neurosurgery,* 22, 259.

CROMPTON, M. R. 1966. The pathogenesis of cerebral aneurysms. *Brain,* 89, 797-814.

DEAN, B. L. 1996. Conventional angiography. *Neuroimaging Clinics of North America* 6, 843-851.
DU BOULAY, G. & VERITY, P. M. 1973. *The Cranial Arteries of Mammals.* William Heinemann Medical Books Limited.
DU BOULAY, G. H., KENDALL, B. E., CROCKARD, A., SAGE, M. & BELLONI, G. 1975. The autoregulatory capability of Galen's Rete Cerebri and its connection. *Neuroradiology,* 9, 171-181.
DU BOULAY, G. H., LAWTON, M. & WALLIS, A. 1998. The story of the internal carotid artery of mammals: from Galen to sudden infant death syndrome. *Neuroradiology,* 40, 697-703.
DYCE, K. M., SACK, W. O. & WENSING, C. J. G. 1996. The Nervous System. *In: Textbook of Veterinary Anatomy.* Second edition. W.B. Saunders.
ELGERSMA, O. E. H., BUIJS, P. C., WUST, A. F. J., GRAAF VAN DER, Y., EIKELBOOM, B. C. & MALI, W. P. T. M. 1999. Maximum internal carotid arterial stenosis: assessment with rotational angiography versus conventional intraarterial *Radiology,* 213, 777-783.
ELLENBERGER, W. & BAUM, H. 1943. Handbuch der vergleichenden Anatomie der Haustiere: as cited by Baptiste, K.E (2004). *Veterinary Journal,* 168, 1-2.
ENDO, H., MANGLAI, FUJISAWA, M., KUROHMARU, M. & HAYASHI, Y. 1998. The guttural pouch is not present in the White Rhinoceros (*Ceratotherium simum*); morphology of the Eustachian tube and nasopharynx. *Anatomy, Histology and Embryology,* 27, 327-330.
EWART, J. C. 1915. Studies on the development of the horse. The development during the third week. *Transactions of the Royal Society of Edinburgh,* 51, 287-329.
FISCHER, M. S. 1989. Hyracoids, the sister-group of perissodactyls. *In: The Evolution of Perissodactyls.* New York. Clarendon Press.
FOX, C. H., JOHNSON, F. B., WHITING, J. & ROLLER, P. P. 1985. Formaldehyde fixation. *Journal of Histochemistry and Cytochemistry,* 33, 845-853.
FRACKOWIAK, H., GIEJDASZ, K. & GODYNICKI, S. 1997. The caroticobasilar artery in species of order Perissodactyla. *Folia Morphologica,* 56, 273-276.
FREEMAN, D. E. Epistaxis: diagnosis and treatment. Annual meeting- Italian association of equine veterinarian, 2003 Pisa, Italy. International Veterinary Information Service.
FREEMAN, D. E. & DONAWICK, W. J. 1980a. Occlusion of internal carotid artery in the horse by means of a balloon-tipped catheter: Clinical use of a method to prevent epistaxis caused by guttural pouch mycosis. *Journal of American Veterinary Medicine Association,* 176, 236-240.
FREEMAN, D. E. & DONAWICK, W. J. 1980b. Occlusion of the internal carotid artery in the horse by means of a balloon tipped catheter : evaluation of a method designed to prevent epistaxis caused by guttural pouch mycosis. *Journal of American Veterinary Medicine Association,* 176, 232-235.
FREEMAN, D. E. & HARDY, J. 2006. Guttural Pouch. *In: Auer and Stick Equine Surgery.* Third edition. Saunders Elsevier.
FREEMAN, D. E., ROSS, M. W., DONAWICK, W. J. & HAMIR, A. N. 1989. Occlussion of the external carotid and maxillary arteries in the horse to prevent hemorrhage from guttural pouch mycosis. *Veterinary Surgery,* 18, 39-47.

FREEMAN, D. E., STALLER, G. S., MAXSON, A. D. & SWEENEY, C. R. 1993. Unusual internal carotid artery branching that prevented arterial occlusion with a balloon-tipped catheter in a horse. *Veterinary Surgery,* 22, 531-534.

FULLER, A., MALONEY, S. K., KAMERMAN, P. R., MITCHELL, G. & MITCHELL, D. 2000. Absence of selective brain cooling in free-ranging zebra in their natural habitat. *Experimental physiology,* 85, 209-217.

FURUHATA, K. 1964. Morphological studies of the trifurcate portions of common carotid arteries and so called intercarotid bone in horse. *Japanese Journal of Veterinary Research,* 12, 47-59.

GILLILAN, L. A. 1974. Blood supply to brains of ungulates with and without a Rete Mirabile Caroticum. *Journal of Comparative Neurology,* 153, 275-290.

GRABHERR, S., DJONOV, V., YEN, K., THALI, M. J. & DIRNHOFER, R. 2007. Postmortem angiography: Review of former and current methods. *American Journal of Roentgenology,* 188, 832-838.

GRANT, E. G., BENSON, C. B., MONETA, G. L., ALEXANDROV, A. V., BAKER, J. D., BLUTH, E. I., CARROLL, B. A., ELIASZIW, M., GOCKE, J., HERTZBERG, B. S., KATANICK, S., NEEDLEMAN, L., PELLERITO, J., POLAK, J. F., RHOLL, K. S., WOOSTER, D. L. & ZIERLER, E. 2003. Carotid artery stenosis: Gray scale and Doppler ultrasound diagnosis. *Radiology,* 229, 340-346.

GRASS, M., KOPPE, R., KLOTZ, E., PROKSA, R., KUHN, M. H., AERTS, H., OP DE BEEK, J. & KEMKERS, R. 1999. Three dimensional reconstruction of high contrast objects using C-arm image intensifier projection data. *Computerized Medical Imaging and Graphics,* 23, 311-321.

GRAY, H. 1918. Anatomy of the Human Body. 20th ed. Philadelphia: Lea & Febiger; Bartleby.com, 2000.

GREEN, N. E., CHEN, J., MESSENGER, J. C., GROVES, B. M. & CARROL, J. D. 2004. Three dimensional vascular angiography. *Current Problem in Cardiology,* 29, 104-42.

GREET, T. R. C. 1987. Outcome of treatment in 35 cases of guttural pouch mycosis. *Equine Veterinary Journal,* 19, 483-487.

HARDY, J. & LÉVEILÉ, R. 2003. Diseases of the guttural pouches. *Veterinary Clinics of North America: Equine Practice,* 19, 123-58.

HATHCOCK, J. T. & STICKLE, R. L. 1993. Principles and concepts of computed tomography. *Veterinary Clinics of North America: Small Animal Practice,* 23, 399-415.

HEAUTOT, J. F., CHABERT, E., GANDON, Y., CROCI, S., ROMEAS, R., CAMPAGNOLO, R., CHEREUL, B., SCARABIN, J. M. & CARSIN, M. 1998. Analysis of cerebrovascular diseases by a new 3-dimensional computerised X-ray angiography system. *Neuroradiology,* 40, 203-209.

HIGGINS, A. J. & WRIGHT, I. M. 1995. *The Equine Manual.* W.B Saunders.

HILDEBRAND, M. 1968. *Anatomical Preparations.* Los Angeles. University of California Press.

HINCHCLIFFE, R. & PYE, A. 1969. Journal of Zoology: as cited by Baptiste K.E (2004). *Veterinary Journal,* 168, 1-2.

HIRAI, T., KOROGI, Y., SUGINOHARA, K., ONO, K., NISHI, T., UEMURA, S., YAMURA, M. & YAMASHITA, Y. 2003. Clinical usefulness of unsubtracted 3D digital angiography compared with rotational digital angiography in the pretreatment evaluation of intracranial aneurysms. *American Journal of Neuroradiology,* 24, 1067-1074.

HOCHMUTH, A., SPETZGER, U. & SCHUMACHER, M. 2002. Comparison of three dimensional rotationla angiography with digital subtraction angiography in the assessment of ruptured cerebral aneurysms. *American Journal of Neuroradiology,* 23, 1199- 1205.

HYDE, D. E., FOX, A. J., GULKA, I., KALAPOS, P., LEE, D. H., PELZ, D. M. & HOLDSWORTH, D. W. 2004. Internal carotid artery stenosis measurement: comparison of 3D computed rotational angiography and conventional digital subtraction angiography. *Stroke,* 35, 2776-2781.

JOHNSON, J. H., MERRIAM, J. G. & ATTLEBERGER, M. 1973. A case of guttural pouch mycosis caused by *Aspergillus nidulans*. *Veterinary Medicine Small Animall Clinic,* 68, 771-774.

JOSEPH, P. M. & SPITAL, R. D. 1978. A method for correcting bone induced artifacts in computed tomography scanners. *Journal of Computer Assisted Tomography,* 2, 100-108.

KIPAR, A. & FRESE, K. 1993. Hypoglossal neuritis with associated lingual hemiplegia secondary to guttural pouch mycosis. *Veterinary Pathology,* 30, 574-576.

KOROGI, Y., TAKAHASHI, M., KATADA, K., OGURA, Y., HASUO, K., OCHI, M., UTSUNOMIYA, H., ABE, T. & IMAKITA, S. 1999. Intracranial aneurysms: detection with three dimensional CT angiography with volume rendering-comparison with conventional angiographic and surgical findings. *Radiology,* 211, 497-506.

KOUSKOURAS, C., CHARITANTI, A., GIAVROGLOU, C., FOROGLOU, N., SELVIARIDIS, P., KONTOPOULOS, V. & DIMITRIADIS, A. S. 2004. Intracranial aneurysms: evaluation using CTA and MRA. Correlation with DSA and intraoperative findings. *Neuroradiology,* 46, 842-850.

LANE, J. G. 1989. The management of guttural pouch mycosis. *Equine Veterinary Journal,* 21, 321-324.

LARSEN, W. J. 2001. *Human Embryology. Third edition.* Churchill Livingstone.

LAUS, E., PAGGI, E., CERQUETELLA, M., SPAZIANTE, D., SPATERNA, A. & TESEI, B. 2011. Guttural pouch mycosis in a donkey (*Equus asinus*): a case report. *Veterinarni Medicina,* 55, 561-565.

LEPAGE, O. M. 2005. Transarterial coil embolisation in 31 horses (1999-2002) with guttural pouch mycosis. *Equine Veterinary Journal,* 37, 430-434.

LEPAGE, O. M. 2011. Personal communication-VetAgro Sup, Veterinary Campus of Lyon. *University of Lyon, France.*

LEPAGE, O. M., PERRON, M. F. & CADORÉ, J. L. 2004. The mystery of fungal infection in the guttural pouches. *Veterinary Journal,* 168, 60-4.

LÉVÉILLE, R., HARDY, J., ROBERTSON, J. T., WILLIS, A. M., BEARD, W. L., WEISBRODE, S. E. & LEPAGE, O. M. 2000. Transarterial coil embolization of the internal and external carotid and maxillary arteries for prevention of hemorrhage from guttural pouch mycosis in horses. *Veterinary Surgery,* 29, 389-397.

LUDWIG, A., GATINEAU, S., REYNAUD, M. C., CADORE, J. L. & BOURDOISEAU, G. 2004. Fungal isolation and identification in 21 cases of guttural pouch mycosis in horses (1998-2002). *Veterinary Journal,* 169, 457-461.

MACDONALD, D. G., FRETZ, P. B., BAPTISTE, K. E. & HAMILTON, D. L. 1999. Anatomic, radiographic and physiologic comparisons of the internal carotid and maxillary artery in the horse. *Veterinary Journal,* 158, 182-189.

MAFF 1968. Ministry of Agriculture, Fisheries and Food & Department of Agriculture and Fisheries for Scotland:A century of agricultural statistics 1866-1966. *London, H.M.S.O.*, 54-55, 61, 129.

MANGLAI, D., WADA, R., ENDO, H., KUROHMARU, M., YOSHIHARA, T., SASAKI, M., OIKAWA, M. & HAYASHI, Y. 2000. Macroscopic anatomy of the auditory tube diverticulum (guttural pouch) in the Thoroughbred equine-a silicon mold approach. *Okajimas Folia Anatomica Japonica,* 76, 335-346.

MARCUS, R. G. 2002. *Untersuchungen zur Therapie der Luftsackmycose des Pferdes-Ligatur der Arteria Carotis Interna Mittels Transendoscopischer Clippaplication*. Doktors der Veterinarmedizin, Tierarztliche Hochschule Hannover.

MARTIN, J. H. 2003. *Neuroanatomy: Text and Atlas. Third edition.* The McGraw-Hill Companies.

MATSUDA, Y., NAKANISHI, Y. & MIZUNO, Y. 1999. Occlusion of the internal carotid artery by means of microcoils for preventing epistaxis caused by guttural pouch mycosis in horses. *Journal of Veterinary Medical Science,* 61, 221-225.

MCCONAGHY, F. F., HALES, J. R. S., ROSE, R. J. & HODGSON, D. R. 1995. Selective brain cooling in the horse during exercise and environmental heat stress. *Journal of Applied Physiology,* 79, 1849-54.

MCKENNA, M. C. 1975. Toward a Phylogenetic Classification of Mammalia: A Multidisciplinary Approach. *In: Phylogeny of the Primates.* Plenum Press, New York.

MCKINNEY, A. M., PALMER, C. S., TRUWIT, C. L., KARAGULLE, A. & TEKSAM, M. 2008. Detection of aneurysms by 64-section multidetector CT angiography in patients acutely suspected of having an intracranial aneurysm and comparison with digital subtraction and 3D rotational angiography. *American Journal of Neuroradiology,* 29, 594-602.

MCKNIGHT, A. L., MANDUCA, A., FELMLEE, J. P., ROSSMAN, P. J., MCGEE, K. P. & EHMAN, R. L. 2004. Motion correction techniques for standing equine MRI. *Veterinary Radiology and Ultrasound,* 45, 513-519.

MEIJLING, H. A. 1938. Bau und innervation von glomus caroticum und sinus caroticus. *Acta Neerl. Morph.,* 1, 193-288.

MENKE, J., LARSEN, J. & KALLENBERG, K. 2011. Diagnosing cerebral aneurysms by computed tomographic angiography: meta analysis. *Annals of Neurology,* 69, 646-654.

MILLER, B. C., WILSON, D. A., MARTIN, D. D., PACE, L. W. & CONSTANTINESCU, G. M. 1998. Complications of balloon catheterization associated with aberrant cerebral arterial anatomy in a horse with guttural pouch mycosis. *Veterinary Surgery,* 27, 450-453.

MITCHELL, D., MALONEY, S. K., JESSEN, C., LABURN, H. P., KAMERMAN, P. R., MITCHELL, G. & FULLER, A. 2002. Adaptive heterothermy and selective brain cooling in arid-zone mammals. *Comparative biochemistry and physiology,* 571-585.

MITCHELL, G., FULLER, A., MALONEY, S. K., RUMP, N. & MITCHELL, D. 2006. Guttural pouches, brain temperature and exercise in horses. *Biology Letters,* 2, 475-477.

MOLINARI, G., SMITH, L., GOLDSTEIN, M. N. & SATRAN, R. 1973. Pathogenesis of cerebral mycotic aneurysms. *Neurology,* 23, 325-332.
MOSTRUM, U. & YTTERBERGH, C. 1986. Artifacts in computed tomography of the posterior fossa: a comparative phantom study. *Journal of Computer Assisted Tomography,* 10, 560-566.
NAKAMURA, T., KIRYU, K., MACHIDA, N., IWATA, T., OIKAWA, M. & KANEKO, M. 1992. Histologic features of the carotid artery trifurcation in Thoroughbreds. *American Journal of Veterinary Research,* 53, 288-290.
NANDA, B. S. 1975. Heart and arteries. *In: The Anatomy of the Domestic Animals.* Philadelphia. Saunders W.B.
NANDA, B. S. & GETTY, R. 1975. Presence of the arteria caroticobasilaris in the horse. *Anatomischer Anzeiger,* 137, 116-119.
NISHIMURA, H., TANIMURA, T., SEMBA, R. & UWABE, C. 1974. Normal development of early human embryos: observation of 90 specimens at Carnegie stages 7 to 13. *Teratology,* 10, 1-8.
OKOHARA, M., KIYOSUE, H., MORI, H., TANOUE, S., SAINOU, M. & NAGATOMI, H. 2002. Anatomic variations of the cerebral arteries and their embryology: a pictorial review. *European Radiology,* 12, 2548-2561.
ORR, J. A., WAGERLE, L. C., KIORPES, A. L., SHIRER, H. W. & FRIESEN, B. S. 1983. Distribution of internal carotid artery blood flow in the pony. *American Journal of Physiology,* 244, H142-H149.
ORT, M. G., GREGG, E. C. & KAUFMAN, B. 1977. Subtraction radiography: techniques and limitations. *Radiology,* 124, 65-72.
OWEN, R. R. 1974. Epistaxis prevented by ligation of the internal carotid artery in the guttural pouch. *Equine Veterinary Journal,* 6, 143-149.
OWEN, R. R. & MCKELVEY, W. A. C. 1979. Ligation of the internal carotid artery to prevent epistaxis due to guttural pouch mycosis. *Veterinary Record,* 104, 100-101.
OZGEL, O. & DURSUN, N. 2007. Arteries that supply the brain and the formation of circulus arteriosus cerebri in donkeys. *Medycyna Weterynaryjna,* 63, 1561-1563.
PADGET, D. H. 1948. The development of the cranial arteries in the human embryo. *Contributions to Embryology,* 32, 205-261.
PAULLUS, W. S., PAIT, T. G. & RHOTON, A. L. 1977. Microsurgical exposure of the petrous portion of the carotid artery. *Journal of Neurosurgery,* 47, 713-726.
PEDICELLI, A., ROLLO, M., DI LELLA, G. M., COLOSIMO, C. & BONOMO, L. 2007. 3D rotational angiography for the diagnosis and preoperative assessment of intracranial aneurysms: preliminary experience. *Radiol. Med.,* 112, 895-905.
PERKINS, J. D., SCHUMACHER, J., KELLY, G., GOMEZ, J. H. & SCHUMACHER, J. 2006. Standing surgical removal of inspissated guttural pouch exudate (chondroids) in ten horses. *Veterinary Surgery,* 35, 658-662.
POLLOCK, J. P. 2007. Diagnosis and management of guttural pouch mycosis. *Equine Veterinary Education,* 19, 522-527.
POLLOCK, J. P. 2011. Personal communication- Weipers Equine Hospital, School of Veterinary Medicine. *University of Glasgow, UK.*
PORAT-MOSENCO, Y., SCHWARZ, T. & KASS, P. H. 2004. Thick section reformatting of thinly collimated computed tomography for reduction of skull-base-related artifacts in dogs and horses. *Veterinary Radiology and Ultrasound,* 45, 131-135.

PRITZ, M. B. 2011. Cerebral aneurysm classification based on angioarchitecture. *Journal of Stroke and Cerebrovascular Diseases,* 20, 162-167.
PROTHERO, D. R. & SCHOCH, R. M. 1989. Origin and evolution of the perissodactyla: summary and synthesis. *In: The Evolution of Perissodactyls.* New York. Clarendon Press.
ROONEY, J. R. 1997. Why guttural pouches? *The Equine Disease Quarterly,* 6, 3.
ROSENSTEIN, D. S., BOWKER, R. M. & BARTLETT, P. C. 2000. Digital angiography of the feet of horses. *American Journal of Veterinary Research,* 61, 255-259.
SADLER, T. W. 1995. *Langman's Medical Embryological. Seventh edition.* Baltimore. Williams & Wilkins.
SCHUIERER, G., HUK, W. J. & LAUB, G. 1992. Magnetic resonance angiography of intracranial aneurysms: comparison with intra-arterial digital substraction angiography. *Neuroradiology,* 35, 50-54.
SCHWARZ, T., SULLIVAN, M., STORK, C. K., WILLIS, R., HARLEY, R. & MELLOR, D. J. 2002. Aortic and cardiac mineralization in the dog. *Veterinary Radiology and Ultrasound,* 43, 419-427.
SCOTT, E. A., THRALL, D. E. & SANDLER, G. A. 1976. Angiography of Equine metacarpus and phalanges - alterations with medial palmar artery and medial palmar digital artery ligation. *American Journal of Veterinary Research,* 37, 869-873.
SEIBERT, J. A. 2006. Flat-panel detectors: how much better are they? *Pediatric Radiology,* 36, 173-181.
SHERLOCK, C. E., HAWKINS, F. L. & MAIR, T. S. 2007. Severe upper airway damage caused by iodine administration into the guttural pouches of a pony. *Equine Veterinary Education,* 19, 515-520.
SHINOZAKI, T., KOMIYAMA, K., JIN, K., TAKEKAWA, S., TAKAHASHI, K., KISHIBE, H. T. S. & SATO, M. 1970. Television applied to X-ray diagnosis report 1: an experimental and clinical study of a simplified television monitor and video recorder for televised fluoroscopy. *Nippon Acta Radiology,* 30, 339-346.
SILBERGLEIT, R., QUINT, D. J., MEHTA, B. A., PATEL, S. C., METES, J. J. & NOUJAIM, S. E. 2000. The persistent stapedial artery. *American Journal of Neuroradiology,* 21, 572-577.
SISSON, S. 1975. The ear. *In: The Anatomy of the Domestic Animal.* Fifth edition. W.B Saunders.
SISSON, S. & GROSSMAN, J. D. 1975. *The Anatomy of the Domestic Animal. Fifth edition.* W.B Saunders.
SKIDMORE, F. D. 1976. An analysis of the age and size of 483 human embryos. *Teratology,* 15, 97-102.
SMITH, B. J., HOLLADAY, S. D. & HUDSON, L. C. 1990. A simplified method of casting the macroscopic airways of lungs. *Acta Anatomica,* 137, 109-113.
SMITH, K. M. & BARBER, S. M. 1984. Guttural pouch haemorrhage associated with lesions of the maxillary artery in two horses. *Canadian Veterinary Journal,* 25, 239-242.
SPEIRS, V. C., HARRISON, I. W., VEENENDAAL, J. C., BAUMGARTNER, T., JOSSECK, H. H. & REUTTER, H. 1995. Is specific antifungal therapy necessary for the treatment of guttural pouch mycosis in horses? *Equine Veterinary Journal,* 27, 151-152.
STEIGER, H. J., POLL, A., LIEPSCH, D. & REULEN, H. J. 1987. Basic flow structure in saccular aneurysms: a flow visualization study. *Heart Vessels,* 3, 55-65.

TANDLER, J. 1901. *Anat. Hefte, Abt.*, 1, 327.

TOGNETTI, F., LIMONI, P. & TESCA, C. 1983. Aneurysm growth and haemodynamic stress. *Surgical Neurology,* 20, 74-78.

TOMMASINI, G., CAMERINI, A., GATTI, A., DERCHI, G., BRUZZONE, A. & VECCHIO, C. 1998. Panoramic coronary angiography. *Journal of American College of Cardiology,* 31, 871-7.

TOMPSETT, D. H. 1970. *Anatomical Techniques. Second edition.* E. & S. Livingstone, Ltd.

TURNER, H. N. 1850. Proceedings of the Zoological Society: as cited by Baptiste, K.E (2004). *Veterinary Journal,* 168, 1-2.

URQUHART, J. 1983. *Animals on the Farm: Their History from the Earliest Times to the Present Day.* London and Sidney. MacDonald and Co.

VAN ROOIJ, W. J., SPRENGERS, M. E., DE GAST, A. N., PELUSO, J. P. P. & SLUZEWSKI, M. 2008. 3D rotational angiography: the new gold standard in the detection of additional intrcranial aneurysms. *American Journal of Neuroradiology,* 29, 976-979.

VAN VALEN, L. 1978. The beginning of the age of Mammals. *Evolutionary Theory,* 4, 45-80.

VITUMS, A. 1951. The development of the aortic arches in the horse. *American Journal of Veterinary Research,* 12, 26-30.

VITUMS, A. 1969. Development and transformation of the aortic arches in the equine embryos with special attention to the formation of the definitive arch of the aorta and the common brachiocephalic trunk. *Anat. Entwickl.-Gesch.,* 128, 243-270.

VON HAGENS, G., TIEDEMANN, K. & KRIZ, W. 1987. The current potential of plastination. *Anatomy and Embryology,* 175, 411-421.

WIBLE, J. R. 1986. Transformation in the extracranial course of the internal carotid artery in mammalian phylogeny. *Journal of Vertebrae Paleontology,* 6, 313-325.

WILSON, J. 1985. Effects of indwelling catheters and povidone iodine flushes on the guttural pouches of the horse. *Equine Veterinary Journal,* 17, 242-244.

WINOGRADOW, P. P. 1928. Uber die variationen der gemeins chaftlichen kopfarterien (Aa. carotides communes) beim pferde. *Anat. Anzeiger,* 66, 273-280.

WISMER, G. L. 1989. Circle of Willis variant analogous to fetal type primitive trigeminal artery. *Neuroradiology,* 31, 366-368.

WOODIE, J., DUCHARME, N., GLEED, R. & SODERHOLM, L. V. 2002. In horses with with guttural pouch mycosis or after stylohyoid bone resection, what arterial ligation (s) could be effective in emergency treatment of haemorrhage crisis? *Veterinary Surgery,* 31, 498.

YOUNG, M., DORSCH, N. W. C. & KINGSTON, R. J. 1999. Pitfalls in the use of spiral CT for identification of intracranial aneurysm. *Neuroradiology,* 41, 93-99.

ZIEHM 2007. Ziehm Vision Vario family operation instructions. Ziehm Imaging Group.